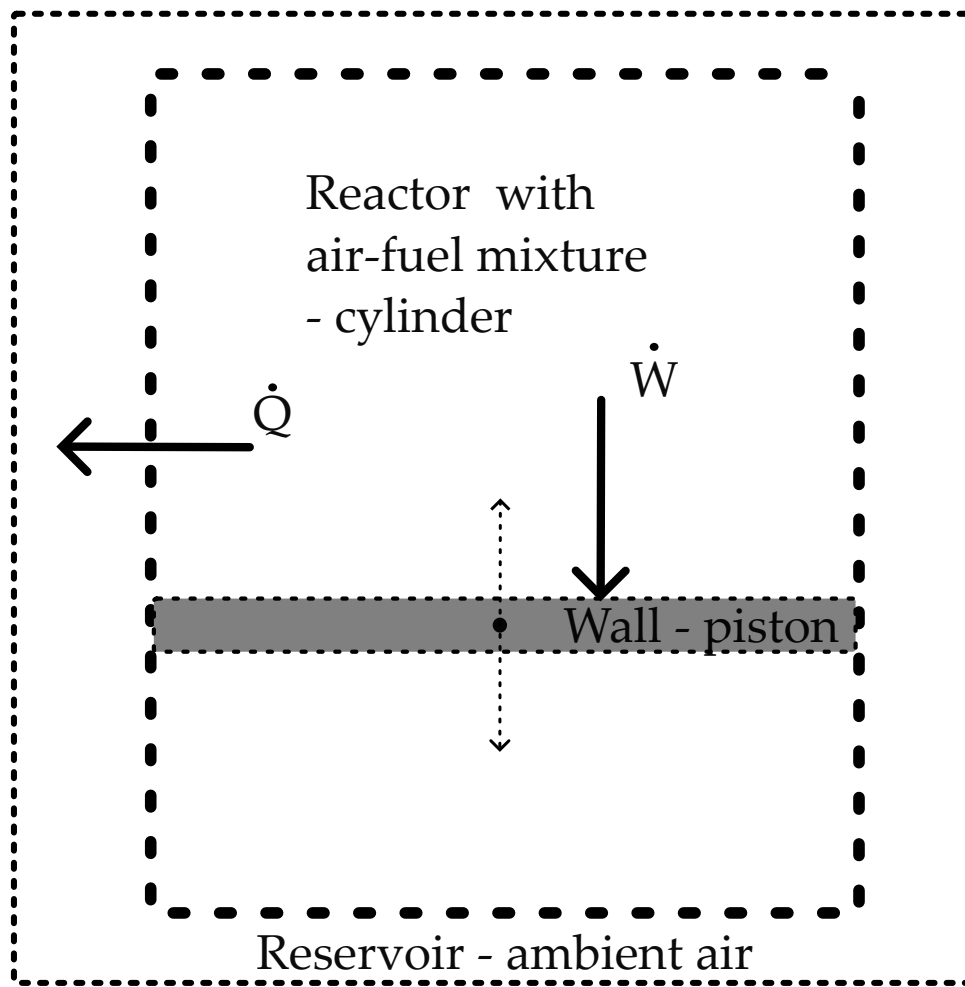
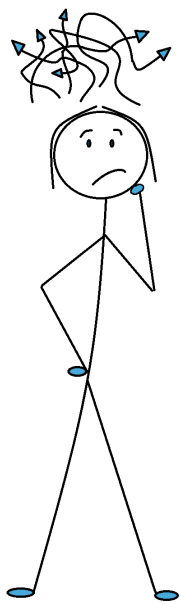


Exploring CI combustion of ammonia and hydrogen in an ICE with a single-zone thermodynamic model incorporating reaction kinetics



Thesis for the degree of MSc in Marine Technology
in the specialization of Marine Engineering.

Exploring CI combustion of ammonia and hydrogen in an ICE with a single-zone thermodynamic model incorporating reaction kinetics

by

Isabelle Jacobs

Performed at

Maritime and Transport Technology department at
Delft University of Technology.

This thesis (MT.22/23.036.M) is classified as confidential in accordance with the general
conditions for projects performed by the TU Delft.

13th of September 2023

Thesis exam committee

Chair	Dr.ir. P. de Vos	Delft University of Technology
Scientific member	Dr.ir. X.L.J. Seykens	TNO Helmond
Scientific member	Ir. K. Visser	Delft University of Technology
Staff member	Ir. T. Eker	Delft University of Technology

Author Details

Student number	1357603
Author contact e-mail	isabellejacobs@protonmail.com

Isabelle Jacobs: *Exploring CI combustion of ammonia and hydrogen in an ICE with a single-zone thermodynamic model incorporating reaction kinetics* (2023)

The work in this thesis was carried out at the Maritime and Transport Technology department at Delft University of Technology.

Supervisors: Dr.ir. P. de Vos Delft University of Technology
Dr.ir. X.L.J. Seykens TNO Helmond

Abstract

This graduation thesis studies the CI combustion of ammonia and hydrogen in an ICE. It contains a review of the literature and a modeling study of the ignition and cylinder performance of the AmmoniaDrive test engine. AmmoniaDrive is a NWO-funded research project that aims to decarbonize shipping by introducing an ammonia-fuelled SOFC-ICE power plant for ships and other heavy-duty applications.

Ammonia (NH_3) has unfavorable properties for combustion, such as a high heat of vaporization, narrow flammability limits, a high flame quenching distance, low flame speed, and most important: a high resistance to autoignition. Those properties have to be overcome and hydrogen (H_2) is known to be capable of playing a role. As the properties of hydrogen are extremely high combustion speed, very wide flammability limits and a very short flame quenching distance. Unfortunately, both ammonia and hydrogen have a high resistance to autoignition, while CI engines need a fuel with low resistance to auto-ignition. For this reason, a carbon-based fuel, like DME or HVO, is considered necessary to achieve ignition.

The state-of-the-art experimentally achieved combustion concepts are an homogeneous charge compression ignition (HCCI) combustion concept of Pochet et al. [2020a] and an reactivity controlled compression ignition (RCCI) combustion concept of Chiera et al. [2022]. The HCCI combustion concept is fueled by NH_3 and H_2 , without a carbon-based fuel. However, it requires a compression ratio (CR) of 22, a high intake temperature, and is limited by the maximum pressure rise rate (MPRR). The RCCI combustion concept is fueled by NH_3 and diesel. This concept can achieve up to 81%_e NH_3 , but still requires 19%_e diesel.

A modeling study is done to investigate how to improve the CI combustion strategies, taking into consideration the context of AmmoniaDrive. The modeling study consists of two closed volume single-zone thermodynamic reactor models: the ignition model and the engine cylinder model. The ignition model is a constant volume model, resembling top dead center (TDC) conditions. The engine cylinder model simulates a closed volume from bottom dead center (BDC) to 90 CAD after TDC and incorporates volume change and the heat loss. Both models make use of the chemical kinetic mechanism of Shrestha et al. [2018] to incorporate the combustion reaction. Due to the limitation imposed by the available species in chemical kinetic mechanisms, the carbon-based fuel in the modeling study is DME. For the future, hydrotreated vegetable oil (HVO) seems a more favorable carbon-based fuel, based on experimental results in a constant volume combustion chamber (CVCC) of Hernández et al. [2023].

The results of the two models indicate that an HCCI combustion concept of ammonia and hydrogen, without a carbon-based fuel, will not ignite within the engine limits of the AmmoniaDrive test engine. An HCCI combustion concept of ammonia, hydrogen, with DME will ignite, but has a limited power output due to the MPRR. An RCCI combustion concept with stratification of DME throughout the cylinder looks promising based on the engine cylinder model results. Stratifying DME concentration, and with that the fuel reactivity, is likely to reduce the MPRR. This would allow for a higher power output due to the possibility to inject more fuel energy without exceeding the engine limits.

Combining the literature and modeling results, it is likely that an RCCI combustion concept with ammonia, hydrogen, and HVO will lead to a higher power output and a decreased required amount of carbon-based fuel, whilst staying within engine limits.

Acknowledgements

With these acknowledgements I'd like to express my gratitude and appreciation to the people who supported me during the graduation project.

First of all, Peter de Vos. Thank you for providing me this amazing graduation project. I feel very fortunate by the trust and supervision given by you. As supervisor, you gave space to find my way, whilst keeping me on track and nudging me forward. And when it was outside your expertise, you found resources outside our faculty or university, to help me. I am so happy to continue our cooperation.

Xander Seykens, thank you for your thorough and incredibly useful explanation and feedback during my graduation project. Sometimes I needed a day to fully grasp it, but your insights have lifted my understanding and this graduation project to a higher level. I very much appreciate your time and effort to provide me with thorough feedback.

Turhan Eker, your expertise regarding chemical kinetic mechanisms has helped me through critical points in this graduation. Thank you for answering all my questions and helping me out.

Klaas Visser, the lecturer who sparked my enthusiasm for internal combustion engines. I'm grateful that you, on your last day as an official employee of the university, are part of my graduation committee. Although you have more than deserved your retirement, I hope you continue to be involved.

Tom Postma, my chemistry hotline. Thank you for taking the time to help me, whether it was to explain chemistry, finding out which books could help me or rephrasing the title. You were there, thank you.

My study friends, thank you for welcoming me back every time I returned from a adventures. The support and warm welcome back has been so much appreciated.

My friends, thank you for supporting me in this winding, adventurous road that was my study. Your continued faith in a good ending, meant so much to me.

Mom, my favorite lastpost, thank you for letting me occupy your dining table and supporting me in many ways. Joost, thank you for your support by doing some chores. This project went pretty well and will continue for four more years. So it would be great if you keep up the good work.

Andrew, thank you for supporting and enduring me during this project.

Contents

1	Introduction	1
1.1	Development	1
1.2	Motivation for this study	2
1.3	Broader perspective	2
1.4	Scope	3
1.5	Content	3
1.6	AmmoniaDrive Research Project	3
1.6.1	Case study W12V31	4
2	Available research	5
2.1	Scientific publications	5
2.1.1	Experimental research	5
2.1.2	Numerical research	6
2.2	Research locations	7
2.3	Non-scientific research	7
3	Fuel	9
3.1	Ammonia	9
3.1.1	Aqueous ammonia	9
3.2	Hydrogen	10
3.2.1	Ringling	10
3.3	The HRF, promoter, or pilot fuel	10
3.4	Fuel mixture	10
3.5	Equivalence ratio	12
3.6	Autoignition	13
3.6.1	Ignition delay time	15
3.7	Flame speed	15
4	Combustion strategies	19
4.1	Conventional Dual-Fuel	19
4.2	HCCI	20
4.3	Partially & premixed charge compression ignition	21
4.4	RCCI	21
4.4.1	Ignition RCCI	22
4.4.2	Reactivity control	22
4.4.3	Ammonia combustion via RCCI	23
4.5	Other combustion mechanisms	23
5	In-cylinder processes	25
5.1	Air intake	25
5.1.1	Exhaust gas recirculation	26
5.2	Injection	26
5.2.1	Injection timing	26

Contents

5.2.2	Multiple injections	27
5.2.3	Injection pressure	28
5.2.4	Spray shape	28
5.2.5	Other injection strategies	28
5.3	Mixing	28
5.4	Ignition	29
5.5	Combustion	30
5.5.1	Pressure rise rate	30
6	Emissions	33
6.1	Measuring global warming effect	33
6.2	CO ₂ and CO	33
6.3	NO _x	33
6.4	N ₂ O	34
6.5	Ammonia	34
6.6	Hydrocarbons	36
6.7	Soot	36
6.8	Selective catalytic reduction	36
7	Engine characteristics	39
7.1	Engine speed	39
7.2	Compression ratio	39
7.3	Fuel delivery system	40
7.3.1	Injectors	40
7.3.2	Plenum	41
7.3.3	Pre-heating	41
7.3.4	Pre-chamber	41
7.4	Piston design	42
7.5	Material factors	42
8	Models in literature	43
8.1	Thermodynamic models	43
8.2	Fluid dynamic models	43
8.3	Phenomenological models	44
8.3.1	Heat transfer model	44
8.3.2	Combustion model	45
8.4	Chemical-Kinetic Mechanisms	45
8.5	Software	46
8.6	Modelling CI combustion concepts with ammonia	46
9	Novel combustion strategies	49
9.1	Novel combustion concepts	49
9.1.1	Concept 1: the RCCI concept	49
9.1.2	Concept 2: the PCCI stratification concept	50
9.1.3	Concept 3: the homogeneous charge hydrogen spark concept	50
9.2	Trade off	51
9.3	Investigating a combustion strategy for the AmmoniaDrive test engine	52
10	Ignition model	55
10.1	Modeling of the ignition and combustion	57

10.2	Equations	58
10.2.1	Governing equations of the ideal gas reactor	58
10.2.2	Definitions	60
10.3	Verification & Validation	60
10.4	Assumptions, limitations, and uncertainties	63
10.5	Results	64
10.5.1	Ammonia and hydrogen, without DME	65
10.5.2	Ammonia, hydrogen, and DME	67
11	Engine cylinder modeling	69
11.1	Equations & definitions	71
11.1.1	Governing equations reactor	71
11.1.2	Definitions & Calculations	72
11.1.3	Heat transfer model	73
11.2	Verification & Validation	74
11.2.1	Verification	74
11.2.2	Validation	74
11.2.3	Comparison with modeling results	75
11.2.4	Comparison with experimental results	76
11.3	Limitations, assumptions, and uncertainties	78
11.4	Results	78
11.4.1	Fueled by ammonia and hydrogen, without DME	78
11.4.2	Fueled by ammonia, hydrogen, with DME	79
11.5	Reflection on modeling method	82
12	Conclusion	85
13	Discussion and Recommendations	89
A	Research questions - Literature research	91
B	Research questions - Thesis	93
C	Experimental studies	95
D	Results Hernández et al. 2023	99
E	Spray shape different fuels	101
F	Background – Fuel	103
G	Results Niki et al.	105
H	Results Niki et al. - Fuel reactivity	107
I	Background - Modeling	109
J	Overview chemical kinetic mechanisms	111
K	Species Chemical Kinetic Mechanism	113

Contents

L	Converting chemical kinetic model to YAML	117
M	Cantera	119
	M.1 Ideal Gas Reactor	119
	M.2 Wall	119
	M.2.1 Wall parameters	119
	M.3 Reservoir	120
N	Ignition model results	121
O	Engine cylinder model results	123

List of Figures

1.1	Overview literature study results in chapters 3-8	4
2.1	Locations where ammonia combustion via a CI mechanism are or have been experimentally investigated	7
3.1	The maximum pressure rise rate (MPRR) and CA50 for a constant intake temperature and hydrogen flow rate, while increasing the ammonia flow rate. From Pochet et al. [2020a]	12
3.2	Laminar flame speeds of NH ₃ /H ₂ /air at 473K and 1/3 at varying H ₂ content. (Symbols: measurements from Lhuillier et al. [2020] and Shrestha et al. [2021]. Dashed lines: model from Shrestha et al. [2018], solid lines: Shrestha et al. [2021]. Figure from Shrestha et al. [2021]	13
3.3	Combustion duration as a function of the NH ₃ % and ϕ	14
3.4	From Dai et al. [2020]: Effect of hydrogen on the ignition delay time at different equivalence ratio's. (a) isobars, (b) isotherms.	16
3.5	Laminar flame speed of NH ₃ /H ₂ /air mixtures at 473K, $\phi=1.1$ and 5–10 bar. Symbols: measurements. Lines: simulations. From Shrestha et al. [2021]	16
4.1	Measured cylinder pressure and HRR by Yousefi et al. [2022b]	20
4.2	Heat release rate and needle lift for a conventional diesel combustion and two HCCI combustion processes (from Heywood [2018])	21
4.3	Constant intake temperature and hydrogen flow with increasing the ammonia flow rate. From Pochet et al. [2020a]	22
4.4	Effect of changing the fuel mixture ratio on the HRR and HRR for two different pilot injection timings, a) -45 CAD after top dead center (ATDC), b) -60 CAD ATDC. Graph from Niki [2021b]	24
5.1	Overview in-cylinder processes	25
5.2	Required intake temperatures for NH ₃ /H ₂ mixtures such that the autoignition occurs close to TDC. ϕ varies between 0.21 @ 100% H ₂ and 0.27 @ 61% NH ₃	25
5.3	Pressure traces of CVCC for different compositions of diesel-ammonia and diesel-hydrogen with $p_0=21$ bar and $T_0= 535^\circ\text{C}$ (blue) and $T_0= 600^\circ\text{C}$ from Hernández et al. [2022]	26
5.4	Range of injection timing for effective combustion of DME-Ammonia (from Ryu et al. [2014a])	27
5.5	Autoignition and flame propagation after an early injection of n-heptane. From: Zhang et al. [2022]	29
5.6	The obtainable IMEP tapers off as the maximum pressure rise rate increases	31
6.1	CO emissions of a CDF combustion as function of the % _{energy} NH ₃ from Yousefi et al. [2022b]	34
6.2	Emissions for varying H ₂ % and equivalence ratio in a SI engine from Lhuillier et al. [2020]	35

List of Figures

6.3	Ammonia limits in ppm from Class guidelines from MMMCZCS [2023]	35
6.4	NOx and NH ₃ emissions for different CR and ϕ . From Mounaïm-Rousselle et al. [2022]	36
6.5	Soot measurements from Reiter and Kong [2011]	37
7.1	Dual fuel injector of Woodward L'Orange: nozzle and spray arrangement. Image from Frankl et al. [2021]	40
7.2	Details of port fuel injectors of Kuta et al. [2023]	41
8.1	Engine model of Frost et al. [2021] illustrating the zones	44
8.2	Comparison conditions assessment heat transfer models of Broekaert et al. [2015] and HCCI runs Pochet et al. [2020a]	45
9.1	Injection timing of the homogeneous charge hydrogen spark concept	50
9.2	Graphical illustration of the three concepts	51
9.3	Graphical representation of the ignition model and the engine cylinder model with the incorporated Cantera objects and what the objects represent.	53
10.1	Mass fractions of NH ₃ , H ₂ and DME during a stoichiometric constant volume combustion of 72.0 % _e NH ₃ , 19.5 % _e H ₂ , and 8.5 % _e DME with initial conditions of $p = 50$ bar and $T = 944$ K.	56
10.2	Graphical overview of the ignition model with the Cantera object Ideal Gas Reactor and what it represents	57
10.3	Results of Dai et al. [2020] for $\phi = 0.5$, $H_2 = 10\%_{mole}$. The points correspond to experimental measurements, the lines correspond to different chemical kinetic mechanisms: the dashed line for Shrestha et al. [2018] , the dotted lines Mathieu and Petersen [2015] , the dash-dot line Klippenstein et al. [2011] , the solid line to the mechanism of Dai et al. [2020]	62
10.4	Results of the ignition model for NH ₃ /H ₂ mixture with 10% _{mole} H ₂	62
10.5	Measured ignition delay times of NH ₃ and DME mixtures at $p_c=60$ bar and $\phi = 0.5$ Dai et al. [2021]	63
10.6	Results for varying ϕ_0 , $p=50$ bar at different T_{TDC}	65
10.7	Results for varying ϕ_0 , $p=50/60/70$ bar and $T_{TDC}=1150$ K.	66
10.8	Results for varying % _e H ₂ for $p=50$ bar and varying T_{TDC}	67
10.9	Results for varying % _e DME, at $p=50$ bar and varying T_{TDC}	67
11.1	Graphical representation of the engine cylinder model with the incorporated Cantera objects and what the objects represent.	69
11.2	Part of the cycle that is covered by the engine cylinder model	70
11.3	p-V diagrams	71
11.4	Evolution of fuel in the modeling results of Chiera et al. [2022]	75
11.5	Resulting heat release and pressure of Chiera et al. [2022]	77
11.6	Cylinder pressure of the experimental result of Chiera et al. [2022]	77
11.7	Pressure and temperature results of 80% _e NH ₃ and 20% _e H ₂	78
11.8	Results of varying the energy fraction of DME fraction, with a constant energy ratio between NH ₃ /H ₂ of 80/20% _e	79
11.9	Results of varying the energy ratio between NH ₃ and H ₂ , with DME fraction constant at 17.5% _e	80
11.10	Effect on the emissions of varying the energy ratio between NH ₃ and H ₂ , with DME fraction constant at 17.5% _e	81

D.1	Pressure traces for different combinations of LRF and HRF from Hernández et al. [2023]	99
E.1	Spray shapes 1 ms after the start of injection of ammonia, gasoline, and methanol at different conditions. From Pelé et al. [2021]	101
G.1	From Niki [2021b]	105
H.1	Effects of different fuel compositions for two pilot injection timings (black = 45 CAD BTDC, red = 60 CAD BTDC). Graphs from Niki [2021b]	107
N.1	Graphical results of the ignition model	121
O.1	Pressure and temperature	124
O.5	Mass fraction H_2O_2	125

List of Tables

2.1	Literature searches and results	6
3.1	Fuel properties. Superscripts: ^a = Dimitriou and Javaid [2020], ^b = Lesmana et al. [2019], ^c = Hernández et al. [2022], ^d = Kurien and Mittal [2022], ^e Szybist et al. [2014], ^f US Department of Energy [2023]	11
3.2	Comparison between definitions of fuel mixture composition for an ammonia-hydrogen mixture at 323K and 1 bar. Based on Lhuillier et al. [2020].	11
3.3	Overview of equivalent ratios in literature for ammonia and hydrogen in an engine	14
4.1	Comparison test engines Chiera et al. [2022] and AmmoniaDrive	23
9.1	Overview models	53
10.1	Comparison of the properties of this study to the experimental studies	61
11.1	Comparison test engines Chiera et al. [2022] and AmmoniaDrive	75
N.1	Export of set-up and results of the ignition model	122
O.1	Export of set-up and results of the engine cylinder model	123

Acronyms

CI	compression ignition	1
AOG	anode off-gas	1
CVCC	constant volume compression chamber	6
AEA	Ammonia Energy Association	5
DEE	di-ethylether	10
CDF	conventional dual-fuel	19
DI	direct injection	19
ATDC	after top dead center	xiii
BTDC	before top dead center	39
CR	compression ratio	39
CAD	crank angle degree	60
ICE	internal combustion engine	1
HCCI	homogeneous charge compression ignition	v
HRF	high reactivity fuel	10
HVO	hydrotreated vegetable oil	10
EGR	exhaust gas recirculation	26
JCCI	jet controlled compression ignition	2
LFL	lower flammability limit	10
LFS	laminar flame speed	12
LRF	low reactivity fuel	10
LHV	lower heating value	74
MMMCZCS	Mærsk Mc-Kinney Møller Center for Zero Carbon Shipping	5
MRR	maximum pressure rise rate	53
PRR	pressure rise rate	65
PFI	port fuel injection	19
RCCI	reactivity controlled compression ignition	v
TDC	top dead center	52
SOFC	solid oxide fuel cell	1
RCM	rapid compression machine	6
PPCI	partially premixed compression ignition	2
PCCI	premixed charge compression ignition	2
SI	spark ignition	3

List of Tables

SODI start of diesel injection	20
SOC start of combustion	20
UHC unburned hydrocarbons	42

1 Introduction

Outline

This graduation research investigates compression ignition (CI) combustion of ammonia and hydrogen in an internal combustion engine (ICE) within the context of the AmmoniaDrive project. AmmoniaDrive is a NWO-funded research project that aims to decarbonize shipping by introducing an solid oxide fuel cell (SOFC)-ICE power plant for ships and other heavy-duty applications. This power plant is fueled by a single fuel: ammonia [de Vos et al., 2022]. The hydrogen for the combustion in the ICE is supplied by the anode off-gas (AOG) of the fuel cells. This study will focus on a compression ignition ICE concept for the AmmoniaDrive power plant.

Ammonia is a carbon-free fuel, but has unfavorable properties for combustion in an ICE, such as a high heat of vaporization, narrow flammability limits, a high flame quenching distance, low flame speed, and most important: a high autoignition temperature. Those properties have to be overcome and hydrogen, also a carbon-free fuel, is known to be capable of playing a role. As the properties of hydrogen are extremely high combustion speed, very wide flammability limits and a very short flame quenching distance [Hernández et al., 2022]. Unfortunately, the property ammonia and hydrogen have in common, is a relatively high resistance to autoignition. An innovative combustion strategy and/or using a promoter fuel are possible solutions to offset the resistance to autoignition. This research provides an overview of the related state-of-the-art knowledge and investigates CI ICE combustion strategies for NH_3 and H_2 with a modeling study.

1.1 Development

The earliest research concerning ammonia as a fuel for ICEs is war-related. First in Belgium, towards the use of ammonia as a fuel for buses for when carbon-based fuels are scarce [Koch, 1945]. Followed by the U.S. Army, which started investigating the use of ammonia in compression ignition engines after World War II and Korea because 65% of the total tonnage supporting combat operations consisted of fuels and lubricants [Pearsall and Garabedian, 1967]. The U.S. Army was interested in fuels that could be produced on-site, with power supplied by a nuclear power generator. Their objective was to use ammonia in slightly adapted diesel engines. Unfortunately, this has not reached the required level of technology readiness to be implemented, but the research and experiments conducted form a foundation for current research.

Later, ammonia regained attention due to its potential to decrease the worldwide emission of greenhouse gases by ICEs. In 2008, experimental research was published on the compression ignition of ammonia. Reiter and Kong [2008] successfully demonstrated a dual-fuel CI engine operation with ammonia and diesel. This dual-fuel CI technology with ammonia and a carbon-based fuel is currently being developed by engine manufacturers for commercial application (MAN Energy Solutions [2019]; Wärtsilä [2020]).

1 Introduction

However, when a carbon-based fuel is used to combust ammonia, carbon dioxide will be formed. Therefore, the challenge is a net-zero carbon ICE. One potential way to achieve this, is combusting ammonia and hydrogen. There are several combustion mechanisms to combust ammonia and hydrogen in an ICE. The first distinction is whether it is spark ignited (SI) or compression ignited (CI). This research focuses on CI.

Focusing on CI, several forms can be distinguished such as HCCI, partially premixed compression ignition (PPCI), premixed charge compression ignition (PCCI), jet controlled compression ignition (JCCI), and RCCI.

The current state-of-the-art of experimental research towards compression ignition of ammonia has been done by Chiera et al. [2022], Pochet et al. [2020a] and Jin et al. [2023]. Chiera et al. developed a successful RCCI combustion strategy with ammonia and diesel, achieving an 81%_{energy} NH₃, however still 19%_{energy} of diesel was required. Pochet et al. achieved a carbon-free HCCI combustion of ammonia and hydrogen, but this required a compression ratio of 22. Jin et al. investigated a PPCI up to 85%_{energy} NH₃, but the lowest GHG emissions were achieved at 50%_{energy} NH₃.

Building on their concepts, this research further explores compression ignition concepts for ammonia and hydrogen, and optionally a carbon-based promoter fuel. The goals are a high percentage of ammonia, low emissions, and feasible engine parameters such as a not too high compression ratio or air intake temperature.

1.2 Motivation for this study

The driving force behind research towards alternative fuels is to lower the harmful emissions of ICEs. Within the realm of alternative fuels, the search continues towards the lowest emissions and good engine performance while combusting a feasible fuel. "Feasible" is a broad concept in this case, in a cargo ship for example, there should be space for payload after the tanks have been put in, and the fuel costs also have to be economically feasible. This research focuses on engine performance, as the operating window of ammonia in CI ICE is still limited.

1.3 Broader perspective

Ammonia is gaining attention throughout society from numerous perspectives. The perspectives originate from a variety of parties involved, for example, citizens, research institutes, fuel suppliers, engine operators, engine manufacturers, transport companies, class societies, insurance companies, legislators and governments, and environmental protection agencies. One of those environmental protection agencies is the DMCR.

The DCMR composes the environmental regulations for companies and monitors the compliance with them in the Rijnmond region, which includes the port of Rotterdam. They have recently stated that the port of Rotterdam is not prepared yet for a transition towards ammonia. The agency has several safety concerns regarding the storage and transportation of ammonia, as well as the uncoordinated approach of the transition towards ammonia [NRC, 2023].

That the transition towards ammonia as a fuel for transportation has started, can be seen from the concrete preparation, for example, by Hy2Gen Inc Canada. They are currently building a green ammonia production facility which is scheduled to be operational in 2026. It will be powered by hydro-electricity and produce 173,000 MT of green ammonia per year [Hy2Gen Inc Canada, 2023]. The DCMR and H2Gen Inc Canada are merely two examples of many that can be found in various media.

1.4 Scope

The scope of this research is set by the AmmoniaDrive project and is limited by graduation project constraints such as available time and experience. This graduation research investigates compression ignition combustion strategies of ammonia, hydrogen, and a carbon-based fuel if necessary. Other research within the AmmoniaDrive project will investigate different ignition strategies, such as spark ignition (SI).

Scope

- 4-stroke engine
- Compression ignition
- Pure ammonia via port fuel injection (PFI)
- Hydrogen via direct injection (DI)
- Optional carbon-based promoter fuel as a promoter fuel via DI

1.5 Content

This study consists of two parts; a literature research and modeling study. The literature part provides an overview of the related state-of-the-art knowledge related to compression ignition of ammonia and hydrogen. It is concluded by potential new compression ignition combustion concepts for ammonia and hydrogen. The second part is a modeling study of the compression ignition combustion of ammonia and hydrogen with and without DME in the AmmoniaDrive test engine.

The literature study consists of eight chapters. First, an overview of the available knowledge is given in chapter 2, followed by the literature study results, which are spread out over chapters 3 to 8. The topics are shown in [Figure 1.1](#). For the readers interested in the research questions for literature study, those are listed in [Appendix A](#). The research questions of the thesis are listed in [Appendix B](#).

Chapters 3 and 8 have an appendix covering some relevant theoretical background knowledge. This is intended to improve the understanding of the literature, without clogging the report.

The literature research is concluded in [chapter 9](#) with several new combustion concepts and the strategy to investigate CI combustion concepts in this research.

The investigation of the compression ignition starts with [chapter 10](#), in this chapter the ignition properties of a mixture of ammonia, hydrogen, and optionally DME is investigated. The results of this ignition study are then used in [chapter 11](#) to create insight into what to expect of compression ignition combustion within the AmmoniaDrive test engine.

1.6 AmmoniaDrive Research Project

The AmmoniaDrive project forms the context for the thesis, and therefore the available literature will be viewed through the lens of AmmoniaDrive. This is applied, for example, when investigating compression ratio's, power output or cylinder bores used in other research. The

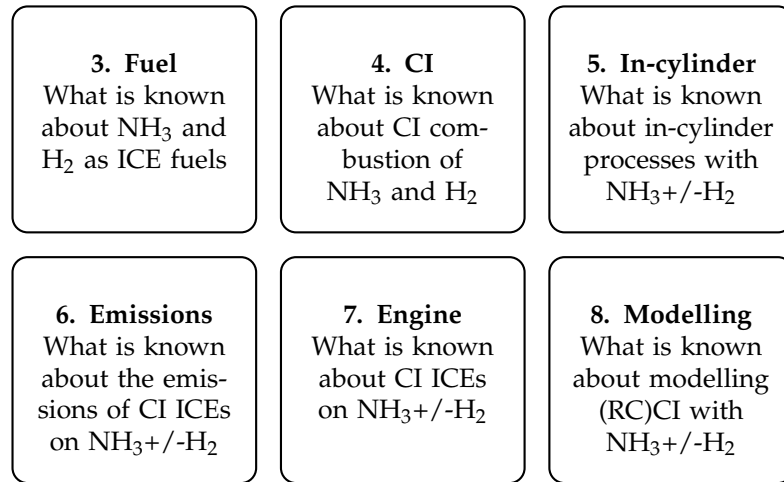


Figure 1.1: Overview literature study results in chapters 3-8

test motor available within AmmoniaDrive has the following properties, based on the provided specification sheet of the S6R2-T2MPTK marine diesel engine;

- 4-stroke
- Bore 170 mm
- Stroke 180 mm
- 1 cylinder
- Compression ratio 14
 - Somewhat variable
- Power output in diesel mode ≈ 90 kW/cylinder

1.6.1 Case study W12V31

A case study has been conducted by [de Vos \[2022\]](#) for the AmmoniaDrive project, based on the Wärtsilä 31 W12V31. The ammonia ICE considered in the case study has the following properties:

- 4-stroke
- 7320 kW
- 750 rpm
- 12 cylinders
- Bore 310 mm
- Stroke 430 mm
- Firing frequency $75 \frac{1}{s}$
- Engine efficiency 0.45 [–]
- 80% load contribution of NH₃
- 20% load contribution of H₂
- Fuel composition
 - Molar fractions: 75% NH₃, 25% H₂
 - Mass fractions: 96% NH₃, 4% H₂

The W12V31 fueled by diesel is estimated to have an engine efficiency of 0.48. This lower efficiency of 0.45 is to allow for a lower combustion efficiency when fueled by ammonia.

2 Available research

Outline

This chapter gives an overview of the available knowledge, related or relatable to the CI combustion of ammonia, hydrogen, and if necessary a promoter fuel.

The scientific literature searches are conducted in Scopus. An overview of the literature searches can be seen in [Table 2.1](#). An overview of relevant experimental studies and their properties is listed in [Appendix C](#).

There is also valuable knowledge outside the scientific community. Some non-scientific research is described in the last section. Institutes conducting research towards ammonia as fuel for shipping are, amongst others, the Mærsk Mc-Kinney Møller Center for Zero Carbon Shipping (MMMCZCS), Ammonia Energy Association (AEA) and the International Maritime Organization (IMO).

2.1 Scientific publications

The literature research started with studying the literature closest to the topic and scope of this research, this related to searches with ID # 1 to 3 in [Table 2.1](#). Then the literature search was expanded to literature searches 4-6 in [Table 2.1](#). There is no age limit set on the literature, as the foundational work done by Gray, Pearsall and Starkman contains valuable experimental work ([Gray et al. \[1966\]](#); [Pearsall and Garabedian \[1967\]](#); [Starkman et al. \[1967\]](#)).

2.1.1 Experimental research

Characteristics of experimental studies are investigated to acquire an initial idea of experiment and engine parameters. An overview of experimental studies and their properties is listed in [Appendix C](#). It is limited to studies in which more than 40%_{energy} ammonia is combusted. The overview is not limited to experiments with solely ammonia and hydrogen, as that number is minimal. The listed properties are:

- Fuel(s)
- % of fuel component
- Combustion mechanism
- Type of machine or engine
- Compression ratio
- Engine speed
- Bore
- Power
- Emissions

The power of the experimental engines is not always provided. In some cases, the power could be calculated from the BMEP, other publications allowed for an educated guess, and for some there was no hint. When it was not provided in the publication and deduced from available data, this is clearly stated in [Appendix C](#).

ID #	Search criteria	Results
<i>First selection</i>		
1	TITLE-ABS-KEY(("reactivity controlled compression ignition" OR RCCI) AND ammonia AND hydrogen)	0
2	TITLE-ABS-KEY(("reactivity controlled compression ignition" OR RCCI) AND ammonia)	6
3	TITLE-ABS-KEY("compression ignition" AND hydrogen AND ammonia) AND (LIMIT-TO(LANGUAGE, "English"))	29
4	TITLE-ABS-KEY("compression ignition" AND ammonia) AND (LIMIT-TO(EXACTKEYWORD, "Ammonia")) AND (LIMIT-TO(LANGUAGE, "English"))	74
5	TITLE-ABS-KEY(ammonia AND hydrogen AND combustion AND engine) AND (LIMIT-TO(DOCTYPE, "ar")) AND (LIMIT-TO(LANGUAGE, "English")) AND (LIMIT-TO(SUBJAREA, "ENER") OR LIMIT-TO(SUBJAREA, "ENGI"))	125
6	TITLE-ABS-KEY(ammonia AND hydrogen AND ignition) AND (LIMIT-TO(SUBJAREA, "ENER") OR LIMIT-TO(SUBJAREA, "ENGI")) AND (LIMIT-TO(LANGUAGE, "English"))	188
Total number of results without duplicates		321

Table 2.1: Literature searches and results

In the appendix, it can be observed that most of the experimental work is done at low power per cylinder. The majority are below 5 kW/cyl, only [Chiera et al. \[2022\]](#) (+- 80 kW/cyl) and [Reiter and Kong \[2011\]](#) (40 kW/cyl) have investigated higher power outputs.

Comparing the bores of the experimental engines to the test engine of AmmoniaDrive, it can be observed that the AmmoniaDrive test engine has a larger bore (170 mm) than all other experimental engines, except for the engine used by [Chiera et al. \[2022\]](#) which also has a bore of 170 mm.

Type of machine or engine

Different machines and engines are used to investigate combustion. The most encountered are a single-cylinder 2 or 4-stroke, a constant volume compression chamber (CVCC) and a rapid compression machine (RCM).

A CVCC is a machine which operates with a constant volume to investigate properties of fuels such as autoignition, a vital property for compression ignition. It is less influenced by variations from cycle-to-cycle and decreases non-fuel effects [[Hernández et al., 2022](#)].

A RCM can be used to investigate the behavior of a fuel in a compression stroke because, in contrast to a CVCC, it mimics the compression stroke.

2.1.2 Numerical research

The following characteristics of numerical studies are investigated to create an overview of which models, theory, and software are used to investigate the combustion of ammonia and hydrogen.

- Model type

- Theory in the model
- Software used

2.2 Research locations

Experimental research on ammonia CI combustion mechanisms has been published by institutes around the world. The institutes, their research, and locations are marked in [Figure 2.1](#). More details on the studies can be found in [Appendix C](#).

A new research consortium is *MarINH3*, led by Nottingham University. They will be investigating ammonia as a fuel for the long-haul shipping [*IMarEST Marine Professional, 2023*]. As there is no published research yet, this consortium is not indicated on the map.

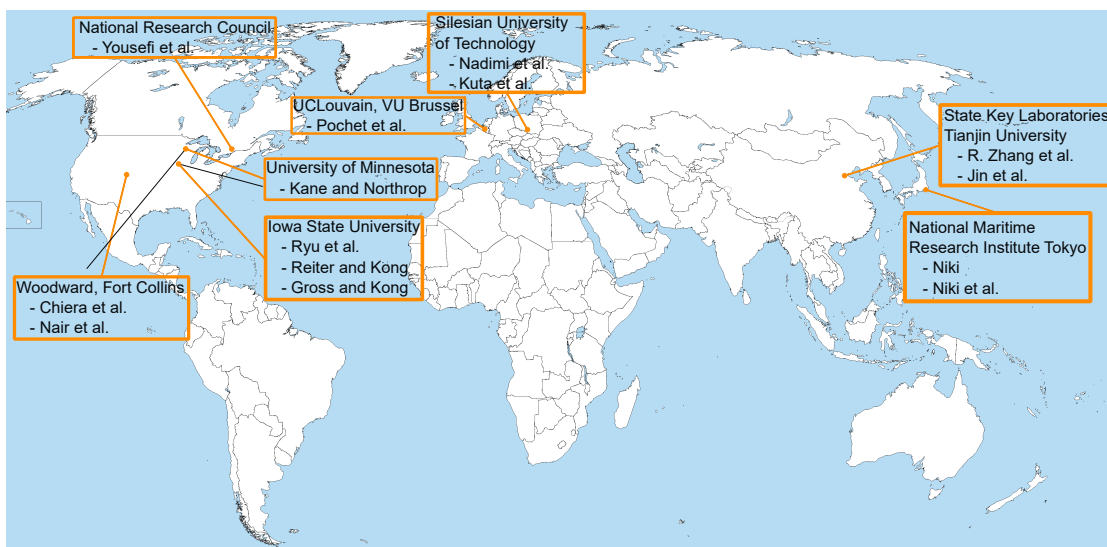


Figure 2.1: Locations where ammonia combustion via a CI mechanism are or have been experimentally investigated

2.3 Non-scientific research

The *MMMCZCS* is a not-for-profit, independent research institute focusing on accomplishing a net-zero maritime industry. They view ammonia as a potential fuel to achieve this. Contributions from the *MMMCZCS* are, for example, a report on “Managing Emissions from Ammonia-Fueled Vessels” which is used in [chapter 6](#) [*MMMCZCS, 2023*].

The *AEA* is a non-profit industry association, which includes 165 corporations. They organize conferences and events, as well as sharing articles and papers related to the sustainable use of ammonia [*AEA, 2023*].

The IMO is responsible for the safety of shipping, and the prevention of marine and atmospheric pollution by shipping. The IMO has a strategy to decrease the GHG emissions from shipping. The so-called “Initial Strategy” was established in 2008 and will be revised this year, 2023. The 2008-version has a target of 50% reduction of the GHG emissions by 2050 and a 70% reduction of CO₂ emissions per transport work compared to 2008 [*IMO, 2023*].

2 Available research

Key points

- There is no literature available on [RCCI](#) combustion of ammonia and hydrogen, and only 6 search results on [RCCI](#) and ammonia.
- There is limited experimental research on the compression ignition combustion of ammonia & hydrogen.
- The power output of experimental [CI ICE](#) fueled by ammonia is low.

3 Fuel

Outline

The scope of this literature research is limited to two fuel options. The first consists of ammonia and hydrogen and the second to a promoter fuel, ammonia, and hydrogen. This chapter describes the fuel properties related to ICEs and identifies knowledge gaps of fuel properties under engine conditions. It is not limited to the behavior in a CI engine, and therefore properties such as flame speed are also discussed. Background knowledge for this chapter can be found in [Appendix F](#).

3.1 Ammonia

Ammonia is often described as 'blue ammonia', 'e-ammonia', or 'gray ammonia'. Blue ammonia refers to ammonia produced with hydrogen originating from conventional methane reforming, where the carbon dioxide is captured. E-ammonia, or electro-ammonia, is produced with hydrogen from the electrolysis of water, powered by renewable energy. Lastly, gray ammonia is produced similarly to blue ammonia, but without carbon capture and is not considered a sustainable fuel [MMMCZCS, 2023].

Ammonia can be employed as pure ammonia or as aqueous ammonia. An important consideration, in both cases, is the effect on the in-cylinder temperature. Pure ammonia has a high heat of vaporization compared to diesel. This reduces the in-cylinder temperature when liquid ammonia is injected and transitions from liquid to gas. The temperature reduction will be larger when additional water is injected.

A beneficial property of ammonia is the relatively low viscosity, this supports the fuel atomization and droplet formation [Kurien and Mittal, 2022]. The viscosity will also affect the turbulence in the fuel flow and spray formation [Lesmana et al., 2019]. Several relevant fuel properties are listed in [Table 3.1](#). Noticeable is the high latent heat of vaporization of ammonia.

As mentioned and can be seen from [Table 3.1](#), ammonia has a long quenching distance. This is likely to cause more incomplete combustion in crevices regions.

3.1.1 Aqueous ammonia

Aqueous ammonia is ammonia dissolved in water to ease the storage and improve safety [Schönborn, 2021]. The safety improves because mixing ammonia with water allows the fuel to be stored at atmospheric pressure while staying liquid. Pure ammonia either requires pressurization to stay liquid (0.43 MPa at 0°C) or cryogenic storage at -35°C. The ignition of aqueous ammonia compared to pure ammonia has been investigated by Schönborn [2021] with a single-zone zero-dimensional model of a 2-stroke engine. The mixture composition of aqueous ammonia was 75%_m water and 25%_m ammonia. They concluded that the ignition of aqueous ammonia required a higher compression ratio than pure ammonia, 24.8 and 26.7 respectively.

A disadvantage of aqueous ammonia is the increase in tank volume, as a 75/25 ratio would result in a four times higher tank volume. When viewing [Table 3.1](#), it can be seen that pure

ammonia already requires a more than three times larger tank than diesel, based on energy density.

3.2 Hydrogen

Hydrogen has good combustion properties, such as a high flame speed and high flame temperature. A remarkable phenomenon about the lower flammability limit (LFL) of hydrogen is the slight narrowing by increasing the pressure [Law, 2006]. The flammability limits of hydrogen vary from an equivalence ratio of 0.1 to 7.1 [Kumar et al., 2015].

Lhuillier et al. [2020] investigated a SI engine fueled with premixed ammonia, hydrogen, and air. Their results indicate that hydrogen was mainly beneficial for the early stage of the combustion.

3.2.1 Ringing

Ringing is a high pitch sound coming from the cylinder. This sound is caused by high-amplitude pressure oscillations generated by the combustion. Combusting hydrogen is known to have a high tendency to induce ringing. Avoiding high intensity ringing is important because it causes an increase in heat loss to the cylinder wall [Pochet et al., 2020a].

3.3 The HRF, promoter, or pilot fuel

The third fuel is the high reactivity fuel (HRF), promoter, or pilot fuel depending on the combustion concept. The reactivity of a fuel is determined by its cetane number, a higher cetane number corresponds to a more reactive fuel.

There have been a few studies towards a RCCI combustion of ammonia with high-reactivity fuels such as diesel [Chiera et al., 2022], n-heptane [Zhang et al., 2022], DME, and di-ethylether (DEE) [Frost et al., 2021]. Frost et al. attempted to blend DEE with aqueous ammonia to obtain autoignition of ammonia without using a pilot fuel, however, this was unsuccessful.

Hernández et al. [2023] investigated different combinations of HRF's and low reactivity fuel (LRF)'s in a CVCC. Ammonia and hydrogen were both considered as an LRF. The results of Hernandez et al. are shown in Appendix D. From their results, it seems that hydrotreated vegetable oil (HVO) could be a more suitable HRF or pilot fuel than diesel. HVO has a higher cetane number than diesel.

3.4 Fuel mixture

Fuel fractions can be expressed in terms of energy, mass, or volume fractions. Table 3.2 contains an example of an ammonia-hydrogen mixture described by percentages based on volume ($\%_{vol}$), energy ($\%_{en}$), and mass ($\%_{m}$).

Several studies have investigated the effect of adding hydrogen to ammonia to improve the combustion. Pochet et al. [2019] concluded based on ignition delay measurements in an RCM that the hydrogen addition has to be more than $10\%_{vol}$ to promote ammonia combustion sufficiently.

Dinesh et al. [2022] studied a spark ignited engine and indicated that the best compromise was $21\%_{en}$ hydrogen. Lhuillier et al. [2020] came to a similar result for a SI engine, namely $20\%_{vol}$ hydrogen.

Property	Ammonia	Hydrogen	Hydrogen	Diesel	DME
Storage method	Compr liquid ^a	Compr liquid ^a	Compr gas ^a	Liquid ^a	Compr liquid ^e
Storage temperature [K]	298 ^a	20 ^a	298 ^a	298 ^a	T _{ambient} ^e
Storage pressure [MPa]	1.03 ^a	0.1 ^a	24.8 ^a	0.10 ^a	0.5 ^e
Mass density [kg/m ³]	602.8 ^a	71.1 ^a	17.5 ^a	838.8 ^a	667 ^d
Energy density [MJ/m ³]	11300 ^a	8539 ^a	2101 ^a	36403 ^a	
Stoichiometric fuel/air ratio	1/6.05 ^c	1/34.33 ^c	1/34.33 ^c	1/17.41 ^c	1/9.0 ^e
LHV [MJ/kg _{fuel}]	18.5 ^b	120 ^b	120 ^b	42.5 ^b	27.6 ^b
LHV _{st} [MJ/kg _{stoich}]	2.62 ^b	2.71 ^b	2.71 ^b	2.74 ^b	2.65 ^b
Flammability limits gas in air (% _{vol})	16-25 ^a	4-75 ^a	4-75 ^a	0.6-7.5 ^a	3.4-18.6 ^e
Latent heat of vaporization (kJ/kg)	1370 ^b	445.6 ^b	-	270 ^b	467 ^b
Autoignition temperature [K]	924 ^a	884 ^a	884 ^a	503 ^a	508 ^e
LBV at $\phi = 1$ [m/s]	0.07 ^d	3.51 ^d	3.51 ^d	0.86 ^d	0.42 ^f
Quenching distance [mm] at $\phi = 1$	7	0.6	0.6		
Octane number [RON]	110 ^a -130 ^d	> 130 ^a	> 130 ^a	-	-
Cetane number [-]	-	-	-	40-50 ^b	> 55 ^e

Table 3.1: Fuel properties. Superscripts: ^a = Dimitriou and Javaid [2020], ^b = Lesmana et al. [2019], ^c = Hernández et al. [2022], ^d = Kurien and Mittal [2022], ^e Szybist et al. [2014], ^f US Department of Energy [2023]

Component	% _{vol}	% _{en}	% _m
H ₂	20	18	5
NH ₃	80	82	95

Table 3.2: Comparison between definitions of fuel mixture composition for an ammonia-hydrogen mixture at 323K and 1 bar. Based on Lhuillier et al. [2020].

3 Fuel

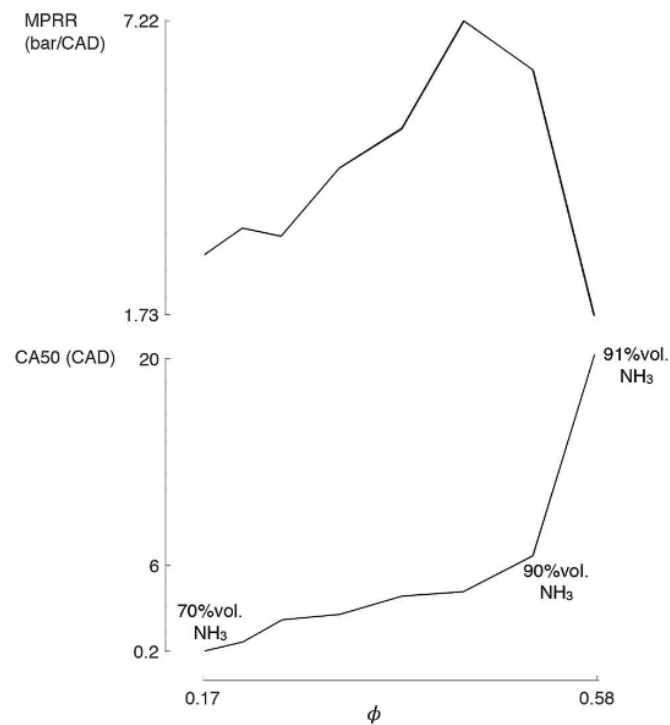


Figure 3.1: The maximum pressure rise rate (MPRR) and CA50 for a constant intake temperature and hydrogen flow rate, while increasing the ammonia flow rate. From Pochet et al. [2020a]

Pochet et al. [2017b] achieved stable combustion with a HCCI ICE up to 70%_{vol} ammonia and 30%_{vol}. In later research, Pochet et al. [2020a], they achieved combustion until 91%. However, an important observation was made regarding the combustion promoting effect of hydrogen. It seems to steeply decline at a certain threshold, based on the operating pressure and temperature. Their experimental results with the clear decline in the combustion promoting effect are shown in Figure 3.1.

3.5 Equivalence ratio

Shrestha et al. [2021] studied the laminar flame speed (LFS) at different equivalence ratios.¹ The highest LFS was found around an equivalence ratio of 1.1, as can be seen in Figure 3.2. When the result of Shrestha et al. is compared to successful ammonia-hydrogen engine experiments described in the literature, there is some variation. Pochet et al. [2017b] achieved stable combustion of 70%_{vol} NH₃ with an equivalence ratio of 0.28, an intake pressure 1.5 bar and intake temperature of 473 K. Pochet et al. also studied the combustion duration as a function of

¹Flame speed is often not a relevant fuel property for compression ignition combustion. However, with a conventional dual fuel (CDF) CI combustion, flame speed is relevant. In CDF the diesel autoignites in a mixture of ammonia and air. The ammonia is then ignited by the diesel, but due to the limited flame propagation in the ammonia rich zone, the combustion stagnates after the diesel rich zone has burned. CDF will be discussed further in the next chapter.

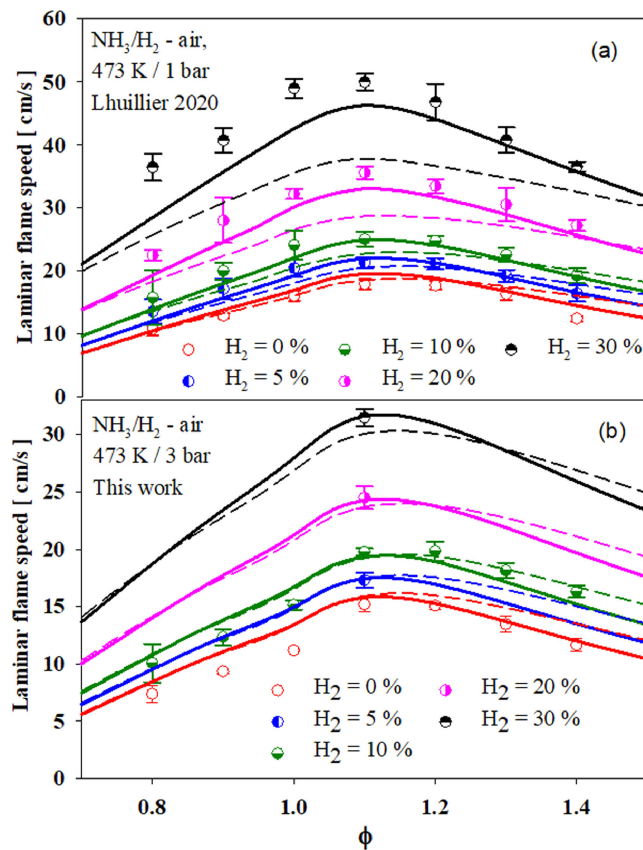


Figure 3.2: Laminar flame speeds of $\text{NH}_3/\text{H}_2/\text{air}$ at 473K and 1/3 at varying H_2 content. (Symbols: measurements from Lhuillier et al. [2020] and Shrestha et al. [2021]. Dashed lines: model from Shrestha et al. [2018], solid lines: Shrestha et al. [2021]. Figure from Shrestha et al. [2021])

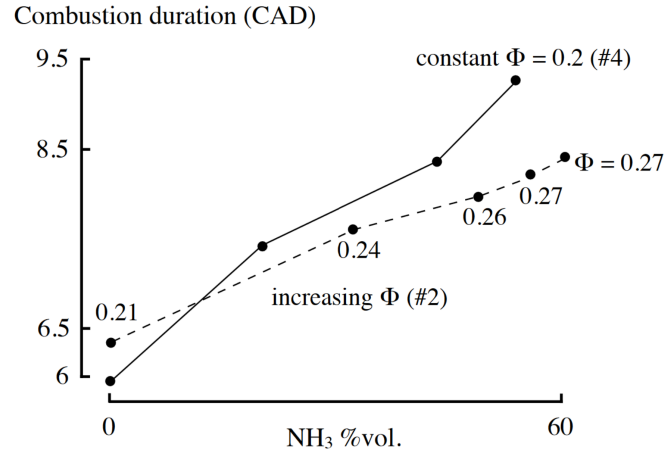
the NH_3 % and the equivalence ratio. The results are shown in Figure 3.3. The same trend can be observed as expected by the results of Shrestha et al., a higher ϕ leads to a short combustion duration.

To create a more comprehensive overview, the equivalence ratio's for the combustion of ammonia and hydrogen in an ICE available in literature, are summarized in Table 3.3.

3.6 Autoignition

Hernández et al. [2022] investigated the effect of partially substituting diesel by ammonia, hydrogen, or methane on the autoignition. A two-stage autoignition was observed, consisting of cool flames and main combustion in all their cases. And it was concluded that the cool flame timing and intensity appears to be dominated by the diesel.

Liu et al. [2022] researched the use of ammonia in a compression ignition engine. The authors investigated the addition of ammonium nitrite and the addition of hydrogen to lower the conditions for autoignition. The addition of hydrogen was not enough to accomplish

Figure 3.3: Combustion duration as a function of the NH₃ % and ϕ

Source	Sim/exp	Ignition	Fuel%	ϕ	Observations
Meng et al. [2023]	Both	PCJII	100% NH ₃	1.1 / 0.65	Pre-chamber jet induced ignition. In the pre-chamber $\phi=1.1$ and in the main chamber $\phi=0.65$
Mounaïm-Rousselle et al. [2022]	Both	SI	100% NH ₃	0.9-1-1.1	SACI is SI with a high compression ratio
Zhang et al. [2022]	RCCI	Exp	50/50 and 70/30 % _{en} NH ₃ /n-heptane	0.89 and 0.87	
Pochet et al. [2017b]	Exp	HCCI	69% _{vol} NH ₃ , 31% _{vol} H ₂	0.28	
Pochet et al. [2017a]	Sim	HCCI	100% NH ₃	0.2-0.4	

Table 3.3: Overview of equivalent ratios in literature for ammonia and hydrogen in an engine

compression ignition.

In experiments done by Frankl et al. [2021], although without ammonia present due to safety reasons, it is observed that the direct injected hydrogen combusts almost instantly when it enters the combustion chamber.

Schönborn [2021] also describes modelling the compression ratio of 23 where the hydrogen combusts but not the ammonia. It may be likely that the flame propagates from the hydrogen to the ammonia and initiates the combustion.

3.6.1 Ignition delay time

Dai et al. [2020] experimentally investigated the autoignition behavior of ammonia with and without hydrogen in an RCM, varying the equivalence ratio from 0.5 to 3.0, pressures from 20 to 75 bar, temperatures from 1040 to 1210 K. The hydrogen addition was 10% at most. Their results indicate that the ignition delay time of NH₃ increases with the equivalence ratio, which can be seen in Figure 3.4.

Similar results to Dai et al. are observed in experiments conducted by Liao et al. [2022]. Their experiments also included 25% hydrogen, which further decreased the autoignition temperature of the mixture. Their experiments, also in an RCM, were conducted under 30 bar and the lowest autoignition temperature was found to be 950 K with 25% hydrogen.

Hernández et al. [2022] investigated the effect of substituting diesel by hydrogen, ammonia, and methane on the autoignition process. The tests were conducted in a CVCC with different temperatures (535-650 °C) and pressures (11-21 bar). Their results indicate that the ignition is delayed by ammonia, hydrogen, and methane. The authors distinguish between the main ignition delay (ID_M) and the cool flames ignition (ID_{CF}). The authors also established an estimation of the main ignition delay time (ID_M) as a function of the energy replacement (E_{LRF}), shown in Equation 3.1. The parameters, A, b, d, e and E_a, in Equation 3.1 are fitting parameters and listed in Table 5 in Hernández et al. [2022]. This equation could be used to compare with the outcomes of the modeling study.

$$ID_M = A * p_0^b * F_r^d * (1 - E_{LRF})^e * \exp\left(-\frac{E_a}{R * T_0}\right) \quad (3.1)$$

3.7 Flame speed

Shrestha et al. [2021] studied the LFS of ammonia and hydrogen mixtures from 1-10 bar and 298-473 K with a CVCC and simulations. The highest LFS was obtained at an equivalence ratio of 1.1. The results of Shrestha et al. are shown in Figure 3.5.

In an ICE there is a turbulent flame. The turbulent flame speed of an ammonia and hydrogen mixture has been investigated by Zitouni et al. [2022]. Their results show an exponential increase in flame propagation speed with increasing hydrogen % and an increasing ratio between turbulent and laminar flame speed with increasing turbulence.

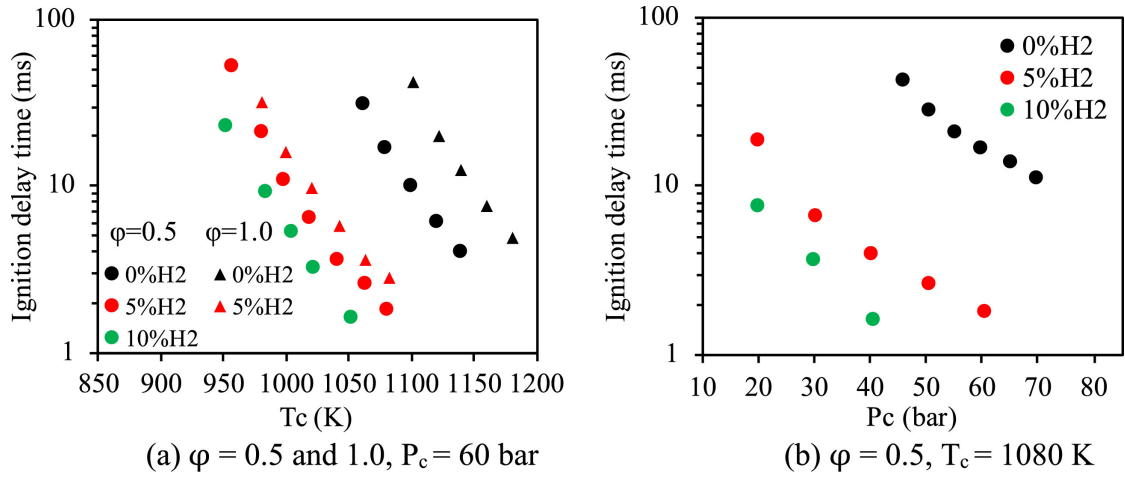


Figure 3.4: From Dai et al. [2020]: Effect of hydrogen on the ignition delay time at different equivalence ratio's. (a) isobars, (b) isotherms.

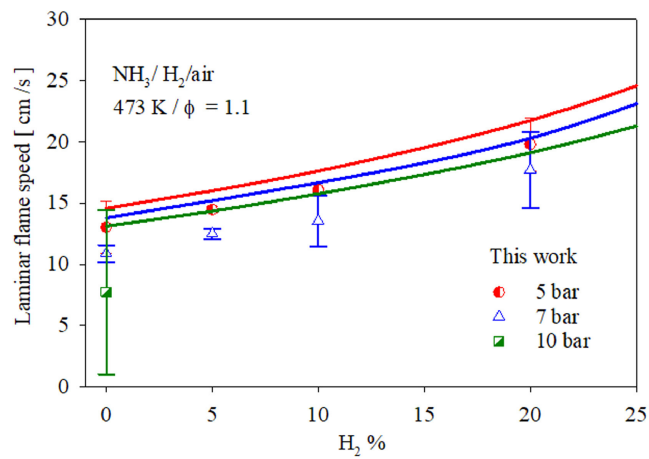


Figure 3.5: Laminar flame speed of NH₃/H₂/air mixtures at 473K, $\phi=1.1$ and 5–10 bar. Symbols: measurements. Lines: simulations. From Shrestha et al. [2021]

Key points

- 70%_{vol} ammonia and 30%_{vol} hydrogen has been successfully experimentally achieved with HCCI
- There is a threshold in the mixture ratio of ammonia/hydrogen where the ammonia combustion promotion by hydrogen steeply declines. The value of this threshold depends on the operating conditions.
- Hydrogen is not considered an [HRF](#).
- HVO seems a more suitable [HRF](#) than conventional diesel.

4 Combustion strategies

Outline

The feasibility of combusting ammonia and hydrogen via a compression ignition combustion mechanism is explored in this literature study. Before an assessment of the feasibility can be made, it should be clear which varieties there are within compression ignition. That is the objective of this chapter. The combustion mechanisms defined in this chapter correspond to the combustion mechanisms in [Appendix C](#).

Experimentally achieved CI of ammonia in literature is found in several studies, an overview is listed in [Appendix C](#). The dual-fuel CI strategies encountered are;

- Conventional dual-fuel (CDF)
- Partially premixed compression ignition (PPCI)
- Premixed charge compression ignition (PCCI)
- Homogeneous charge compression ignition (HCCI)
- Reactivity controlled compression ignition (RCCI)
- Other mechanisms such as SACI and JCCI

Spark assisted compression ignition (SACI) does not qualify as compression ignition, as a spark is used to ignite the fuel mixture.

4.1 Conventional Dual-Fuel

The conventional dual-fuel (CDF) combustion strategy is the most encountered strategy within ammonia combustion via compression ignition. In this strategy, the ammonia is injected early in the compression stroke via port fuel injection (PFI), mixes with the air and close to TDC, diesel is injected via direct injection (DI). The diesel ignites shortly after injection. The ammonia combustion relies on the diesel combustion and cannot firmly propagate a flame after being ignited, according to CFD research conducted by [Chiera et al. \[2022\]](#).

Chiera et al. also concluded that this combustion strategy cannot achieve more than 50%_{vol}. It is hampered by the limited flame propagation within the ammonia and the decrease in turbulence when there is less diesel injected. The conclusion of [Chiera et al. \[2022\]](#) is supported by [Reiter and Kong \[2008\]](#), [Reiter and Kong \[2011\]](#).

Reiter et al. experimentally investigated an ammonia-diesel dual-fuel combustion and compared the emissions and performance to a conventional diesel. Their findings show that above 40-60%_{en} did not lead to further reductions in GHG emissions.

CDF combustion is also experimentally investigated by [Nadimi et al. \[2023\]](#). Nadimi et al. achieved an 84.4%_{en}, however, above 61.6%_{en} the coefficient of variation of the maximum

4 Combustion strategies

pressure, and of the IMEP indicate that the combustion became unstable. Therefore, it can be concluded that Nadimi et al. successfully combusted 61.6%_{en} NH₃.

Yousefi et al. [2022b] investigated the effect of shifting the start of diesel injection (SODI) on the combustion of ammonia. When the SODI is -14.2 CAD ATDC, the combustion resembles a CDF combustion, however, when the SODI is -24 CAD ATDC, it starts to show characteristics of a partially premixed compression ignition (PPCI). This can be seen from Figure 4.1, as the SODI is 10 CAD earlier, the start of combustion (SOC) is not delayed by 10 CAD, this indicates that there is time available to partially mix before the autoignition.

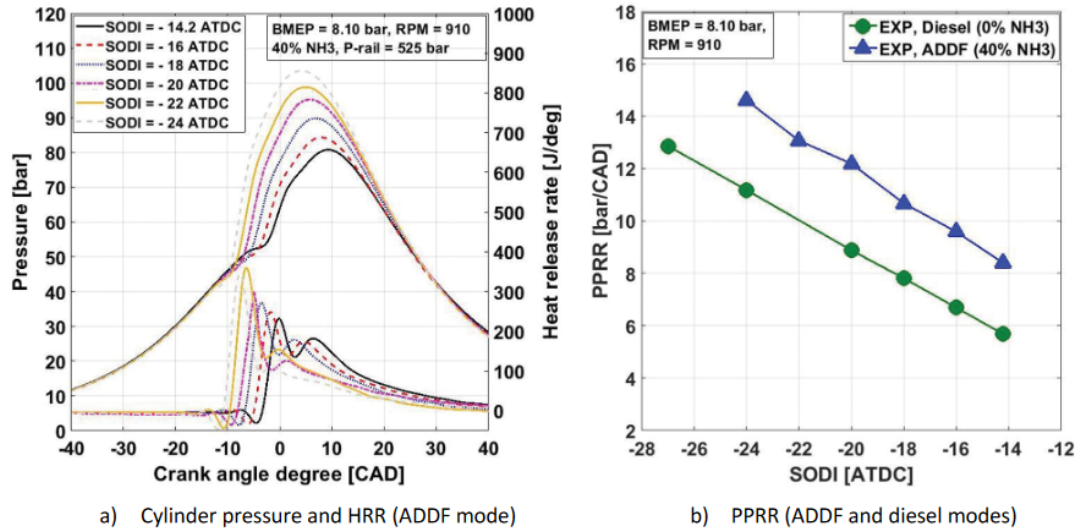


Figure 4.1: Measured cylinder pressure and HRR by Yousefi et al. [2022b]

4.2 HCCI

In an HCCI combustion concept, all fuel is mixed homogeneously with the oxidizer in the combustion chamber before autoignition occurs. The HRR and needle lift of an HCCI combustion is shown in Figure 4.2. There is early injection of the fuel(s) and this allows the fuel(s) and oxidizer to mix to homogeneous mixture before the start of combustion. As a result, the combustion will mainly consist of a premixed combustion phase and less of a diffusion combustion phase. To ensure a homogeneous mixture is formed, a plenum can be used to premix the fuel(s) and oxidizer, as done by Pochet et al. [2017b] with ammonia and hydrogen.

HCCI combustion concepts experience difficulties with combustion phasing and high rates of pressure rise at high loads. And for the HCCI combustion of ammonia and hydrogen, a high compression ratio and high air-intake temperature is required for high percentages of ammonia.

The HCCI combustion of ammonia and hydrogen has been extensively researched by Maxime Pochet (Pochet et al. [2017b]; Pochet et al. [2019]; Pochet et al. [2020a]). They concluded that selecting the blending ratio of ammonia and hydrogen is a practical and quick way to control the load and combustion timing. Although it is not “reactivity controlled” because there is no difference in the autoignition point, it shows great resemblance to it. Their results are shown in Figure 4.3 and more (engine) details are listed in Appendix C.

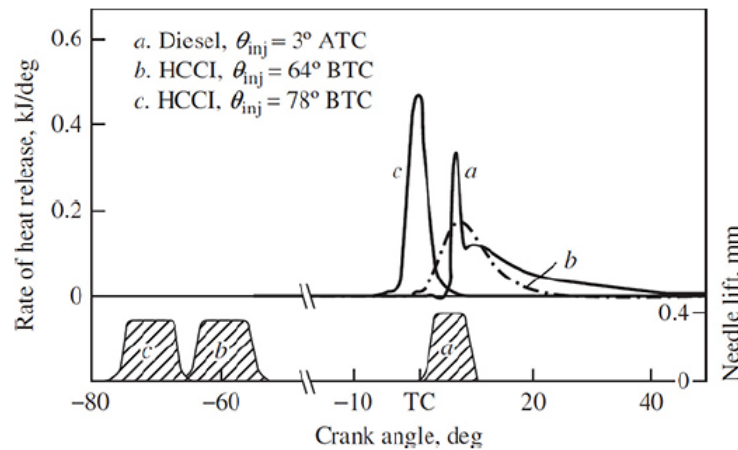


Figure 4.2: Heat release rate and needle lift for a conventional diesel combustion and two HCCI combustion processes (from Heywood [2018])

Ryu et al. [2014b] investigated an HCCI combustion of ammonia and dimethyl ether (DEE). Details of this study are listed in Appendix C.

4.3 Partially & premixed charge compression ignition

PCCI is similar to HCCI, but the fuel is not homogeneously mixed. PPCI is similar to PCCI, but has a second, later injection. This allows for more control on the combustion process. The second injection is typically of higher pressure. In research by Yousefi et al. [2022a], the effect of a split diesel injection is investigated. Two optimum points are identified, in both points 40% of the diesel is injected at 57 CAD BTDC and the remainder is injected at either 16 CAD BTDC or 20 CAD BTDC.

PCCI and PPCI experience difficulties with combustion phasing and are limited at high loads due to high rates of pressure rise.

4.4 RCCI

The RCCI concept is based on varying the mixture composition of two fuels with different autoignition properties. This controls the ignition delay, combustion phasing and combustion duration. Important parameters are the injection strategy and the in-cylinder fuel blending. The initial set-up was with a PFI of gasoline and early cycle DI of diesel. Varying the fuel reactivity made it possible to control the combustion phasing and rate of pressure rise. Generally, the low reactivity fuel (LRF) is injected early and the high reactivity fuel (HRF) shortly before TDC. The HRF injection creates a high reactivity region which functions as an ignition source [Kokjohn et al., 2011].

RCCI has been developed at the Engine Research Center at the University of Wisconsin-Madison in 2010. They published fundamental papers regarding RCCI (Kokjohn et al. [2010]; Splitter et al. [2010]; Hanson et al. [2010]; Kokjohn et al. [2011]) and an extensive review [Reitz and Duraisamy, 2015].

4 Combustion strategies

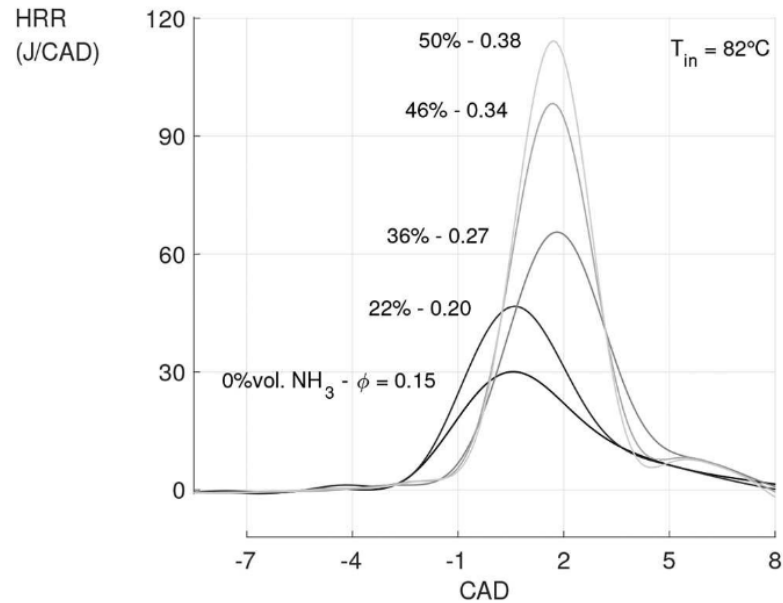


Figure 4.3: Constant intake temperature and hydrogen flow with increasing the ammonia flow rate. From Pochet et al. [2020a]

RCCI combustion is hampered by a load-limit because at higher loads the maximum pressure rise rate becomes too large. This was already identified in the initial research by Kokjohn et al. [2011]. The authors concluded that stratification of the fuel reactivity is needed to overcome this load-limit.

4.4.1 Ignition RCCI

Chiera et al. [2022] state, based on their CFD results for the RCCI combustion of ammonia and diesel, that in RCCI there is not a “*turbulent propagating flame front*” but more a “*wave of auto-ignition precursors*”. This does not fully match the modelling results of Kokjohn et al. [2010] for the RCCI combustion of diesel and gasoline blends. They report that the ignition location for all cases was the location with the highest concentration of diesel, the high reactivity fuel. However, in a follow-up study of the same research group, they focused on the ignition process. They concluded that the combustion reaction starts globally by the more reactive fuel, only the regions with lower reactivity exhibit a lower reaction progression rate in the beginning [Splitter et al., 2010].

4.4.2 Reactivity control

The reactivity of the mixture in the combustion chamber can be controlled by adjusting the mixture composition. When two fuels have a different reactivity, adjusting the mixture composition will adjust the reactivity of the fuel. This is the initial strategy used by Kokjohn et al. [2010]. This could potentially be expanded to the mixture ratio of the fuels, air, and EGR. The application of EGR will be discussed in chapter 5.

4.4.3 Ammonia combustion via RCCI

Chiera et al. [2022] investigated RCCI combustion with ammonia and diesel with CFD modeling and 1-cyl engine experiments. The results are very promising and substitution rates up to 81% were experimentally achieved with a good power density, an improved indicated efficiency compared to conventional dual fuel and lower GHG emissions. Their experimental work has been performed with an engine that is comparable to the AmmoniaDrive test engine. The engines are compared in Table 4.1.

Parameter	Chiera et al.	AmmoniaDrive	unit
Stroke	210	220	mm
Bore	170	170	mm
Compression ratio	17	14	-
Inlet temperature	65	up to 45	°C
Inlet pressure	2.4		bar

Table 4.1: Comparison test engines Chiera et al. [2022] and AmmoniaDrive

Their concept is named “diesel seeded premixed” (DSP). First, ammonia is port fuel injected. Then, a small amount of pilot diesel fuel is injected before the compression temperature reaches the autoignition temperature of diesel. This allows droplets to spread and mix with the ammonia and air charge and partly vaporize. Then the diesel ignition seeds are distributed throughout the premixed charge and available to initiate localized ignition once the conditions are reached.

A noteworthy property of the autoignition in this DSP concept, is that an early injection causes a longer ignition delay. This is due to the more homogeneously distributed diesel and thus less high local reactivity. Therefore, the timing of the diesel injection can be used to control the combustion phasing. In the experiments of Chiera et al., this is done by a control logic which adjusts the diesel injection timing based on the CA10. It is emphasized by the authors, that this is a very non-linear and stochastic process, as the autoignition does not only depend on the local diesel concentration, but also on the temperature history.

Zhang et al. [2022] experimentally investigated RCCI combustion of ammonia and n-heptane, with 50-70%_{en} ammonia. The focus within their research was the effect of turbulence and mixture reactivity on the ignition. The results of their results will be discussed in chapter 5.

Niki [2021b] experimentally demonstrated control of the combustion phasing by altering the mixture ratio of diesel and ammonia. The control of the combustion phasing by using different fuel compositions is shown in Figure 4.4. In the depicted experiments, the injected diesel pilot flow is kept constant, and the ammonia flow is altered. It can be seen, especially from the normalized cumulative heat release, how the mixture ratio influences the combustion phasing. Other effects of different fuel compositions are shown in Appendix H. The red solid line in the bottom graph represents the specific GHG emissions for a conventional diesel fuel. From Appendix H it can be seen that it is difficult to point out the optimal solution.

4.5 Other combustion mechanisms

Mounaim-Rousselle et al. [2022] investigated a spark-assisted compression ignition (SACI), a concept that was also identified by Pearsall and Garabedian [1967]. Contrary to what the name SACI seems to imply, there is no compression ignition or autoignition. It is a spark ignited

4 Combustion strategies

engine with a high, CI-like, compression ratio, but it uses the spark plug to ignite at every load. In both publications, an CI engine is retrofitted with a spark plug.

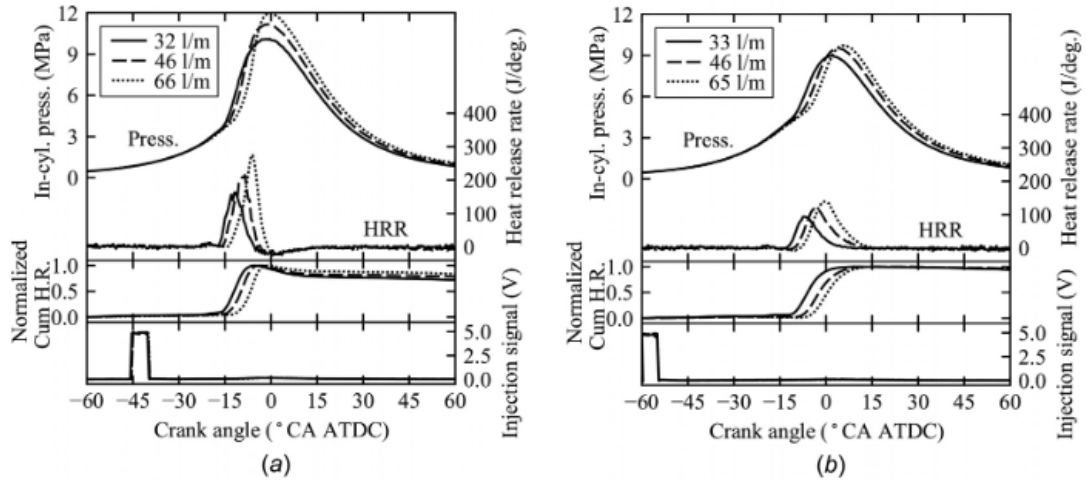


Figure 4.4: Effect of changing the fuel mixture ratio on the HRR and HRR for two different pilot injection timings, a) -45 CAD ATDC, b) -60 CAD ATDC. Graph from Niki [2021b]

Key points

- Conventional dual fuel (CDF) with diesel and ammonia is incapable to successfully combust more than 40-60%_{load} ammonia. CDF is limited due to the limited flame propagation in the ammonia rich zone, after the diesel rich zone has burned. Thus, to achieve higher %_{load} of ammonia, other combustion strategies have to be used.
- RCCI with ammonia and diesel has experimentally been achieved up to 81% ammonia by Chiera et al. [2022] in an engine comparable to the AmmoniaDrive test engine.
- With RCCI combustion, the reactivity of the fuel adjustable and with that, the ignition delay and the combustion phasing controllable.
- The stratification of fuel reactivity influences the pressure rise rate.

5 In-cylinder processes

Outline

This chapter reports on the available knowledge regarding in-cylinder processes for a CI ICE ammonia engine. Five in-cylinder processes are distinguished, shown in Figure 5.1.



Figure 5.1: Overview in-cylinder processes

5.1 Air intake

The required air intake temperature has been experimentally and numerically studied by Pochet et al. [2017b]. Their results are shown in Figure 5.2. When injecting the ammonia into the air-in-take manifold, the cooling effect of the vaporization is something to consider.

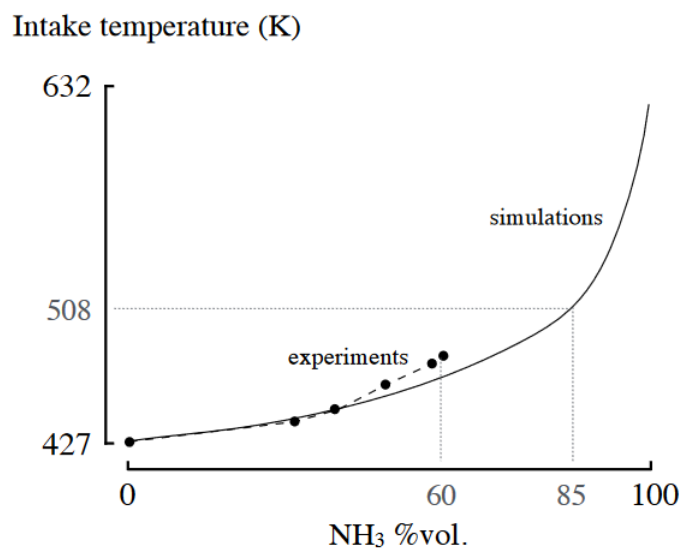


Figure 5.2: Required intake temperatures for NH₃/H₂ mixtures such that the autoignition occurs close to TDC. ϕ varies between 0.21 @ 100% H₂ and 0.27 @ 61% NH₃

In the study of Zhang et al. [2022] towards the RCCI combustion of ammonia and n-heptane,

the intake temperature was kept at 313 K (40°C). The effect of different cylinder temperatures has also been investigated by [Hernández et al. \[2022\]](#) in a CVCC, their results are shown in [Figure 5.3](#). The difference between $T_0 = 535^\circ\text{C}$ (blue) and $T_0 = 600^\circ\text{C}$ (green) for the combustion of different ammonia substitutions and diesel, is significant.

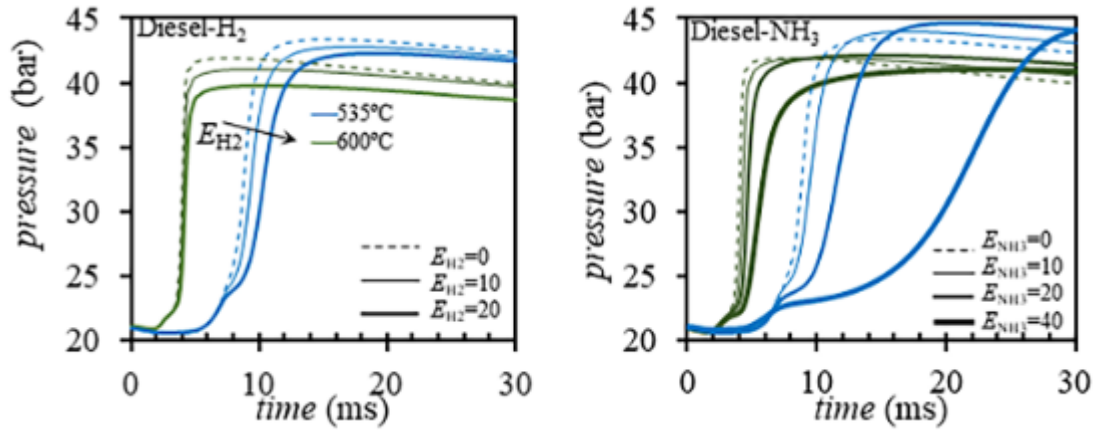


Figure 5.3: Pressure traces of CVCC for different compositions of diesel-ammonia and diesel-hydrogen with $p_0 = 21$ bar and $T_0 = 535^\circ\text{C}$ (blue) and $T_0 = 600^\circ\text{C}$ from [Hernández et al. \[2022\]](#)

5.1.1 Exhaust gas recirculation

The exhaust gas of an ammonia-hydrogen combustion contains water vapor. Therefore, it can decrease the cylinder temperature increase if that is required. [Pochet et al. \[2020a\]](#) observed a three-fold reduction of fuel-related NO_x emissions by exhaust gas recirculation (EGR) with an HCCI combustion, unfortunately it increased the N₂O and unburned ammonia emissions. Another effect observed by [Pochet et al. \[2020a\]](#), was the decrease of NO_x due to reduced oxygen availability as a result of the EGR.

5.2 Injection

The injection strategy has several variables, such as the method of injection, the timing, splitting up the injection into multiple injections, pressure, and shape of the spray. The AmmoniaDrive project has pre-set the injection of ammonia via PFI and hydrogen via DI. This section therefore discusses the timing, multiple injections, injection pressure and shape of the spray.

5.2.1 Injection timing

[Niki \[2021b\]](#) investigated the effect of the diesel pilot injection timing on the combustion performance. Their experiments had a 45% load contribution of ammonia (more details in [Appendix C](#)). The diesel pilot injection timing was varied between 10-65 CAD BTDC. Earlier than 65 CAD BTDC led to a sudden instability of the load and speed. The results of [Niki \[2021b\]](#) investigating the effect of diesel pilot injection timing is shown in [Appendix G](#) and [Appendix H](#). As can be seen from the graphs in the appendix, it is difficult to define an optimum diesel

pilot injection timing. The GHG effect of the emissions and the possibilities to capture them will influence what the optimal injection timing is.

Zhang et al. [2022] have conducted an experimental investigation towards the influence of injection properties on a RCCI combustion of ammonia and n-heptane. Their results highlight the importance of in-cylinder turbulence and n-heptane injection timing for the combustion of ammonia.

Ryu et al. [2014a] tested different injection timings with diesel and ammonia. Their results are shown in Figure 5.4. It can be seen that when there is more ammonia, the timing of the injection is advanced to achieve successful engine operation. This is explained by the authors, by the high latent heat of vaporization and increased ignition delay due to the ammonia.

Gray et al. [1966] already observed that combustion could only be achieved when ammonia was injected early into the cylinder, not later than 40 CAD before the end of the diesel injection, otherwise misfiring was occurred [Gray et al., 1966].

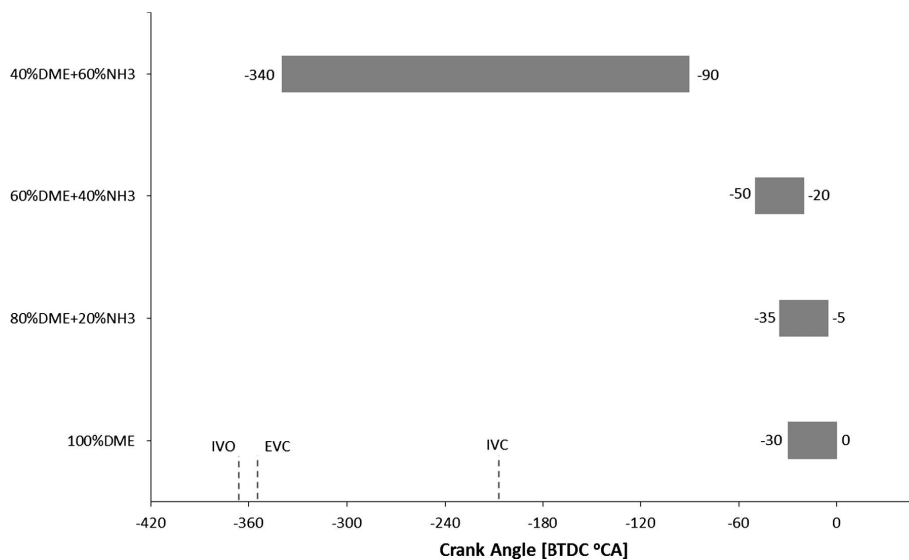


Figure 5.4: Range of injection timing for effective combustion of DME-Ammonia (from Ryu et al. [2014a])

5.2.2 Multiple injections

Niki et al. [2019] investigated a pilot and post injection in addition to a main injection, to improve the combustion of ammonia and diesel. This study, however, has a low ammonia substitution, maximum 15%. Based on this work, Niki et al. suggest multiple diesel fuel injections to reduce emissions. This is done in their subsequent work, Niki [2021a]. Unfortunately, this is not retrievable.

Nair et al. [2019] investigated a dual injection strategy to overcome the load limit of an RCCI combustion and create a multi-stage combustion. The first injection created a RCCI combustion and the second injection a diffusion flame. With this strategy, higher loads were achieved. Both Chiera et al. who investigated the RCCI combustion of ammonia and diesel and Nair et al. are part of Woodward, a “designer, manufacturer and service provider of energy control and optimization solutions” [Woodward, 2023].

Yousefi et al. [2022a] investigated the effect of splitting the diesel injection in an ammonia-diesel engine with 40%_{heat} of ammonia. The split diesel injection strategy increased the ITE from 38.62% to 39.72% and reduced the unburned ammonia emissions by 83.5%, compared to the best results for a single diesel injection.

5.2.3 Injection pressure

In the experimental work of Frost et al. [2021], although with ammonium hydroxide, diesel was direct injected with a pressure of 500 bar.

A consideration is a variable pressure pulse (VPP) injection system, used in Kokjohn and Reitz [2010]. This system can deliver multiple injections at different pressures within one cycle. This could be interesting when one wants to achieve reactivity stratification.

5.2.4 Spray shape

The spray shape of an injection depends on the fuel and injection variables. The shape can be, for example, parabolic, triangular, or rectangular. As discussed earlier, ammonia has a relatively low viscosity of ammonia, which will influence the atomization, droplet formation, turbulence, and spray formation. These properties will influence the combustion efficiency [Li et al., 2022].

Research has been done by Pelé et al. [2021] towards the spray shape of ammonia after DI. DI of ammonia is outside the scope of AmmoniaDrive, however, it does illustrate the different spray shapes and indicates the demand for additional research. The different spray shapes can be viewed in Appendix E.

5.2.5 Other injection strategies

Sun et al. [2007], of the ERC of the UW-Madison where later RCCI was developed, investigated adaptive injection strategies (AIS). AIS entails a variable geometry spray (VGS), variable injection pressure (VIP) and using multiple injections. The background of this research was the problems experienced within HCCI combustion, such as spray-wall impingement and the extension to higher loads. They concluded that 1) AIS was an effective method to minimize spray-wall wetting, 2) low-pressure injection is to be preferred to high pressure for HCCI and 3) a low pressure early injection, followed by a high pressure late injection produces two-stage combustion (TSC) which results in lower emissions. Although this research is slightly older, since the HCCI combustion of ammonia and hydrogen encounters similar problems [Zheng, 2020], their solutions could be valuable.

5.3 Mixing

Mixing is dependent on a considerable number of parameters. Several, not all, parameters are listed;

- Injection properties
 - Timing, spray shape, pressure, turbulence
- Time available to mix
 - Dependent on the fuel(s), pressure, injection timing

- Geometry of the piston and combustion chamber
- Fuel(s)
 - Autoignition behavior, phase, temperature

These variables illustrate the interaction between the properties and how immensely correlated it is.

5.4 Ignition

Zhang et al. [2022] has optically investigated the RCCI combustion of ammonia and n-heptane. The authors varied three things:

- The timing of the n-heptane injection: early or late.
- The mixture ratio: 70/30%_{energy} (H30) and 50/50%_{energy} (H50) ammonia/n-heptane.
- Turbulence intensity: lower turbulence intensity (type 1) and higher turbulence intensity (type 2).

The images from the autoignition and flame propagation of Zhang et al. [2022] are shown in Figure 5.5. The 'a' in the picture marks autoignition kernels.

The authors observed that the location of autoignition kernels is closely related to local concentration of n-heptane and in a more homogeneous mixture, due to higher turbulence intensity, the autoignition and combustion phasing are later delayed. This adds another mechanism to control the combustion phasing, namely controlling the turbulence.

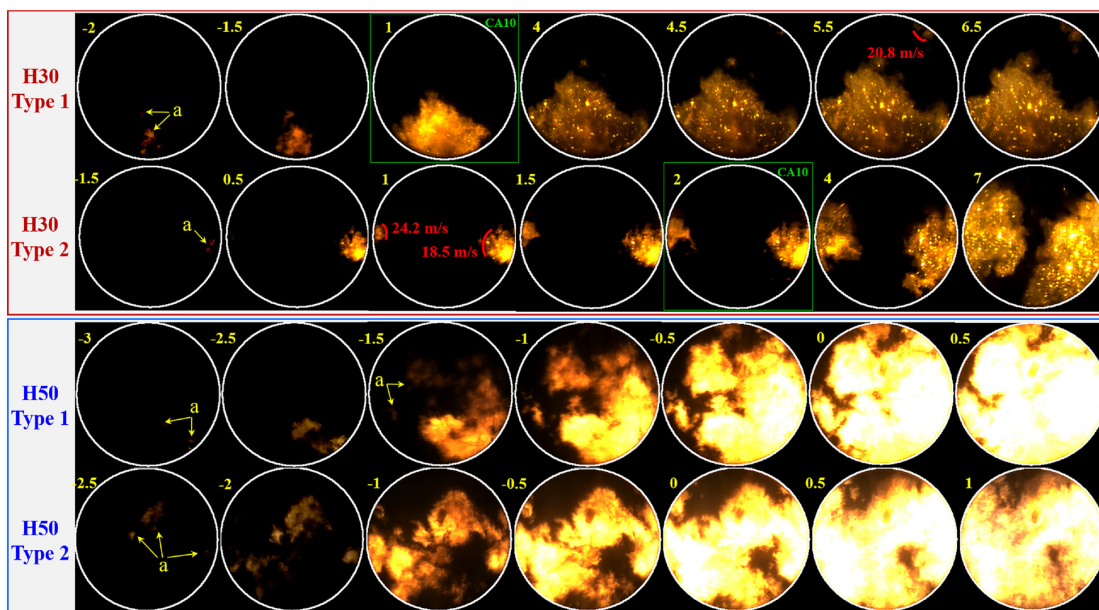


Figure 5.5: Autoignition and flame propagation after an early injection of n-heptane. From: Zhang et al. [2022]

5.5 Combustion

The combustion can be characterized based on the classification of fundamental combustion phenomena based on Law [2006] and Heywood [2018]. Classifying the combustion will give direction to which theories and models can be applied.

- Pre-mixed versus non-premixed combustion
- Laminar versus turbulent combustion
- Subsonic versus supersonic combustion
- Homogeneous versus heterogeneous combustion

The typical DI diesel combustion is non-premixed combustion, also known as diffusion combustion. However, when ammonia is port fuel injected, the combustion becomes a more pre-mixed combustion due to the higher premixed ratio and the ignition delay caused by ammonia. This has been confirmed in experiments by Reiter and Kong [2011] and Nadimi et al. [2022]. Yousefi et al. [2022b] investigated ammonia/diesel dual-fuel operation mode experimentally and numerically. The results indicated that due to the low flame speed of ammonia, the thermal efficiency was decreased by increasing the ammonia energy fraction. The slow flame speed in a premixed ammonia-air mixture generated a significant amount of unburned ammonia. This will be improved by mixing ammonia and hydrogen, as shown in a study by da Rocha et al. [2019]. Da Rocha et al. combined several experimental data sets and numerical models together to compare their results. It is shown that adding hydrogen, as expected, increases the laminar flame speed and the laminar flame speed is plotted against the H₂ mole fraction.

HCCI combustion has been experimentally investigated by Pochet (Pochet et al. [2017b]; Pochet et al. [2020a]) and by Zheng [2020]. Pochet et al. report that the successful combustion is very dependent on the charge air temperature and Zheng concluded in his thesis that a HCCI combustion of ammonia & hydrogen is not optimal in a SOFC-ICE configuration.

5.5.1 Pressure rise rate

Pochet et al. [2020a] identified the maximum pressure rise rate (MPRR) as the limiting factor for HCCI. This is shown in Figure 5.6. The tapering off the achievable IMEP is due to increased friction and heat losses. Here lies a potential opportunity for reactivity controlled compression ignition, to decrease the MPRR.

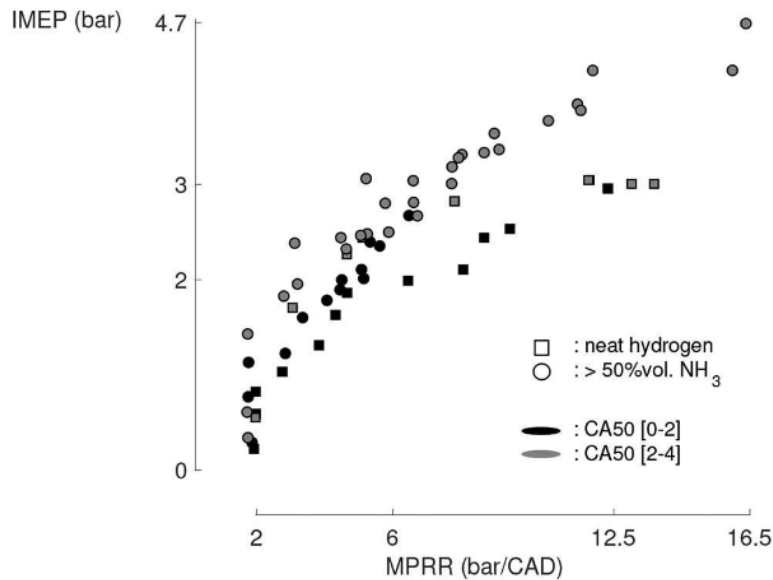


Figure 5.6: The obtainable IMEP tapers off as the maximum pressure rise rate increases

Key points

- The HCCI combustion of ammonia and hydrogen requires a high air intake temperature. A lower air intake temperature is worthwhile to investigate, and this could potentially be achieved by a small amount of diesel.
- Turbulence has a significant effect on the ammonia ignition in an RCCI or HCCI combustion with ammonia and a carbon-base fuel. Because an increase in turbulence delays the ignition due to creating a more homogeneous mixture.
- Combining RCCI with PPCI, by employing a second injection causing a diffusion combustion, could be a method to achieve a higher combustion efficiency.
- Properties of ammonia-hydrogen mixtures under engine conditions are starting to become available in literature.
- RCCI can potentially decrease the MPRR, which is a limiting factor for achieving a higher IMEP via HCCI.

6 Emissions

Outline

Emissions are one of the main driving forces behind alternative fuels, as mentioned in the introduction. Ammonia and hydrogen are carbon-free molecules, which is viewed as their key selling point. However, the emission of nitrogen oxides is a concern, also due to the fuel-bound nitrogen. Fortunately, the MMMCZCS concluded that if there is industry-wide collaboration, then the emissions from ammonia fueled power trains will not become a 'showstopper' [MMMCZCS, 2023].

This chapter will elaborate on the harmful emissions related to the CI combustion of ammonia, hydrogen, and a carbon-based fuel.

6.1 Measuring global warming effect

The Global Warming Potential (GWP) is a measure to compare the global warming effect of different gases. It indicates how much energy a gas will absorb over a period of time (usually 100 years), relative to carbon dioxide.

The GWP also considers the time a certain gas will be present in the atmosphere. As an example, CO₂ is present for thousands of years, while the lifespan of nitrous oxide is 114 years on average [US EPA, 2023].

6.2 CO₂ and CO

As mentioned, CO₂ is a long-lived greenhouse gas. The amount of CO₂ is directly related to the amount of combusted carbon-based fuel. The technology to remove the CO₂ from the exhaust and renew it to fuel, is energetically not attractive due to the stability of the CO₂-molecule and also economically not viable yet.

Carbon monoxide (CO) results from incomplete combustion. The results of Niki et al. in [Appendix H](#) for a PPCI combustion show that CO increases for a higher amount of NH₃ when the diesel is injected 45 CAD BTDC, but even decreases slightly with an earlier diesel injection of 60 CAD BTDC.

The results of [Yousefi et al. \[2022b\]](#) for a CDF combustion are shown in [Figure 6.1](#), there the CO emissions increase with increasing %_{en} NH₃. This indicates the dependency of CO emissions on the combustion efficiency.

6.3 NO_x

NO_x consists of nitric oxide (NO) and nitrogen dioxide (NO₂). Another distinction is made between fuel NO_x and thermal NO_x. Fuel NO_x originates from the fuel, which is relevant for ammonia. And thermal NO_x is formed from nitrogen in the combustion air.

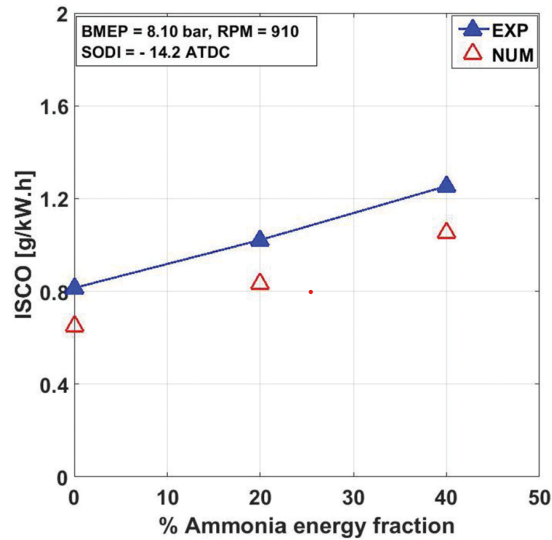


Figure 6.1: CO emissions of a CDF combustion as function of the $\%_{energy} \text{NH}_3$ from Yousefi et al. [2022b]

Lhuillier et al. [2020] investigated the emissions from the combustion of an ammonia-hydrogen mixture in SI engine, the results are shown in Figure 6.2. Details of this study can be viewed in Appendix C.

Exhaust gas recirculation (EGR) decreases the amount of NO but increases the amount of NO_2 , as can be seen from the experiments of Pochet et al. [2020a]. The decrease of NO is thought to be realized by the lower amount of oxygen available, and therefore the favoring of N_2 formation instead of NO_x [Pochet et al., 2020a].

6.4 N_2O

Nitrous oxide (N_2O), also known as laughing gas, has a GWP that is 298 times higher than CO_2 . It has an average life-span of 114 years [US EPA, 2023]. Over the past 150 years, increasing atmospheric N_2O concentrations have contributed to stratospheric ozone depletion and climate change.

N_2O is an intermediate species in the combustion of ammonia and can thermally decompose above 1073 K [Niki, 2021b]. There is an unfortunate interaction between NO_x and N_2O , which can be clearly viewed in the results of Niki et al. in Appendix G and Appendix H. When N_2O emissions decrease, NO_x emissions rise. Where the optimum is for an engine, also heavily relies on the possible exhaust treatment.

6.5 Ammonia

The MMMCZCS has identified three sources of ammonia emissions related to ICEs fueled by ammonia. These are boil-off gas (BOG) from fuel tanks, ammonia from venting and purging operations, and unburned ammonia from the ICE [MMMCZCS, 2023]. Accumulating evidence indicates that ammonia has to be prevented from entering the atmosphere. Although

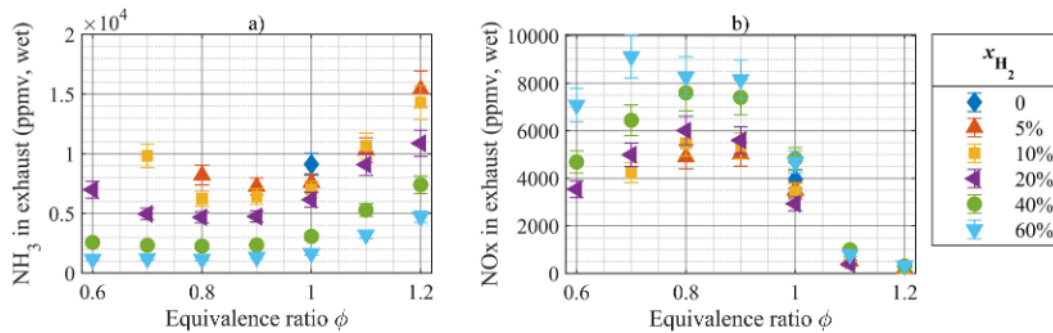


Figure 6.2: Emissions for varying $\text{H}_2\%$ and equivalence ratio in a SI engine from Lhuillier et al. [2020]

Classification Society	ppm limits for release, alarm, and safety systems activation	Source
ABS	10 ppm as release/exhaust limit, gas alarms at 25 ppm and safety systems activated at 150 ppm	ABS, "Guide for Ammonia Fueled Vessels", September 2021
BV	30 ppm exposure limit, triggering shut down and other safety measures	Bureau Veritas, "AMMONIA-FUELED SHIPS TENTATIVE RULES - NR671 - JULY 2022". 2022
Class NK	25 ppm as release/exhaust limit, same safety and alarm provisions as Korean Registry	ClassNK, "Guidelines for Ships Using Alternative Fuels (Edition 2.0) - Methy/Ethyl Alcohol/LPG/Ammonia, June 2022
DNV	30 ppm as release/exhaust limit, gas alarms at 150 ppm and safety systems activated at 350 ppm	DNV, RULES FOR CLASSIFICATION, Ships, "Part 6 Additional class notations, Chapter 2 Propulsion, power generation and auxiliary systems", July 2022
Korean Register	Safety systems activated at 300 ppm. Alarm sounds at 25 ppm	Korean Register, "Guidelines for ships using Ammonia as fuels (2021.26)", 2021
Lloyd's Register	Prevent venting in normal and abnormal conditions. Safety systems activated at 220 ppm and alarm sounds at 25 ppm.	Lloyd's Register, Notice No. 1, Rules and Regulations for the Classification of ships using Gases or other Low-flashpoint Fuels, December 2022

Figure 6.3: Ammonia limits in ppm from Class guidelines from MMMCZCS [2023]

the mechanisms are not fully understood yet, it appears that ammonia can create secondary organic aerosols and PM [Kane and Northrop, 2021]. Secondary organic aerosols are a combination of gas- and solid-phase molecules. The molecules are formed by multi-generation oxidation of a parent organic molecule, ammonia in this case [Yee et al., 2012].

The MMMCZCS has listed the ammonia limits in ppm from class guidelines, their table is shown in Figure 6.3. 10-35 ppm is listed as acceptable as an exhaust limit. Comparing these numbers to the emissions listed in Appendix C, it can be concluded that there is still a large gap between what is achieved and what is required by class.

It can be observed in the results of Lhuillier et al. [2020], shown in Figure 6.2, that an increasing % of hydrogen and a leaner mixture, decreases the amount of the unburned ammonia. However, it increases the NO_x emissions.

Ammonia emissions will increase with a higher compression ratio, this can be seen in the results of Mounaim-Rousselle et al. [2022] shown in Figure 6.4. This could be explained by more ammonia trapped in the crevices at higher compression ratio's.

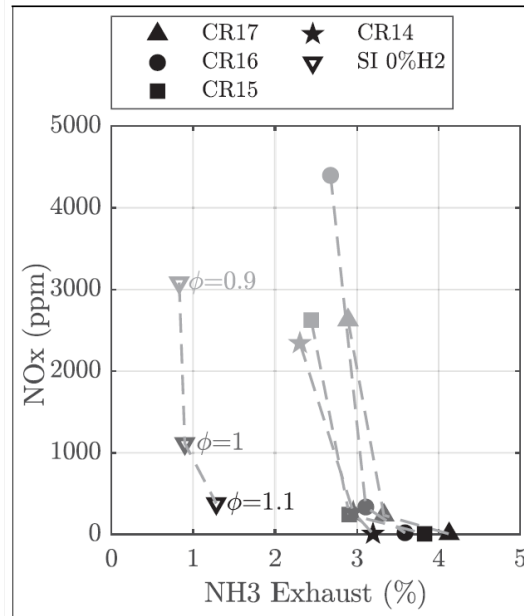


Figure 6.4: NO_x and NH₃ emissions for different CR and ϕ . From Mounaim-Rousselle et al. [2022]

6.6 Hydrocarbons

Hydrocarbon emissions originate from carbon-based fuels. It appears that an earlier injection of diesel, causes more hydrocarbon emissions. This can be observed in the results of Niki [2021b] in Appendix G and Appendix H.

6.7 Soot

There are not many experimental studies reporting on soot emissions. Reiter and Kong [2011] did measure soot and their results are shown in Figure 6.5. It is noteworthy that for lower contributions of ammonia, the soot emissions rise compared to the diesel-only combustion. When the contribution of ammonia is further increased, the soot emissions decrease.

6.8 Selective catalytic reduction

The AmmoniaDrive Research Project and other researchers describe the use of the unburned ammonia in an SCR to reduce the NO_x in the exhaust. Pochet et al. [2020a] refer to a ratio of $[\text{NH}_3]/[\text{NO}_x] \simeq 1$ for effective reduction. Chiera et al. [2022] proposes a similar strategy with a ratio of 1.2:1 for $[\text{NH}_3]/[\text{NO}_x]$.

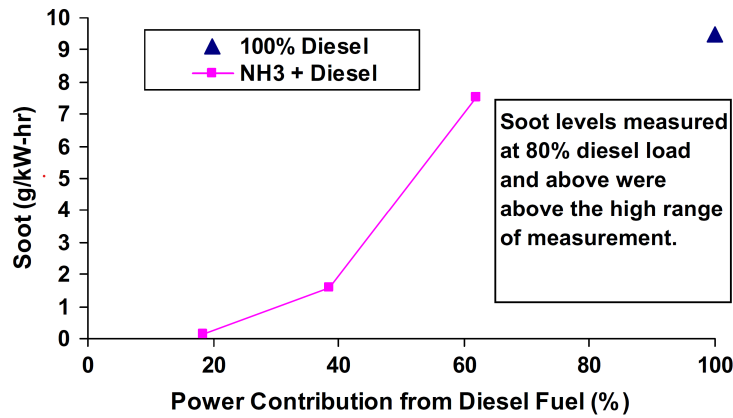


Figure 6.5: Soot measurements from Reiter and Kong [2011]

Key points

- H_2 can decrease the unburned ammonia emissions, but increases the NO_x , although more in leaner mixtures than in more fuel rich mixtures.
- There appears to be a reciprocity between N_2O and NO_x , when one decreases, the other increases.
- There is a considerable gap between the maximum allowable level of emissions and the level from experimental research.
- When comparing the emissions, this can only be achieved when all harmful emissions and countermeasures, such as an SCR, are taken into account.

7 Engine characteristics

Outline

This chapter reports on the engine characteristics, relevant to know preparing for experiments. In addition, it covers some employed technologies to improve the (RC)CI combustion of ammonia and hydrogen. The literature, on which this chapter is based, is largely experimental literature.

7.1 Engine speed

Ammonia has a high autoignition resistance and low flame speed, and therefore it appears a logical consequence that ammonia engine speeds are lower. This is supported by [Ryu et al. \[2014b\]](#) reporting on limitations on the engine speed when substituting DEE with ammonia. In several other experimental studies with (partly) ammonia fueled engines, the engine speed is also lower compared to diesel engines. This can be observed in [Appendix C](#). The engine in the experiments of [Yousefi et al. \[2022a\]](#) with 40%_{mass} ammonia ran at 910 rpm. However, the recent study of [Wang et al. \[2023\]](#) did achieve 1800 rpm with an ammonia substitution of 70%_{load}.

7.2 Compression ratio

[Gray et al. \[1966\]](#) determined a required compression ratio (CR) of 35 for the combustion of pure ammonia in a diesel engine. These very high compression ratios are unfavorable due to the high friction it will induce [[Pochet et al., 2017b](#)]. Fortunately, [Pochet et al. \[2020a\]](#) has achieved a HCCI combustion with 94%_{volume} ammonia and hydrogen with a compression ratio of 22.

The CR has also been studied numerically. [Schönborn \[2021\]](#) studied the influence of the compression ratio on the ignition of ammonia and aqueous ammonia with a zero-dimensional single-zone combustion model. This simulation study of Schönborn resulted in a required CR for pure ammonia of 24.8 and for aqueous ammonia a CR of 26.7 (25:75%_{mass} ammonia:water). Schönborn also investigated the effect of a direct injection of hydrogen at 3 CAD before top dead center (BTDC) on the ignition of aqueous ammonia with a zero-dimensional two-zone model. This resulted in a required CR of 24, and it is likely that a CR of 23 could also ignite the aqueous ammonia due to flame propagation.

When comparing the required compression ratios in the literature with the test engine available in the AmmoniaDrive project, the required compression ratio for the autoignition of pure ammonia & hydrogen is unlikely to be achievable by the test engine. Although Schönborn does not report results for pure ammonia & hydrogen, knowing the difference in the required CR for combustion of pure ammonia without hydrogen, 24.8 versus 26.7, it is not likely to be within reach for the AmmoniaDrive test engine.

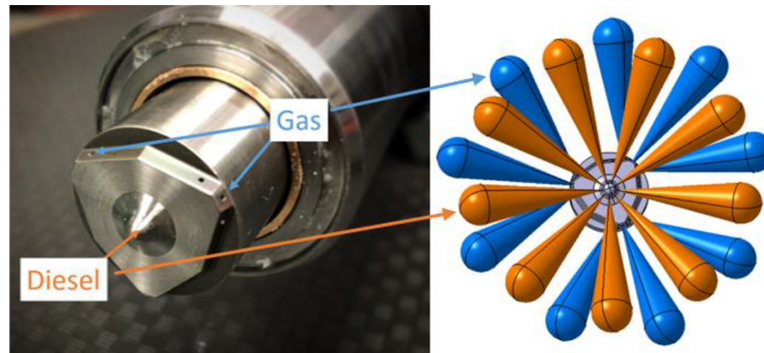


Figure 7.1: Dual fuel injector of Woodward L'Orange: nozzle and spray arrangement. Image from Frankl et al. [2021]

7.3 Fuel delivery system

Zhu and Fan [2022] have investigated fuel delivery systems for alternative fuel engines and identified factors that have to be considered.

- **Sealing and lubrication** due to phase transformations at certain pressures & temperatures.
- **Capacity of fuel flow** due to the potential lower energy density.
- **Corrosion** due to the corrosive nature of alternative fuels
- **Multiple fuels** may require co-axial and/or multiple injectors

7.3.1 Injectors

Multiple injectors and/or co-axial injectors can be used to inject different fuels. When ammonia is injected via PFI, hydrogen & a HRF can be injected via a DI co-axial injector. This also limits the number of items having to be placed on the cylinder head.

Frankl et al. [2021] used a dual fuel injector of Woodward L'Orange, which can inject two fuels independently. The main fuel can be injected at maximum 500 bar and the pilot fuel at maximum 1800 bar. This type of injector could be suitable when one wants to achieve reactivity stratification. The spray arrangement and injector nozzle are shown in Figure 7.1.

Yousefi et al. [2022a] injected ammonia via PFI and used two solenoid gas injectors (Gs60 model of Alternative Fuel System Inc.) to inject the ammonia into the intake manifold.

Kuta et al. [2023] used ammonia via PFI and the details of their ammonia port injection are shown in Figure 7.2. Niki [2021b] used a Quantum gas injector (type: 110764) to inject gaseous ammonia into the intake manifold. Another ammonia injection related technology, is the use of an intake adapter to influence the in-cylinder turbulence, as done by Zhang et al. [2022] while investigating the RCCI combustion of ammonia and n-heptane.

Bao et al. [2022] investigated a hydrogen engine with direct injection of hydrogen. Their hydrogen injector achieved a maximum flow rate of 2.66 mg/ms with the injection pressure of 14 MPa.

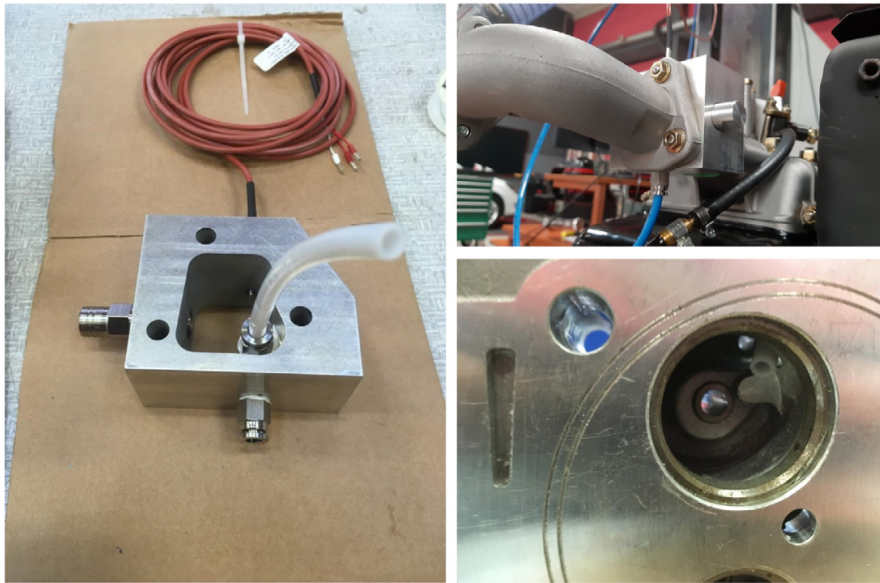


Figure 7.2: Details of port fuel injectors of Kuta et al. [2023]

7.3.2 Plenum

To ensure a homogeneous mixture is formed, a plenum can be used. This is done by Pochet et al. [2017b] to achieve HCCI with an ammonia and hydrogen mixture. It could be sensible to investigate the in-cylinder pre-combustion behavior of the fuels and assess which measures should be taken to ensure the desired stratification or homogeneous distribution is achieved.

7.3.3 Pre-heating

Frigo and Gentili [2013] used a heated vaporizer in ammonia experiments, to counteract the higher latent heat of vaporization. Niki [2021b] offset this by heating the ammonia cylinders to 40°C to maintain the pressure of the ammonia gas supply. Reiter and Kong [2011] also report on chilling of the ammonia tanks due to the phase transformation from liquid to gas of ammonia. This caused the tank pressure and fuel flow to drop.

The result of a numerical study of Frankl et al. [2021] shows that pre-heating the ammonia will improve the combustion efficiency, their reference point is 350 K ($\approx 77^\circ\text{C}$). This is also done in the experimental study by Lhuillier et al. [2020], where the fuel is premixed (ammonia, hydrogen, and air) and heated to 323 K ($\approx 50^\circ\text{C}$).

7.3.4 Pre-chamber

The effect of pre-chamber jet-induced ignition on the combustion of pure ammonia has been investigated by Meng et al. [2023], experimentally in a CVCC and with a CFD model. They spark ignite a rich mixture of ammonia and air in the pre-chamber. The results indicate it to be an effective way to counteract the low flammability of ammonia and accelerate the combustion speed in the main chamber.

Wang et al. [2022] studied the feasibility of hydrogen jet flame ignition, specifically in marine large-bore low speed engines, and concluded it to be a viable option. The jet flame was

developed by spark igniting hydrogen in a pre-combustion chamber to form a hydrogen jet flame. The jet flame ignited the ammonia in the cylinder. With this ignition strategy, it would be possible to eliminate the need for diesel as a pilot fuel. The hydrogen energy corresponded to 1.68% of the total fuel energy.

7.4 Piston design

HCCI and PCCI were troubled by high CO and unburned hydrocarbons (UHC) emissions due to a low combustion efficiency. This has been greatly improved by innovations in the piston design and by limiting the crevice volumes [Kokjohn et al., 2011]. Another solution is to minimize the crevice volume, as done by Pochet et al. [2020a] for their HCCI combustion experiments of ammonia and hydrogen by using a flat piston.

Regardless of the combustion mechanism, ammonia is expected to be difficult to combust around crevice regions due to the low flame speed and long quenching distance, this confirms the need for a well-designed piston.

7.5 Material factors

Ammonia is corrosive to copper, copper alloys, nickel and plastics [Dimitriou and Javaid, 2020]. Therefore, Kuta et al. [2023] use an ammonia-resistant elastic pipe of PTPE and Reiter and Kong [2011] replaced brass, copper, and rubber components with mild steel and Teflon counterparts. In the experimental work of Zhang et al. [2022] with ammonia and n-heptane, the components of the ammonia supply system are constructed of SS316L stainless steel. A preventive measure could be flashing with conventional fuels after using a corrosive fuel as ammonia, according to Starkman et al. [1967].

Kurien and Mittal [2022] report on hydrogen embrittlement and hydrogen ICE having signs of hydrogen embrittlement in intake valves after longer operation.

Key points

- Engine speeds of CI ICE (partly) running on ammonia are often lower than the same engine fueled by diesel only.
- Fuel injectors for the PFI of ammonia and DI of hydrogen are present in experimental studies.
- Measures to offset the high latent heat of vaporization of ammonia have to be considered.
- It could be sensible to assess which measures, such as a plenum or piston design, should be taken to minimize crevice regions and to ensure the desired distribution of fuel is achieved.
- Material factors, such as the corrosive nature of ammonia, have to be considered.

8 Models in literature

Outline

This chapter reports on the available literature related to the modeling of a CI combustion of ammonia and hydrogen. The background knowledge for this chapter can be found in [Appendix I](#).

First, the two main model types are discussed; thermodynamic and CFD models. Followed by phenomenological models and chemical-kinetic mechanisms, which are employed by the thermodynamic and CFD models to incorporate phenomena or chemical reactions.

8.1 Thermodynamic models

[Zheng \[2020\]](#) used a single-zone zero-dimensional model in this thesis, based on the work of Dr.ir. Harsh Sapra to model the HCCI combustion of ammonia and hydrogen.

[Pochet et al. \[2017b\]](#) used a single-zone zero-dimensional model with a hydrogen-ammonia kinetic mechanism. The goal of their model was to predict the timing of an HCCI combustion.

[Mounaïm-Rousselle et al. \[2022\]](#) investigated the combustion of pure ammonia via SACI with a zero-dimensional two-zone model. The two zones consisted of unburned fuel/air/EGR and burned gases.

[Schönborn \[2021\]](#) employed a two-zones zero-dimensional model to investigate the ability of a hydrogen injection to ignite a mixture of ammonia and air. Both zones consisted of a homogeneously premixed mixture of aqueous ammonia and air, with hydrogen being injected at 3°CA before TDC into zone 1 of the reactor model.

[Frost et al. \[2021\]](#) also used a two-zones zero-dimensional model to investigate the effect of substituting diesel by ammonium hydroxide at different engine loads. Both zones initially consist of an ammonia-air mixture and zone 1 receives a diesel injection. As zone 1 is surrounded by zone 2, the heat transfer to the walls only occurs in zone 2. The model is shown in [Figure 8.1](#)

8.2 Fluid dynamic models

[Chiera et al. \[2022\]](#) used a CFD model to do a feasibility study before experimentally investigating the RCCI combustion of ammonia and diesel.

[Yousefi et al. \[2022a\]](#) used a CFD model to study the split diesel injection and observed that their simulation results correspond well to the experimental data.

[Wang et al. \[2023\]](#) have investigated high pressure compression ignition with diesel of ammonia and hydrogen by conducting experiments and simulations. The results of their CFD simulations are the pressure and heat release rate are very consistent with their obtained experimental data.

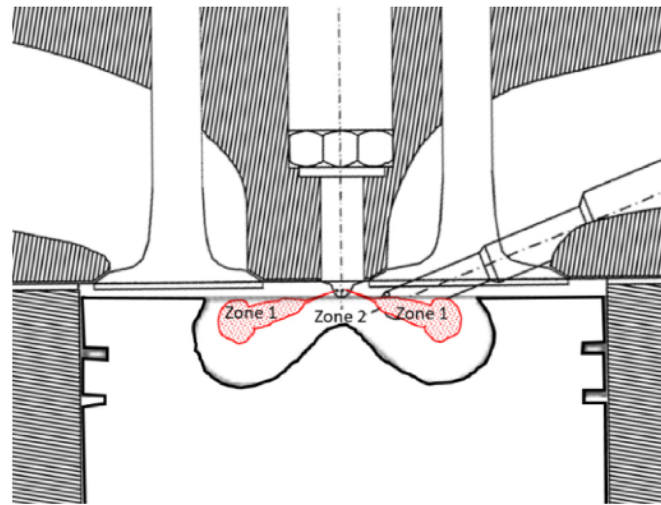


Figure 8.1: Engine model of Frost et al. [2021] illustrating the zones

8.3 Phenomenological models

Phenomenological models can be employed to incorporate phenomena, such as the heat transfer to the wall and the combustion, into an engine model or simulation. In some literature, a heat transfer model is referred to as a heat transfer correlation.

This overview will show the demand for more accurate phenomenological models for the HCCI/RCCI combustion of ammonia and hydrogen. Especially for initial design and control studies, these low-fidelity, phenomenological models are useful because they require less computational time than CFD models.

8.3.1 Heat transfer model

In a thermodynamic model, the heat transfer to the wall is typically modelled by an empirical model. The applicability of several empirical heat transfer models for modelling HCCI combustion is assessed by Broekaert et al. [2015]. The models of Annand, Hohenberg and Hensel were deemed to be able to predict the heat transfer to the wall in a HCCI combustion. However, it was concluded that the model coefficients are only accurate for one operating point.

The conditions Broekaert et al. [2015] used to assess the heat transfer models are shown in Figure 8.2a. When these are compared to the operating conditions of the HCCI combustion ammonia & hydrogen of Pochet et al. [2020a], shown in Figure 8.2b, it can be seen that the intake temperature for the combustion of a high ammonia % is significantly higher. A larger deviation can be seen in the equivalence ratios.

The model of Hohenberg for the heat transfer is employed by Pochet et al. [2017a], investigating HCCI combustion of ammonia and hydrogen. In subsequent research, Pochet et al. [2020a] updated the heat transfer model of Hohenberg, based on their experimental data. The reasoning behind choosing for the Hohenberg model is described further in a separate publication, Pochet et al. [2020b].

It will be a challenge to model a RCCI combustion of ammonia and hydrogen, due to the changing operating points, which could require changing the heat transfer model coefficients.

Operating point	Inlet air temperature [°C]	Air-to-fuel equivalence ratio λ	Operating mode
1	28	-	motored
2	160	4.0	fired
3	150	4.0	fired
4	150	4.7	fired
5	130	3.7	fired
6	115	2.7	fired

(a) Conditions assessment heat transfer models of Broekaert et al. [2015]

Run (#)	T_{in} (°C)	NH_3 (%vol.)	ϕ_0 (-)
All	50–240	0–94	0.1–0.65
1	175	37–77	0.22
2	50–205	0–91	0.25–0.38
3	52, 177	0, 92	0.26, 0.65
4	82	0–50	0.15–0.38
5	175	70–91	0.17–0.58
6	110–210	50	0.17
7	130	33	0.19–0.26
8	175	37–82	0.23
	175	37–75	0.23
	175	21–63	0.22

– indicates a continuous range.

, indicates specific points.

All were operated at 1,500 RPM and 1 bar intake pressure.

(b) HCCI runs Pochet et al. [2020a]

Figure 8.2: Comparison conditions assessment heat transfer models of Broekaert et al. [2015] and HCCI runs Pochet et al. [2020a]

Additionally, the accuracy of the heat transfer models for RCCI combustion of ammonia and hydrogen should be considered.

8.3.2 Combustion model

The Wiebe model is a phenomenological model for the combustion, and it can drive simulation models of in-cylinder processes [Stapersma, 2010b]. Pochet et al. [2020a] use the Wiebe for the combustion of ammonia and hydrogen with a duration of 8 CAD. It is also used by Lasocki et al. [2019] in a simulation feasibility study. However, their results are not validated with experimental data.

A phenomenological model, used for the HCCI combustion of ammonia and hydrogen, is Seiliger in the thesis work of Zheng [2020].

Recently published work of De Bellis et al. [2022] describes a multi-zone phenomenological model for a RCCI combustion which can describe the autoignition and flame propagation. This model has not yet been used in literature.

8.4 Chemical-Kinetic Mechanisms

The chemical-kinetic mechanism used by Pochet et al. [2017b] to model the HCCI combustion of ammonia and hydrogen, was based on Mathieu and Petersen [2015]. This mechanism is validated at 30 bar and for lean conditions (equivalence ratio 0.5-1.0). However, Pochet et al. observed an underestimation of the resistance to autoignition when comparing their experiments with the simulations. In their subsequent research, Pochet et al. [2020a] use the

same 0-dimensional model, but the kinetic mechanism of Song et al. [2016] is employed. This is also used by Schönborn [2021].

The chemical kinetic mechanism of Song et al. [2016] is validated for pressures of 30–100 bar, and temperatures of 450–925 K. From the experimental investigations of Pochet et al. it can be seen that the temperature range of this mechanism is too low.

For the combustion of diesel and ammonia, Convergent Science provides a mechanism, used by the CFD model of Chiera et al. [2022]. This mechanism is partly based on Stagni et al. [2020], which is also used by Mounaïm-Rousselle et al. [2022] to model the SACI in a zero-dimensional, two-zone model. The chemical-kinetic mechanism of Stagni et al. [2020] is based on higher temperatures, 500–2000 K but the experimental data is only from pressures close to atmospheric pressure.

The chemical-kinetic mechanism of Stagni et al. [2020] has been improved by Bertolino et al. [2021]. The resulting chemical-kinetic mechanism is employed by Convergent Science, a software developer, and this is used by the CFD model of Chiera et al. [2022].

It can be concluded from the literature that there is no chemical-kinetic mechanism available that has been validated for CI engine conditions.

8.5 Software

One software used to model the combustion of ammonia is Chemkin Pro, which is available within ANSYS. This software is used by Mounaïm-Rousselle et al. [2022], da Rocha et al. [2019] and Reiter and Kong [2008]. It has several built-in models, such as a single-zone zero-dimensional HCCI model and zero-dimensional 2-zone SI model.

Cantera is another widely used software to model combustion. Schönborn [2021] and Frost et al. [2021] use Cantera for a zero dimensional 2-zone model of an aqueous solution of ammonia.

And lastly, there is CONVERGE by Convergent Science, a computational fluid dynamic modelling software. This is employed by, among others, Chiera et al. [2022] and Yousefi et al. [2022b].

8.6 Modelling CI combustion concepts with ammonia

The RCCI combustion mechanism with the diesel seeded premix of Chiera et al. [2022], cannot be modelled with a zero-dimensional single-zone thermodynamic model. Because the ignition delay of the fuel is based on local autoignition of diesel. Counterintuitively, an earlier injection leads to a more homogeneous charge and therefore a longer ignition delay. A later injection leads to larger droplets of diesel, which leads to a short ignition delay. This effect cannot be captured by a single-zone thermodynamic model.

An HCCI combustion concept of Pochet et al. [2020a] can be modeled with a single zone thermodynamic model. However, when stratification is employed to control the combustion, this has to be modelled with a multi-zone thermodynamic model, because of the different zones.

Multiple runs of a single zone thermodynamic model with varying input parameters, such as the mixture composition or equivalence ratio, can provide insight into the required stratification for RCCI combustion. An example is to vary the mixture composition or equivalence ratio and investigate the effect on the ignition delay. But to assess the engine cylinder performance, a multi zone model is required.

Key points

- Modelling an RCCI combustion cannot be done with a single-zone zero-dimensional thermodynamic model.
- There is a demand for improved phenomenological models and chemical-kinetic mechanisms for the combustion of ammonia validated at CI engine conditions.

9 Novel combustion strategies

Outline

Different strategies to combust ammonia via CI combustion were encountered in the literature study. And until this chapter, everything that has been written came from available research. This chapter introduces the first steps into an unexplored area. It contains conceptual ideas for new NH_3 & H_2 CI combustion strategies, inspired by the results present in literature and the AmmoniaDrive combustion concept. Then the chapter will converge to the first steps to be taken to assess a combustion strategy for the AmmoniaDrive test engine.

9.1 Novel combustion concepts

The three combustion concepts are an RCCI concept, a PCCI stratification concept and a homogeneous charge hydrogen spark concept.

9.1.1 Concept 1: the RCCI concept

The RCCI concept is based on controlling the reactivity by changing the mixture composition of ammonia, hydrogen, air, and HVO. Additionally, more reactivity control can be achieved by controlling the timing of the HVO injection. This concept builds on the combustion concepts of [Chiera et al. \[2022\]](#) and [Pochet et al. \[2020a\]](#).

Compared to the RCCI combustion concept of Chiera et al., there are two modifications: the addition of hydrogen and the replacement of diesel by HVO. Both modifications are aimed at minimizing the required amount of HRF by improving the combustion of ammonia. Hydrogen has been proven to be capable of this [[Lhuillier et al., 2020](#)]. And HVO has proven to be more capable than diesel in combusting ammonia [[Hernández et al., 2023](#)]. The results of Hernandez et al. are shown in [Appendix D](#)

Compared to the HCCI combustion concept of Pochet et al., the addition is the HVO. HVO is added to lower the required compression ratio and air intake temperature. The compression ratio of concepts fueled by a carbon-based promoter fuel and ammonia, are considerably lower than the required compression ratio of 22 for the HCCI combustion of ammonia and hydrogen. This can be seen in [Appendix C](#).

The mixture composition of ammonia, hydrogen, air, and HVO will depend on operating conditions, such as load and charge air temperature. The dependence on the latter could mitigate the issues due to variations in charge air temperature, as encountered by [Pochet et al. \[2017b\]](#). Furthermore, this concept could potentially widen the operating window of the HCCI combustion concept of Pochet et al. by decreasing the maximum pressure rise rate at high loads by decreasing the reactivity at those loads.

The RCCI combustion concept requires a control system that adapts the fuel mixture based on operating conditions, such as the measured charge air temperature, the ignition delay, or

load. In terms of hardware, it requires a controllable and flexible fuel delivery system.

9.1.2 Concept 2: the PCCI stratification concept

The PCCI stratification concept is based on controlling the combustion by varying the stratification in the combustion chamber. This concept is illustrated in [Figure 9.2](#).

The stratification can, for example, create a more ammonia rich zone in the middle of the combustion chamber and a more hydrogen rich zone towards the wall of the cylinder. As the temperature is normally highest in the middle of the combustion chamber, this could dampen the pressure rise rate. A more hydrogen rich zone towards the cylinder wall should leave less unburned ammonia in the crevice regions.

Ammonia and hydrogen may be suitable for the stratification concept, because of their difference in mass. Achieving the in-cylinder stratification and adapting it to operational conditions, would require a sophisticated injection and control system. And in terms of modelling, this injection would probably require a CFD simulation. If it is assumed that stratification is achieved, then the stratified charge before autoignition, could be set as the initial condition in a multi-zone zero-dimensional thermodynamic model. This would limit the required computational resources and make it easier to do an initial feasibility assessment.

9.1.3 Concept 3: the homogeneous charge hydrogen spark concept

The third concept is a combination of a homogeneous charge and dual hydrogen injection. The ammonia and early hydrogen injection form a homogeneous mixture. This results in a slightly lower autoignition temperature or higher flame speed once ignited, compared to a pure ammonia charge. The second hydrogen injection causes a local hydrogen rich region. This region should autoignite, and then there are two options. The first is a propagating flame which ignites the homogeneous ammonia-hydrogen mixture. The second option is an increase in temperature, due to the combustion of the second hydrogen injection, which causes the homogeneous ammonia-hydrogen mixture to autoignite.

The injection strategy is shown in [Figure 9.2](#) and is inspired by the work [Nair et al. \[2019\]](#) and [Yousefi et al. \[2022a\]](#).

Modelling this concept can be done with a multi-zone thermodynamic model. A simplifying assumption would be that there is no mass transport between the second hydrogen injection and the homogeneous mixture of ammonia and hydrogen.

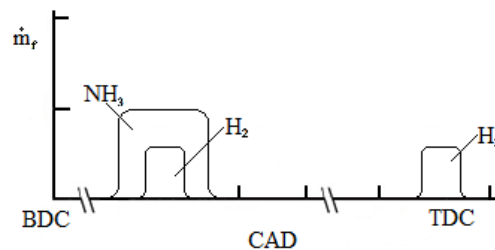


Figure 9.1: Injection timing of the homogeneous charge hydrogen spark concept

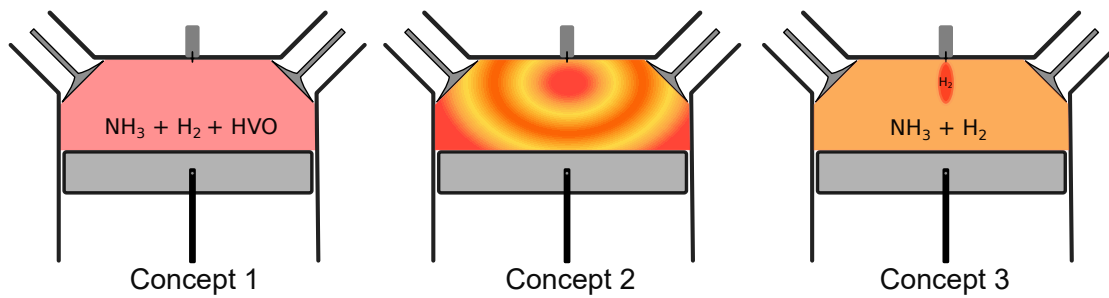


Figure 9.2: Graphical illustration of the three concepts

9.2 Trade off

Three CI combustion concepts for ammonia and hydrogen have been introduced: an RCCI concept, a PCCI stratification concept, and a homogeneous charge hydrogen spark concept. These concepts have not been investigated yet in available literature. An initial estimation of their feasibility could have been done within this thesis work. However, a trade-off had to be made to determine the focus of the thesis work. Factors involved within this trade-off are what is valuable for the AmmoniaDrive Research Project, what can be modelled with the available knowledge, what fits within the constraints of the thesis, and what is the most promising to explore.

Considering the three concepts from the perspective of the AmmoniaDrive project, a first point of interest is the compression ratio of the test motor, which is approximately 14. Using a carbon-based fuel, lowers the required compression ratio compared to the required compression ratio of 22 for an HCCI combustion of ammonia and hydrogen. Given the compression ratio of the test motor, the combustion concept to be investigated will probably have to make use of a carbon-based fuel to ignite.

The next discussion point is the type of carbon-based fuel. Chiera et al. used diesel, however considering the findings of [Hernández et al. \[2023\]](#), HVO seems more promising. The results of Hernandez et al. are shown in [Appendix D](#). When viewing the top two graphs in the middle, HVO seems to be better capable of supporting the ammonia combustion. There is some controversy surrounding HVO because of possible competition with food production. However, waste and residues form more than 80% of the input [[Hernández et al., 2023](#)] and the amount for an RCCI combustion should be less than 19%^{energy}. Based on this, HVO seems promising to investigate as the carbon-based fuel.

The decision to make use of a carbon-based fuel, excludes the third concept, the homogeneous charge hydrogen spark, as a thesis focus. The RCCI and PCCI stratification concepts can both be carried out with ammonia, hydrogen, and HVO. Given the two concepts, the RCCI combustion concept seems a logical start because the RCCI involves a homogeneous charge of the combustion chamber. This can be modelled by a single-zone zero-dimensional model. If the RCCI appears to be limited due to a high maximum pressure rise rate, stratification can be employed. This corresponds to the PCCI stratification concept. Then the model has to be expanded to a multi-zone zero-dimensional thermodynamic model. Concluding, the focus of the thesis work will be the RCCI combustion concept.

To model phenomena such as heat loss, heat release rate, and the combustion, more accurate phenomenological models and chemical-kinetic mechanisms are required. The models and chemical-kinetic mechanisms currently available do not fully cover the conditions encoun-

tered in the CI combustion of ammonia and hydrogen. Without those accurate phenomenological models and chemical-kinetic mechanisms, it could prove difficult to accurately assess the feasibility of a RCCI combustion of ammonia and hydrogen. This should be considered when evaluating the modelling results.

On the other side, [Pochet et al. \[2020a\]](#) did achieve modelling results which were consistent with their experimental data with a single-zone zero-dimensional thermodynamic model. Their result indicates that it is possible to do an initial estimation of the feasibility. The model, developed during the thesis, can be tested with the experimental results of [Pochet et al. \[2020a\]](#) and [Chiera et al. \[2022\]](#). This will not be a validation, as not all data is available, but it will give some indication of the reliability of the model.

9.3 Investigating a combustion strategy for the AmmoniaDrive test engine

The previous chapters have provided an overview of the state-of-the-art knowledge in the literature regarding ammonia as a fuel for a compression ignition engines. The overview has been concluded by several novel combustion concepts in this chapter. These concepts could potentially increase the feasibility of a (partially) ammonia fuelled CI ICE. An initial assessment of the feasibility of new concepts, can be done with modelling. Therefore, in this graduation research, two models have been developed to investigate some compression ignition combustion strategies.

The first model focuses solely on the ignition by investigating the ignition behavior of different mixture compositions at varying top dead center (TDC) conditions with the so-called "ignition model". This is a single zone thermodynamic constant volume reactor model. This model and the results of the ignition research are covered in [chapter 10](#).

Subsequently, the ignition model is used as a basis for the "engine cylinder model", The objective of this model is to provide an initial estimate on the engine cylinder performance. The model incorporates several CI ICE phenomena, such as a varying closed volume and a heat loss model. The engine cylinder model is a single zone thermodynamic reactor model. This model and the results of the single engine cylinder research are covered in [chapter 11](#). An overview of both models is listed in [Table 9.1](#).

As this research aims to provide input for the AmmoniaDrive project, the top dead center conditions and other engine parameters are chosen to be comparable to the AmmoniaDrive test engine of TNO Helmond.

9.3 Investigating a combustion strategy for the AmmoniaDrive test engine

	Ignition model	Engine cylinder model
<i>Type</i>	Single zone thermodynamic constant volume reactor model	Single zone thermodynamic reactor model
<i>Variables</i>	<ul style="list-style-type: none"> - Mixture composition - equivalence ratio - T_{TDC} - p_{TDC} 	<ul style="list-style-type: none"> - Fuel composition based on energy - Equivalence ratio - Inlet temperature - Compression ratio - Engine speed - Stroke and bore - Heat loss
<i>Output</i>	<ul style="list-style-type: none"> - Ignition (CA10) relative to t_0 - Temperature @ CA10 - Pressure @ CA10 - Pressure rise rate @ CA10 - Injected fuel energy 	<ul style="list-style-type: none"> - Injected fuel energy - Ignition (CA10) relative to TDC - Pressure rise rate @ CA10 - Heat release rate - Pressure - Temperature - maximum pressure rise rate (MPRR) - Timing MPRR - Combustion duration - Efficiency W_{out}/Q_{in} - Emissions

Table 9.1: Overview models

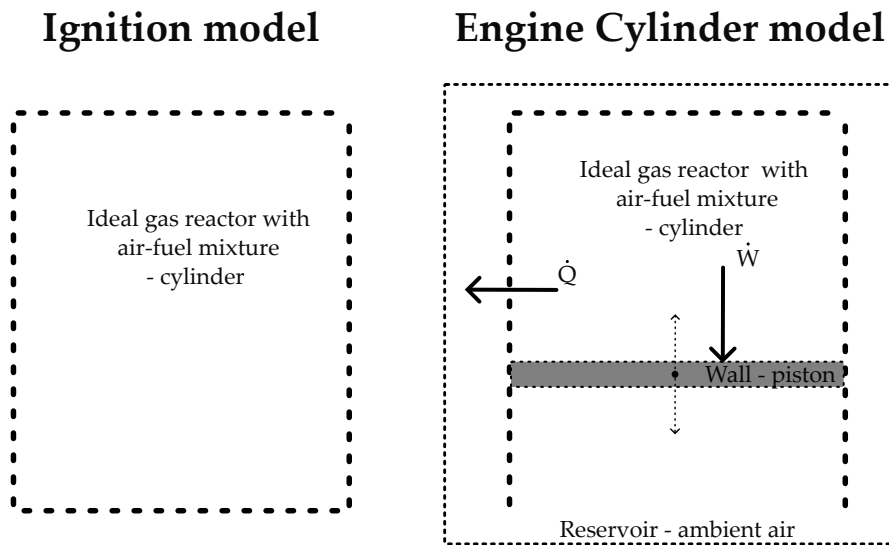


Figure 9.3: Graphical representation of the ignition model and the engine cylinder model with the incorporated Cantera objects and what the objects represent.

10 Ignition model

Outline

This chapter describes the research on the ignition of ammonia, hydrogen, and DME mixtures. It consists of five parts.

- The introduction including definitions, an overview, and context
- Governing equations and definitions of the ignition model
- Validation & Verification of the ignition model
- Limitations, assumptions, and uncertainties
- Results of the ignition model

The first objective of this chapter is to understand the effect of parameters such as the equivalence ratio, the mixture composition, pressure, and temperature. The second objective is to identify a range of feasible fuel properties. For example, to identify a range of equivalence ratios which are worthwhile to investigate further.

The results of this chapter are used in the next chapter with the engine cylinder model, to create insight into the possibilities and limitations of compression ignition combustion in the AmmoniaDrive test engine.

First, “the ignition” has to be defined. In this research, the ignition is defined as the crank angle where 10% of the fuel mass has combusted, CA10. In this report, CA10 and ignition are interchangeable.

The investigated ignition properties are;

- The ignition delay, which is defined as the timing of CA10 relative to t_0 (start of simulation). This will be different at the engine cylinder model, where the CA10 is relative to TDC.
- The pressure rise rate at CA10.
- The temperature rise at CA10.

The variables are:

- The fuel mixture composition
- The equivalence ratio
- The initial pressure (p_{TDC})
- The initial temperature (T_{TDC})

The initial pressure and temperature should be interpreted as the average conditions around top dead center. Therefore, the CA10 identified by this model is not relative to TDC, but to relative to the start of the simulation. The CA10 identified in the next chapter, by the engine cylinder model, is relative to TDC. An example of the full output of the ignition model is shown in [Appendix N](#).

In this phase, it is not possible yet to set definitive target numbers, solely an order or magnitude. For the ignition delay, this is approximately 2 CAD ATDC, which is approximately

10 Ignition model

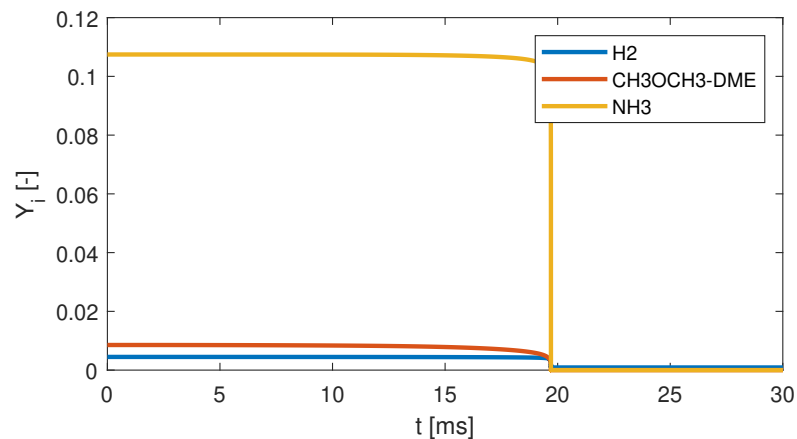


Figure 10.1: Mass fractions of NH_3 , H_2 and DME during a stoichiometric constant volume combustion of 72.0 % $_{\text{e}}$ NH_3 , 19.5 % $_{\text{e}}$ H_2 , and 8.5 % $_{\text{e}}$ DME with initial conditions of $p = 50$ bar and $T = 944$ K.

CA10 of 4 CAD for the ignition model. Pochet et al. [2020a] investigated an HCCI combustion of ammonia and hydrogen. They attempted to maintain a CA50 of 4 CAD ATDC. At their engine speed of 1500 rpm, 4 CAD is equal to 0.44 ms. In this research, the engine speed is set to 1200 rpm, then 4 CAD equals 0.56 ms. These numbers give an order of magnitude for the timing of the ignition.

The MPRR will likely be a limiting factor. The MPRR of the test engine employed by AmmoniaDrive is still unknown, but it was mentioned that “10 bar/cad is already pretty noisy”. Another order of magnitude can be deduced from other experimental studies. For example, the test engine of Pochet et al. [2020a] had an MPRR of 12 bar/cad.

The results of the ignition research provide insight in when a homogenous mixture will ignite. This homogeneous mixture can be interpreted as a cylinder with an homogeneous charge, or as a local condition within the cylinder. Interpreting it as a local condition is, among other things, relevant for local ignition in case of a fuel stratification. Such a stratification can be intended to dampen the pressure rise rate. Investigating the ignition of different mixture compositions will give some indication of the required stratification to achieve a dampening effect of the pressure rise rate.

To investigate the ignition, a single zone thermodynamic constant volume reactor model is employed. The constant volume is analogous to conditions around top dead center, where the volume change is small.

The constant volume has the consequence that the motion of the piston, which varies the volume, is not included. This leads, among other things, to a higher MPRR than in an ICE, as the increasing volume after TDC is not included. The varying volume will be considered in the second part of the research, when the combustion of NH_3 , H_2 , and DME is studied with more CI ICE aspects included.

To create some context, an example is shown in Figure 10.1, this shows the mass fractions of NH_3 , H_2 , and DME during a stoichiometric constant volume compression ignition combustion of 72.0 % $_{\text{e}}$ NH_3 , 19.5 % $_{\text{e}}$ H_2 and 8.5 % $_{\text{e}}$ DME with initial conditions of $p = 50$ bar and $T = 944$ K. The fuel ignites at 19.7 ms. This is equivalent to 35.5 CAD at 1200 rpm, which is much too late. This example shows the necessity to investigate the ignition properties of different fuel compositions at varying initial conditions to achieve ignition closer to top dead center.

The investigation of the ignition properties is broken down into several research questions.

- How does the mixture composition of ammonia, hydrogen, DME, and air affect the ignition properties?
- How do the p_{TDC} and T_{TDC} affect the ignition?
- What effect does the addition of hydrogen to a mixture of ammonia, air, and DME have on the required amount of carbon-based fuel to accomplish an ignition with adequate properties?

10.1 Modeling of the ignition and combustion

The modeling of the ignition model is carried out in Matlab and Cantera. Cantera is a software suite of tools which can integrate chemical kinetics into a model. The three Cantera Objects that are relevant for this thesis are the Ideal Gas Reactor, the Reservoir, and the Wall. These three objects are introduced here to be able to understand the governing equations of the ignition model.

- **Ideal gas reactor:** is a reactor with a homogeneous phase and distribution of ideal gases. It is defined by four state variables; the reactor volume, temperature, the mass of the content, and the mass fraction of each species.
- **Reservoir:** this is a reactor that has a constant state. Therefore, the reservoirs' temperature, pressure, and chemical composition never change from their initial values.
- **Wall:** this is an object in between reactors which, among other things, can change the volume of adjacent reactors and transfer heat between reactors.

The ignition model only employs the Ideal Gas Reactor, as can be seen from the schematic overview in [Figure 10.2](#). This seems a trivial figure, but it forms the basis of the model in the next chapter, where the engine cylinder model employs the three objects to incorporate more ICE phenomena. A more detailed description of the employed Cantera objects can be found in [Appendix M](#).

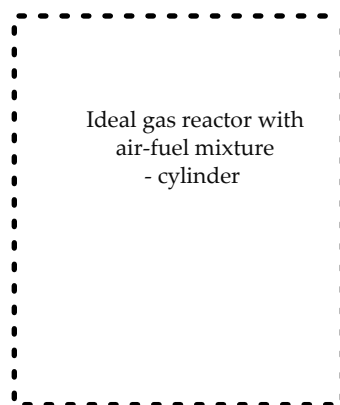


Figure 10.2: Graphical overview of the ignition model with the Cantera object Ideal Gas Reactor and what it represents

The models will make use of a chemical kinetic mechanism to provide the ignition and heat release of the combustion. As chemical kinetic mechanism can predict, among other things, the chemical heat release rate and the ignition delay of a chemical reaction. It contains the sequence of elementary reactions by which the overall reaction occurs. Therefore, the chemical kinetic mechanism also provides insight into the intermediate species during the combustion reaction.

Cai et al. [2023] provides an overview of available kinetic mechanisms for ammonia combustion. This overview is shown in Appendix J. As can be seen in the overview, there is no chemical kinetic mechanism yet which focuses on ammonia, hydrogen and a carbon-based fuel. The chemical kinetic mechanism of Shrestha et al. [2018] does contain these fuel components.

The mechanism of Shrestha et al. contains 125 species (chemical compounds) and 1090 elementary chemical reactions. The species in the chemical mechanism of Shrestha et al. are listed in Appendix J. Many species are reaction intermediates, these are species that are the result of previous elementary reactions and are consumed in later elementary reactions. Reaction intermediates, therefore, do not appear in the overall reaction. The species in the mechanism of Shrestha et al. are listed in Appendix K and includes intermediate species.

The chemical kinetic mechanism is distributed by three TXT files. These three files carry the kinetic mechanism, the transport properties, and the thermochemistry. Appendix L describes how the TXT files have been converted into the chemical kinetic mechanism in YAML-format, which is employed in both the ignition model and the engine model.

10.2 Equations

This section will describe the governing equations of the ignition model, a single-zone constant volume thermodynamic model.

10.2.1 Governing equations of the ideal gas reactor

The 'ideal gas reactor' is the Cantera object that represents the system where the combustion takes place. There are four state variables and four governing equations for the ideal gas reactor Cantera [2023a].

The state variables are:

- The mass of the reactor's contents [kg]
- The reactor volume [m^3]
- The temperature [K]
- The mass fractions for each species [-]

There are four governing equations for the ideal gas reactor object of Cantera. The first equation, Equation 10.1, describes the mass content of the reactor.

$$\frac{dm}{dt} = \sum_{in} \dot{m}_{in} - \sum_{out} \dot{m}_{out} + \dot{m}_{wall} \quad (10.1)$$

$$\frac{dm}{dt} = 0 - 0 + 0$$

The mass flows, \dot{m}_{in} and \dot{m}_{out} , are zero because the ignition model is a closed volume. And the ignition model does not contain the Cantera object 'Wall', thus $\dot{m}_{wall} = 0$. Therefore, Equation 10.1 equals zero for the ignition model.

The second governing equation, Equation 10.2, describes the volume change. The subscript 'w' refers to the Cantera object 'Wall'.

$$\frac{dV}{dt} = \sum_w f_w A_w v_w(t) \quad (10.2)$$

$$\frac{dV}{dt} = 0$$

In the ignition model, there is no Wall and thus no volume change. Equation 10.2 equals zero for the ignition model.

The third governing equation, Equation 10.3, originates from the first law of thermodynamics and describes the temperature.

$$mc_v \frac{dT}{dt} = -p \frac{dV}{dt} + \dot{Q} + \sum_{in} \dot{m}_{in} \left(h_{in} - \sum_k u_k Y_{k,in} \right) - \frac{pV}{m} \sum_{out} \dot{m}_{out} - \sum_k \dot{m}_{k,gen} u_k \quad (10.3)$$

For the ignition model, the third governing equation can be simplified to Equation 10.4, because:

- There is no volume change, $\frac{dV}{dt} = 0$.
- There is no heat flow across reactor boundaries, $\dot{Q} = 0$.
- There is no mass flow, $\dot{m}_{in} = \dot{m}_{out} = 0$.

In the ignition model, the change in species due to the chemical reaction ($\dot{m}_{k,gen}$) and the internal energy of the present species (u_k) fully determine the temperature of the Ideal Gas Reactor.

$$mc_v \frac{dT}{dt} = \sum_k \dot{m}_{k,gen} u_k \quad (10.4)$$

The change in species due to the chemical reaction ($\dot{m}_{k,gen}$), and the internal energy of the present species (u_k) are provided by the chemical kinetic mechanism of Shrestha et al. [2018].

The fourth governing equation of the ideal gas reactor describes each homogeneous phase specie:

$$m \frac{dY_k}{dt} = \sum_{in} \dot{m}_{in} (Y_{k,in} - Y_k) + \dot{m}_{k,gen} - Y_k \dot{m}_{wall} \quad (10.5)$$

There is no mass flow in, $\dot{m}_{in} = 0$, and no mass flow through a Wall, $\dot{m}_{wall} = 0$. Therefore, the change in species ($m \frac{dY_k}{dt}$), is equal to the change in species due to the chemical reaction ($\dot{m}_{k,gen}$). The fourth governing equation for the ignition model becomes:

$$m \frac{dY_k}{dt} = \dot{m}_{k,gen} \quad (10.6)$$

More details on these equations can be found here:

<https://cantera.org/science/reactors/idealgasreactor.html>

10.2.2 Definitions

Here are several definitions to understand the results.

Equivalence ratio

$$\phi = \frac{m_f/m_{ox}}{(m_f/m_{ox})_{stoic}} \quad (10.7)$$

$\phi > 1$ corresponds to a fuel rich combustion and $\phi < 1$ to a lean combustion.

Fuel energy

The fuel energy is defined as in Equation 10.9, in which the subscript 'i' indicates the different fuel components such as ammonia, hydrogen, DME.

$$Q_f = \sum_i LHV_i \cdot m_i \quad (10.8)$$

Fuel component energy percentage

$$\%_{fuel_i} = \frac{LHV_i \cdot m_i}{\sum_i LHV_i \cdot m_i} \quad (10.9)$$

CA10

Simulation results give a time for CA10, this is converted to crank angle degree (CAD). The CA10 is calculated based on an engine speed of 1200 rpm.

$$CA10 = \frac{t_{CA10} \cdot 1200 \cdot 360}{60} \quad (10.10)$$

10.3 Verification & Validation

The verification and validation are based on Thacker et al. [2004]. Their work originates from the decreasing possibilities for nuclear weapon testing, but the continued wish to develop new nuclear weapon technology. Therefore, there was a need for a verification and validation of models. So, the development could continue without, or at least with a decreased amount of, tests.

The verification is considered first. The goal of the verification is to show that the model implementation corresponds with the conceptual description. Therefore, the model behavior is compared with reality. This is done by analyzing the modeling results for scenario's with a known outcome, such as a stoichiometric combustion which should leave no oxygen.

The verification is done by comparing the results with expectations. The following tests have been executed:

- When the combustion is stoichiometric, no fuel or oxygen is left.
- In a fuel rich combustion, fuel remains.
- In a fuel lean combustion, oxygen remains.
- Higher temperatures lead to lower ignition delays.
- Higher pressures lead to lower ignition delays.

It can be concluded from these verification tests that the determination of the stoichiometric ratio is accurate, and the overall trends are as expected from first principles. After the verification, the validation is done by comparing the modeling results to experimental results. The objective of the validation has been well-phrased by [Thacker et al.](#):

Validation

"The process of determining the degree to which a model is an accurate representation of the real world from the perspective of the intended uses of the model." [[Thacker et al., 2004](#)]

For the validation, outcomes of the model are compared with experimental and numerical data from literature. With this comparison, it will be shown that the modeling outcomes are close to the experimental outcomes. Unfortunately, the ignition model can only be compared to results of ammonia-hydrogen mixtures and ammonia-DME mixtures, as there are no experimental results of the ignition of ammonia-hydrogen-DME available.

The two experimental studies used for the validation both originate from the Energy and Sustainability Research Institute of the University of Groningen. [Dai et al. \[2020\]](#) investigated the autoignition behavior of an ammonia-hydrogen mixture and [Dai et al. \[2021\]](#) studied ignition delay times of ammonia-DME mixtures. [Table 10.1](#) shows the properties of the experimental studies of [Dai et al.](#) and of this study. It can be concluded from this overview, that the TDC conditions studied in this research are close or within the range of the experimental results. This ensures that the experimental results of [Dai et al. \[2020\]](#) and [Dai et al. \[2021\]](#) suitable for the validation of the ignition model.

When reviewing the results of [Dai et al.](#), it should be noted that the fractions used in the two publications of [Dai et al.](#) are mole fractions and not energy fractions. Also the definition of ignition used in both publications is *"The ignition delay time was defined as the interval between the end of compression and the maximum in the rate of pressure increase during ignition"*. This complicates a direct comparison difficult.

- In the NH_3/H_2 mixture, 5%_{mole} H_2 equals 7.8%_e H_2 .
- In the NH_3/DME mixture, 5%_{mole} DME equals 17.2%_e DME.

	Dai et al. [2020]	Dai et al. [2021]	This study
Type	Experimental	Experimental	Modeling
Mixture composition	NH_3 with 0-10% _{mole} H_2	NH_3 with 0, 5, and 100 % _{mole} DME	NH_3
Pressure	20-75 bar	10-70 bar	50-70 bar
Equivalence ratio	0.5 and 1.0	0.5, 1.0 and 2.0	0.1-0.45
Temperature	1040-1210 K	610-1180 K	1100-1175 K

Table 10.1: Comparison of the properties of this study to the experimental studies

[Dai et al. \[2020\]](#) compared their experimental results to the chemical kinetic mechanism of [Shrestha et al.](#) and concluded that the mechanism underpredicts the ignition delay. Their results are shown in [Figure 10.3](#).

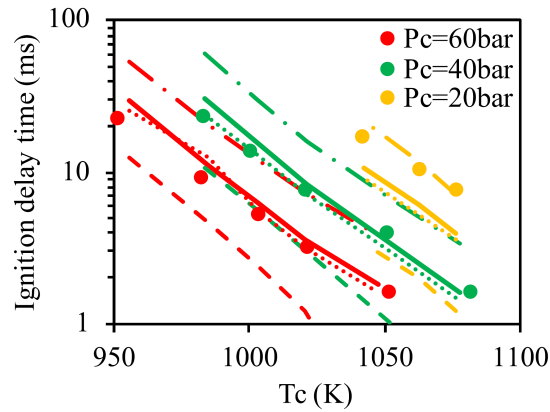


Figure 10.3: Results of Dai et al. [2020] for $\phi = 0.5$, $H_2 = 10\%_{mol}$. The points correspond to experimental measurements, the lines correspond to different chemical kinetic mechanisms: the dashed line for Shrestha et al. [2018], the dotted lines Mathieu and Petersen [2015], the dash-dot line Klippenstein et al. [2011], the solid line to the mechanism of Dai et al. [2020]

The results of the ignition model with the parameters of Dai et al. [2020] are shown in Figure 10.4. The results match the results of the Shrestha et al. [2018] in Figure 10.3. This confirms the implementation of the chemical kinetic mechanism. However, it can be seen that, as Dai et al. [2020] concluded as well, the ignition delay is underestimated. The mechanism used in Dai et al. [2020] is the mechanism of Glarborg et al. [2018] with some modifications described by Dai et al.. For future research, this could be an interesting chemical kinetic mechanism to explore, as will be discussed in the Discussion.

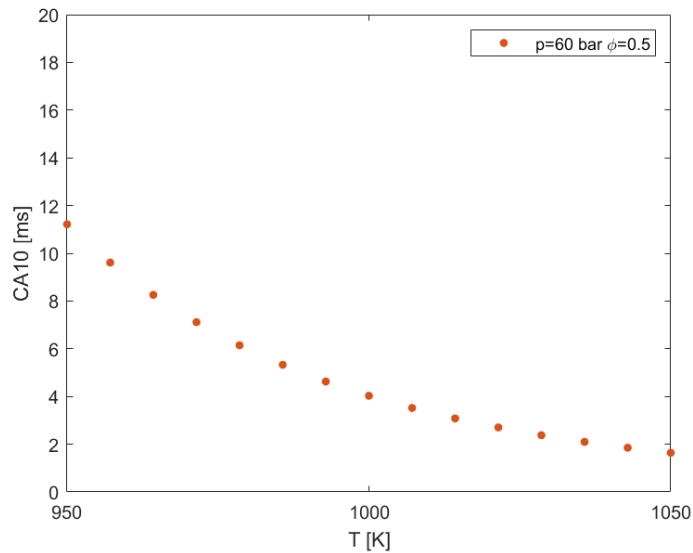


Figure 10.4: Results of the ignition model for NH_3/H_2 mixture with $10\%_{mole} H_2$

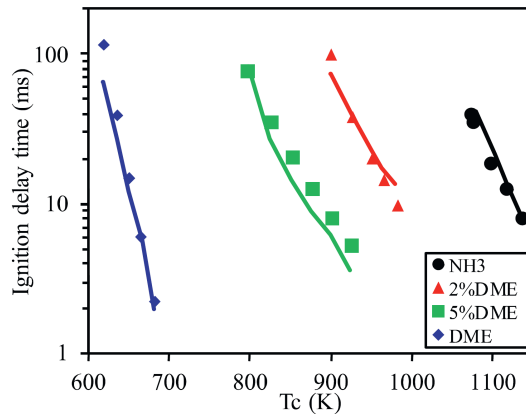


Figure 10.5: Measured ignition delay times of NH₃ and DME mixtures at $p_c=60$ bar and $\phi = 0.5$ Dai et al. [2021]

The ignition model predicts that there is no ignition before approximately 880 Kelvin for the NH₃/DME mixture at $p=60$ bar and with $\phi = 0.5$. For 900 K, the ignition model predicts an CA10 of 23 ms. Although the definitions of ignition differ, this is likely to be an underestimation of the ignition delay time.

The conclusions on the validation of the ignition model are;

- The ignition delay time of NH₃/DME is somewhat overestimated (the ignition occurs earlier in RCM measurements).
- The ignition delay of NH₃/H₂ is somewhat underestimated.
- There is no experimental data available regarding the ignition delay of ammonia, hydrogen, and DME.

For the objective of this model, gaining insight into the order of magnitude and trends, the validation is acceptable but shows the need for additional experimental data.

10.4 Assumptions, limitations, and uncertainties

Most of the assumptions, limitations, and uncertainties of the ignition model are also applicable to the engine cylinder model in the next chapter. Therefore, both models will be mentioned to avoid cluttering the report and only engine cylinder model specific points will be mentioned in the next chapter.

The models have several assumptions and limitations due to their set-up and due to the properties of a single-zone thermodynamic model. The main assumptions are:

- Constant volume (only the ignition model)
- Single-zone
- No incorporation of fluid dynamics
- Gaseous fuel
- Ideal gas

10 Ignition model

The constant volume of the ignition model leads to an overestimation of the pressure rise rate at CA10 compared to a combustion in an engine cylinder. The pressure rise rate at varying volume will be investigated in the next chapter with the engine cylinder model.

A single-zone models a homogeneous charge. Although an initial insight can be gained into the required stratification, a limitation of both models is that they cannot predict the ignition and performance of a stratified cylinder charge.

The single-zone cannot take into account the effect of crevice regions on the combustion efficiency. The effect of crevice regions is relevant because of ammonia's high quenching distance, as discussed in [section 3.1](#). These crevice regions will affect the combustion efficiency and unburned ammonia emissions.

Another consequence of the single-zone is that everything is instantaneous. For example, adding or removing heat will result in a homogenous change in temperature throughout the cylinder. This is not relevant for the ignition model because there is no heat flow from the reactor, but will be relevant for the engine cylinder model. A similar consequence is when, for example, hydrogen is added. The hydrogen instantaneously is mixed homogeneously throughout the reactor, although in reality it may combust directly after injection and have no time to mix. This limits this modeling method in accurately modeling late or multiple fuel injections.

Both models are thermodynamic models and therefore do not consider fluid dynamics. As seen in [chapter 5](#), in-cylinder turbulence plays a substantial role in the combustion. This effect is not considered in both models.

Ammonia has a high heat of vaporization. Therefore, assuming that all fuel is gaseous will lead to an overestimation of the efficiency, as the heat loss of the vaporization is not accounted for in this model. In this model, it is assumed that the ammonia vaporizes before it enters the combustion chamber.

The high latent heat of vaporization of ammonia also leads to a low speed of vaporization. This low speed of vaporization will cause a larger ignition delay than will be predicted by this model, where the fuel is gaseous when entering the combustion chamber.

Both models make use of the Cantera 'Ideal Gas Reactor' and assume that all gases behave like ideal gases. An ideal gas follows the ideal gas law, [Equation 10.11](#) [[Stapersma, 2009](#)].

$$pV = n\bar{R}T \quad (10.11)$$

In which:

- p is the pressure in Pa
- V is the specific volume in m^3
- n is the number of moles
- \bar{R} is the ideal gas constant in $\text{J}/(\text{mol}\cdot\text{K})$
- T is the temperature in Kelvin

For an ideal gas the internal energy (u) and enthalpy (h) are only dependent on temperature.

The main uncertainty comes from the chemical kinetic mechanism. The mechanism of [Shrestha et al.](#) is validated for the combination of ammonia and hydrogen. However, the mechanism has not been validated by the authors for the combination of ammonia-hydrogen-DME. To reduce this uncertainty, the outcomes of the ignition model have been compared to experimental studies with ammonia/DME and ammonia/hydrogen within the validation.

10.5 Results

The research starts with the ignition of the fuel mixture with a composition of 80%_e NH₃ 20%_e H₂ and no DME. This is the composition used in the case study of [de Vos](#), which is described

in the introduction. The pressure is initially set at 50 bar and the ignition of the mixture is studied at different equivalence ratios and temperatures (T_{TDC}). The initial pressure of 50 bar is chosen based on the experimental results of Chiera et al.. In the results of their motored experiments, without ignition, the maximum pressure is 60 bar. As the compression ratio of the AmmoniaDrive test engine is lower, CR of 14 vs. CR of 17, a lower initial pressure is chosen.

For the mixture composition of Ammonia and hydrogen, without DME, the effect of the temperature, pressure, equivalence ratio, and NH_3/H_2 on the CA10 and PRR at CA10 is investigated.

Then the ignition research continues with mixtures of ammonia, hydrogen, and DME. For this mixture, the effect of the $\%_e$ on the CA10 and PRR at CA10 is investigated.

Three remarks on the graphical representation of the results in the figures in this chapter:

- The unit of the ignition delay is CAD, the ignition delay in ms is converted to crank angle degree (CAD), based on 1200 rpm.
- Every marker represents a simulation, with an initial pressure, initial temperature, fuel composition and equivalence ratio.
- Markers are colored and occasionally encircled. The same color, between different figures, refers to the same initial temperature and the same initial pressure. And encircled markers of the same color are the same within different figures. This means the fuel composition, the initial pressure, the initial temperature, and equivalence ratio are the same.

10.5.1 Ammonia and hydrogen, without DME

As mentioned, the research starts with the ignition of 80% $_e$ NH_3 20% $_e$ H_2 , and no DME. The results of these simulations are shown in Figure 10.6a and Figure 10.6b.

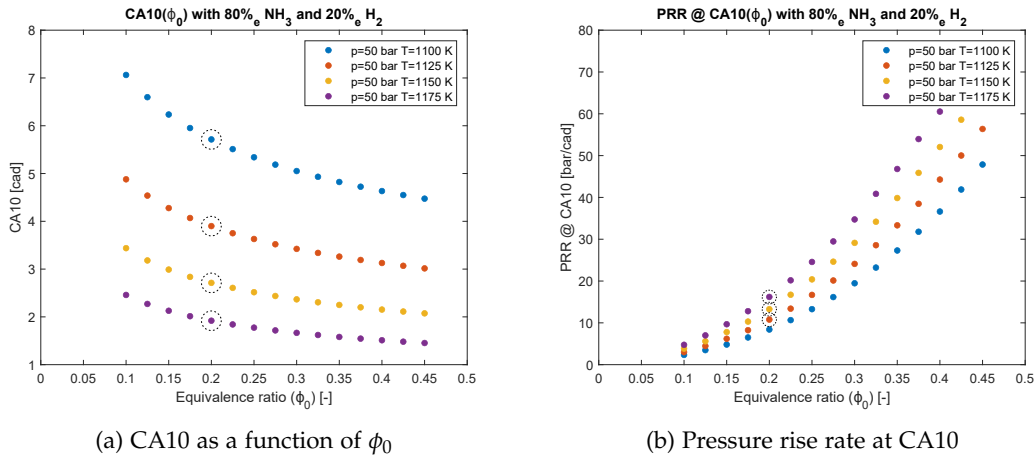


Figure 10.6: Results for varying ϕ_0 , $p=50$ bar at different T_{TDC} .

Figure 10.6a shows the ignition delay for different equivalence ratio's at different temperatures. Figure 10.6a shows the corresponding pressure rise rate (PRR) at CA10. The limit for the PRR is approximately 10-15 bar/CAD, higher PRRs exceed the engine limits. Figure 10.6b

10 Ignition model

shows that an equivalence ratio above 0.225 starts to have PRR above 10-15 bar/CAD. This implies that the equivalence ratio probably has to be lower than approximately 0.225. Based on this, a starting point of $\phi = 0.2$ is chosen for the engine cylinder model in the next chapter. From these results, it can also be concluded that to achieve ignition within the required time frame with this mixture composition, the temperature around TDC should be 1125-1150 Kelvin, if the pressure at TDC is 50 bar.

The next step is to study the effect of the initial pressure. The yellow encircled data point of Figure 10.6a is the same in Figure 10.7a. In Figure 10.7a, it can be seen that an initial pressure of 60 and 70 bar, lowers the ignition delay by approximately 0.4 CAD. Unfortunately, it can be seen in Figure 10.6b that the pressure rise at CA10 increases significantly. Therefore, the ignition research continues with a p_{TDC} of 50 bar.

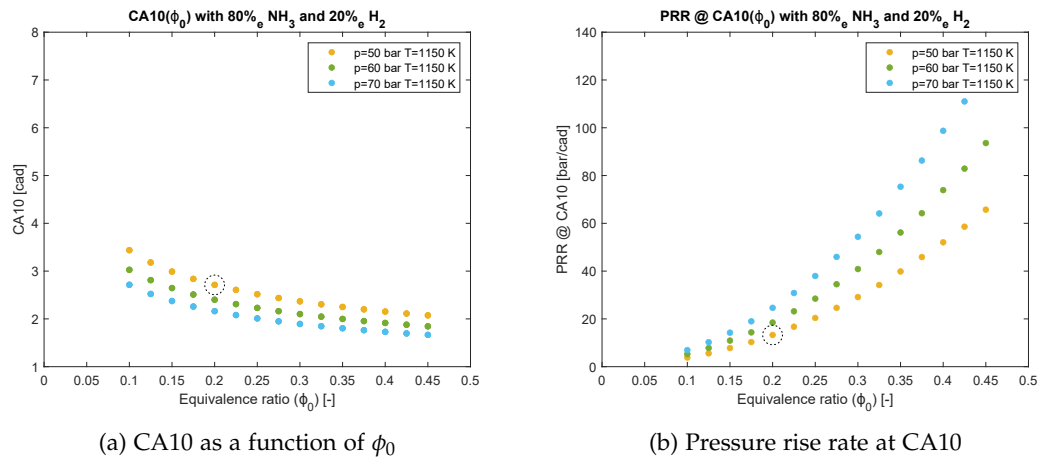


Figure 10.7: Results for varying ϕ_0 , $p=50/60/70$ bar and $T_{TDC}=1150$ K.

The following step is to vary the mixture composition, still without DME. The results are shown in Figure 10.8a and Figure 10.8b. From these results, it can be seen that increasing the hydrogen fraction advances the ignition. However, this also increases the pressure rise rate at CA10 beyond engine limits. Therefore, the hydrogen energy fraction is maintained at 20%.

The next step is to add DME. The energy ratio between ammonia/hydrogen continues to be 80/20%. As an example, when the DME energy fraction is 10%, from the remaining 90%, 72% comes from ammonia and 18% from hydrogen.

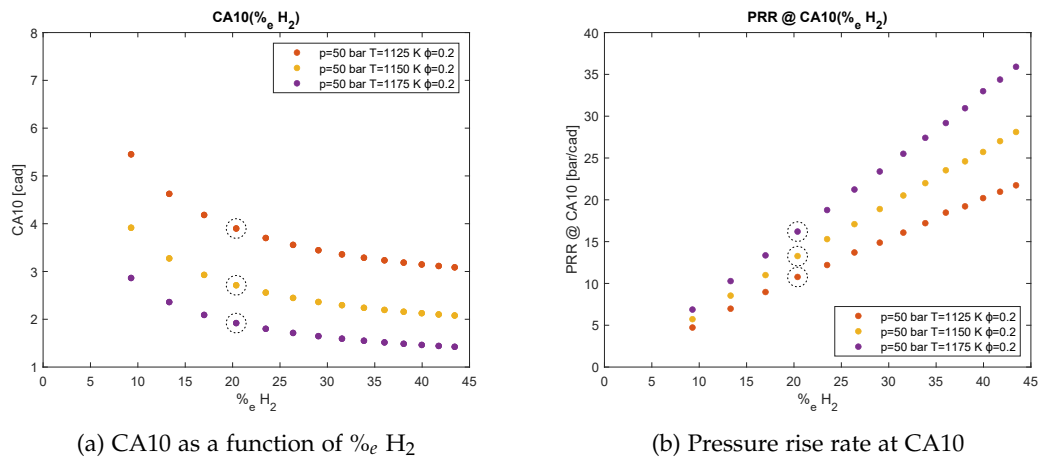


Figure 10.8: Results for varying %_e H₂ for p=50 bar and varying T_{TDC}

10.5.2 Ammonia, hydrogen, and DME

The ignition research continues with an ammonia, hydrogen, and DME fuel mixture. The results are shown in Figure 10.9a and Figure 10.9b. It can be seen that increasing the DME fraction advances the ignition and with less PRR increase than hydrogen. This results in a lower required temperature for achieving an ignition within the required time (crank angle) frame. Especially for lowest temperature (1075K) the effect is noteworthy. 10%_e DME decreases the ignition delay by 3 CAD.

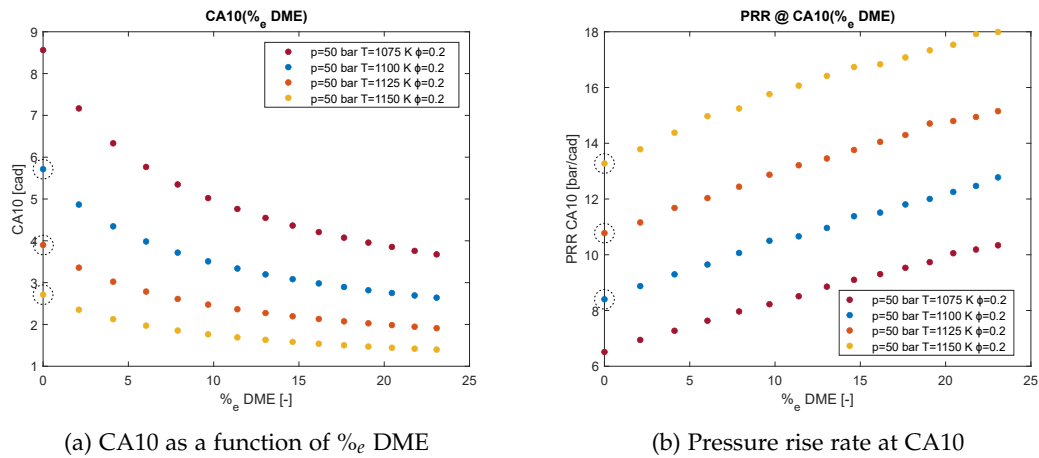


Figure 10.9: Results for varying %_e DME, at p=50 bar and varying T_{TDC} .

Conclusion and next steps

Conclusions on ignition

The ignition of fuel compositions has been investigated with and without DME.

- Ammonia and hydrogen, without DME
 - An equivalence ratio above 0.225 starts to have PRR above 10-15 bar/CAD, which exceeds engine limits.
 - With a p_{TDC} of 50 bar, the T_{TDC} has to be around 1125-1150 K to achieve ignition within the required time frame.
 - Increasing the initial pressure decreases the ignition delay somewhat, but it is accompanied by a significant increase in pressure rise rate.
 - Increasing the hydrogen fraction advances the ignition, however, this also increases the pressure rise rate at CA10 beyond engine limits.
- Ammonia, hydrogen and DME
 - Increasing the DME fraction advances the ignition. Especially at the lower temperature of 1100 Kelvin (50 bar and $\phi = 0.2$), the ignition is advanced by ± 2 CAD by 10%_e DME. This results in a lower possible temperature while still achieving an ignition within the required time (crank angle) frame.
 - The ignition advance due to DME comes with less rise of the pressure rise rate compared to increasing hydrogen. This allows to stay within engine limits.

Next steps

The ignition behavior of different fuel compositions has been investigated at varying top dead center conditions. This led to a narrowing down of potential feasible fuel compositions. In the next chapter, the combustion of these fuel compositions is investigated with an engine cylinder model.

The engine cylinder has several ICE properties that are not considered in the ignition model. For example, the volume is not constant and the p_{TDC}/T_{TDC} are not set, as they were in the ignition model. These properties are consequences of other parameters such as the compression ratio, piston speed, inlet temperature, and heat loss.

With the engine cylinder model, the following questions will be investigated:

- What is the expected engine cylinder performance (CA10 and MPRR) of a CI combustion of ammonia and hydrogen, without DME, in the AmmoniaDrive test engine?
- What is the expected engine cylinder performance (CA10 and MPRR) of a CI combustion of ammonia, hydrogen, and DME in the AmmoniaDrive test engine?
- What is the relationship between the mixture composition and (maximum) pressure rise rate?
- How does the mixture composition affect the emissions?

11 Engine cylinder modeling

Outline

This chapter provides an estimate of what to expect when using ammonia, hydrogen, and DME in the AmmoniaDrive test engine. The objective is to create insight into the performance and possibilities of the AmmoniaDrive test engine.

This estimation is done with the so-called 'engine cylinder model, which incorporates more CI ICE phenomena than the ignition model of the previous chapter. Table 9.1 provided an overview of the variables of the engine cylinder model and the ignition model.

The engine cylinder model is a single zone closed volume thermodynamic reactor model. It simulates an HCCI compression ignition combustion in a single cylinder. The modeling of the engine cylinder is carried out in Python & Cantera, in contrast to the ignition model, which is developed in Matlab & Cantera. The reason for the switch to Python & Cantera, was that the heat loss could not be incorporated well with the Matlab & Cantera combination.

The model is constructed with several Cantera objects. An overview of the engine cylinder is shown in Figure 11.1. The Cantera objects used for the engine cylinder model are the reactor, wall, and reservoir. The reactor represents the cylinder, the wall represents the piston, and the reservoir represents the ambient air. Figure 11.1 shows a graphical representation of the engine cylinder model.

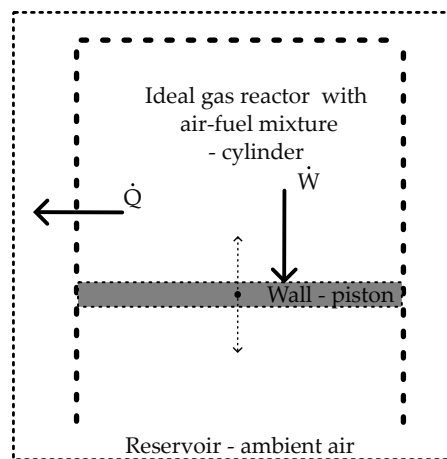


Figure 11.1: Graphical representation of the engine cylinder model with the incorporated Cantera objects and what the objects represent.

Using Cantera and a chemical kinetic mechanism to model a combustion is a not widely used approach within the TU Delft Marine Engineering department. Therefore, exploring the software started with simple tests to discover the methods and possibilities of the software.

Cantera provides several examples on their website [Cantera, 2023b]. These examples formed the starting point of the engine cylinder model.

The engine cylinder model is a closed volume model to avoid issues with mass flow. The part of the cycle that is covered by the engine cylinder model is shown in Figure 11.2. It starts with the fuel and air present at bottom dead center, with p_{BDC} and T_{BCD} . Then the model compresses the cylinder content until TDC and expands from TDC to the end of simulation of 45 CAD ATDC. Whether ignition and combustion take place, depends on the fuel-air mixture and engine parameters.

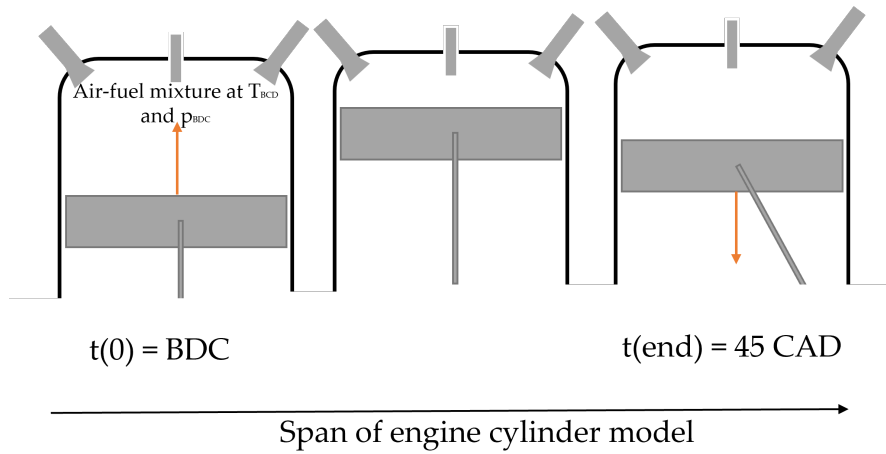
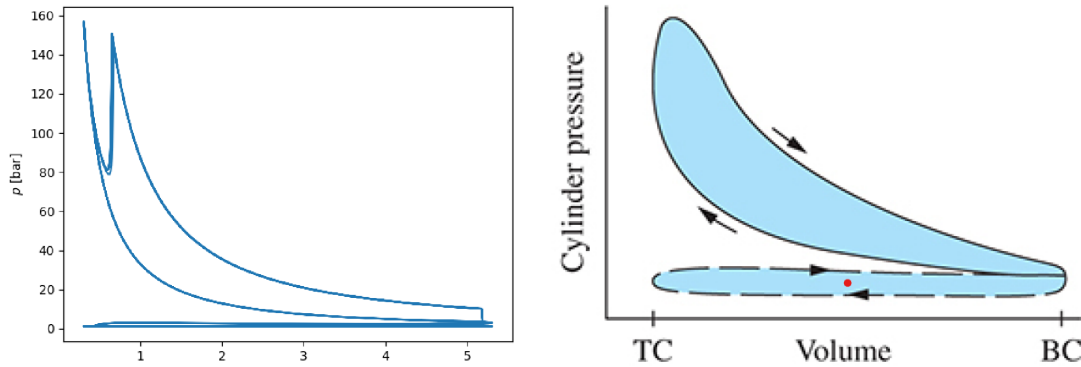


Figure 11.2: Part of the cycle that is covered by the engine cylinder model

An overview of the engine cylinder model output of a single simulation can be seen in Appendix O. An example of a p-V diagram is shown in Figure 11.3a to provide context why the modeling of the engine cylinder is important after the ignition research. In this figure, an undesirable dip can be seen at the top left of the p-V diagram. This indicates that the fuel did not ignite close enough to TDC. For comparison, Figure 11.3b shows a regular p-V diagram, where the ignition timing is closer to TDC. A shorter ignition delay can be achieved by, for example, a higher inlet temperature, higher initial pressure, higher compression ratio or a different mixture composition.

This model provides an initial answer to the following research questions:

- What is the expected engine cylinder performance (CA10 and MPRR) of a CI combustion of ammonia and hydrogen, without DME in the AmmoniaDrive test engine?
- What is the expected engine cylinder performance (CA10 and MPRR) of a CI combustion of ammonia, hydrogen, and DME in the AmmoniaDrive test engine?
- What is the relationship between the mixture composition and (maximum) pressure rise rate?
- How does the mixture composition affect the emissions?



(a) Result of engine cylinder model: p-V diagram (b) p-V diagram of 4-stroke turbocharged engine by Heywood [2018] where the ignition is too late

Figure 11.3: p-V diagrams

11.1 Equations & definitions

This section will describe the governing equations of the engine cylinder model, a single-zone thermodynamic model.

11.1.1 Governing equations reactor

The governing equations for the engine cylinder model are partially different compared to the equations of the ignition cylinder. This is due to the Wall object, that represents the piston, and the heat loss that is incorporated.

The first equation, Equation 11.1, describes the mass content of the reactor.

$$\frac{dm}{dt} = \sum_{in} \dot{m}_{in} - \sum_{out} \dot{m}_{out} + \dot{m}_{wall} \quad (11.1)$$

$$\frac{dm}{dt} = 0 - 0 + 0$$

The mass flows, \dot{m}_{in} and \dot{m}_{out} , are zero because the engine cylinder model is a closed volume. There is no mass transfer through the Cantera object 'Wall', thus $\dot{m}_{wall} = 0$. Therefore, Equation 11.1 equals zero.

The second governing equation, Equation 11.2, describes the volume change. The subscript 'w' refers to the Cantera object 'Wall'. This governing equation is different from the ignition model, as there is Wall object representing the piston with a velocity.

$$\frac{dV}{dt} = \sum_w f_w A_w v_w(t) \quad (11.2)$$

The variables in Equation 11.2 are:

- f_w determines the direction of the Wall, this determines whether it decreases or increases the volume of the reactor. In this case, f_w is -1, because a positive (upward) velocity of the piston, should lead to a decrease in the reactor.

11 Engine cylinder modeling

- A_w is the wall area. This is equal to the area of the piston.
- $v_w(t)$ is the set piston velocity.

The piston velocity is approximated as a sinusoidal velocity.

$$v(t) = l \cdot \pi \cdot f \cdot \sin(\theta(t)) \quad (11.3)$$

In which,

- l is the stroke in meter
- f is the engine speed in rps
- θ is the crank angle

Substituting [Equation 11.3](#) and the other variables into [Equation 11.2](#) leads to:

$$\frac{dV}{dt} = -1 \cdot \left(\frac{d}{2}\right)^2 \cdot l \cdot \pi^2 \cdot f \cdot \sin(\theta(t)) \quad (11.4)$$

The third governing equation, [Equation 10.3](#), originates from the first law of thermodynamics and describes the temperature.

$$mc_v \frac{dT}{dt} = -p \frac{dV}{dt} + \dot{Q} + \sum_{in} \dot{m}_{in} \left(h_{in} - \sum_k u_k Y_{k,in} \right) - \frac{pV}{m} \sum_{out} \dot{m}_{out} - \sum_k \dot{m}_{k,gen} u_k \quad (11.5)$$

There is no mass flow, $\dot{m}_{in} = \dot{m}_{out} = 0$, \dot{Q} equals the heat loss, and $\frac{dV}{dt}$ is defined by [Equation 11.4](#). This simplifies the third governing equation to [Equation 11.6](#).

$$mc_v \frac{dT}{dt} = -p \frac{dV}{dt} + \dot{Q} - \sum_k \dot{m}_{k,gen} u_k \quad (11.6)$$

The fourth governing equation of the ideal gas reactor describes each homogeneous phase specie:

$$m \frac{dY_k}{dt} = \sum_{in} \dot{m}_{in} (Y_{k,in} - Y_k) + \dot{m}_{k,gen} - Y_k \dot{m}_{wall} \quad (11.7)$$

The fourth governing equation can be simplified to [Equation 11.8](#) because there is no mass flow in or mass flow through a Wall object.

$$m \frac{dY_k}{dt} = \dot{m}_{k,gen} - Y_k \quad (11.8)$$

11.1.2 Definitions & Calculations

The definitions of Q_f ([Equation 10.8](#)) and $\%_e$ of a fuel component ([Equation 10.9](#)), defined in the previous chapter, are also applied for the engine cylinder model.

Work

The indicated work of a cycle has been defined as [Equation 11.9](#) [[Stapersma, 2010a](#)]. In this research, the indicated work (W_i) is the work during the closed cylinder process.

$$W_i = \oint p dV \quad (11.9)$$

Power

The indicated work is used to calculate the power in Equation 11.10. In this equation, the factor two accounts for the 4-stroke.

$$P_i = \frac{W_i}{2 \cdot (1/f)} \quad (11.10)$$

Indicated cylinder efficiency

Analogue to Stapersma [2010a], the indicated cylinder is defined as;

$$\eta_i = \frac{W_i}{Q_f} \quad (11.11)$$

In which Q_f is the available heat in the fuel. This is calculated based on the lower heating values of the fuel components.

Emissions

The produced emissions are calculated in g/kWh by Equation 11.12.

$$Emission_i = \frac{X_{end,i} \cdot m_{cyl}}{P_i} \quad (11.12)$$

In Equation 11.12 $X_{end,i}$ is the mass concentration of specie 'i' at t_{end} of the simulation and m_{cyl} is the mass present in the cylinder.

11.1.3 Heat transfer model

Zheng [2020] investigated an HCCI combustion of NH_3 and H_2 in his graduation research and simulated the engine of the experimental set-up of Pochet et al. [2020a]. Pochet et al. [2020b] explains that the Hohenberg model was used to model their HCCI combustion and Zheng also used the model of Hohenberg to incorporate the heat transfer.

A more in-depth investigation on the accuracy of heat transfer models with an HCCI combustion has been done by Broekaert et al. [2015]. Broekaert concludes that there is not an accurately predicting heat transfer model. For the engine cylinder model, the Hohenberg heat transfer model is used, as it is an easily implemented heat transfer model and there is no suitable alternative yet. With the objective of this model, that is acceptable, as the heat transfer likely has the right order of magnitude.

The model and parameters of Hohenberg are based on measurements in conventional diesel engines. The heat transfer coefficient, h , is given by Equation 11.13 [Hohenberg, 1979].

$$h = C_1 \cdot V_c^{-0.06} \cdot p^{0.8} \cdot \bar{v}_p^{-0.4} (\bar{v}_p + C_2)^{0.8} \quad (11.13)$$

In which,

The heat transfer to the wall mainly depends on the flow conditions close to the wall [Hohenberg, 1979]. And the model of Hohenberg is based on conventional diesel engines with in-cylinder turbulence induced by late diesel injections. But a HCCI combustion with ammonia and diesel will not have the same in-cylinder turbulence as conventional diesel engines have. This discrepancy in flow conditions is where the uncertainty regarding the heat loss stems from, as the flow conditions for an HCCI combustion of NH_3 and H_2 are unlike a conventional diesel combustion.

11 Engine cylinder modeling

h	heat transfer coefficient	$[\frac{W}{m^2K}]$	T	mean gas temperature	K
C_1	constant	-	\bar{v}_p	mean piston speed	m/s
V_c	cylinder volume	m^3	C_2	constant	-
p	pressure	bar			

11.2 Verification & Validation

The engine cylinder model is an extended version of the ignition model. Therefore, the verification & validation (V&V), described in [section 10.3](#), of the ignition model forms the basis of the V&V of the engine cylinder model. The V&V of the engine cylinder model consists of [section 10.3](#) and this section.

11.2.1 Verification

The verification of the engine cylinder model is consists of two parts. The first is verifying the behavior of the components of the model, such as the heat loss and cylinder volume. In the second part of the verification, the behavior of the entire model is compared to known engine cylinder behavior.

Verification of model components

The model components that are inspected for behavior are:

- Cylinder volume change
- Cylinder pressure change without combustion
- Cylinder temperature as a function of crank angle
- The combustion reaction by confirming that the heat release from the combustion reaction corresponds to the supplied fuel energy (Q_f) based on the lower heating value (LHV)s.
- The fuel composition by confirming that the energy fraction of the fuels present at $t=0$ matches the fractions set as input variables.

Verification of complete model

In the second part of the verification, the behavior of the complete model is evaluated. The behavior is evaluated at:

- Fuel cut off scenario
- Varying the mixture composition
- Varying engine parameters
 - Inlet temperature
 - Compression ratio
 - Engine speed

11.2.2 Validation

The validation performed for the ignition model is also applicable here, as the engine cylinder model is an extended version of the ignition model. The base of both models are the Cantera object 'ideal gas reactor' and the chemical kinetic mechanism.

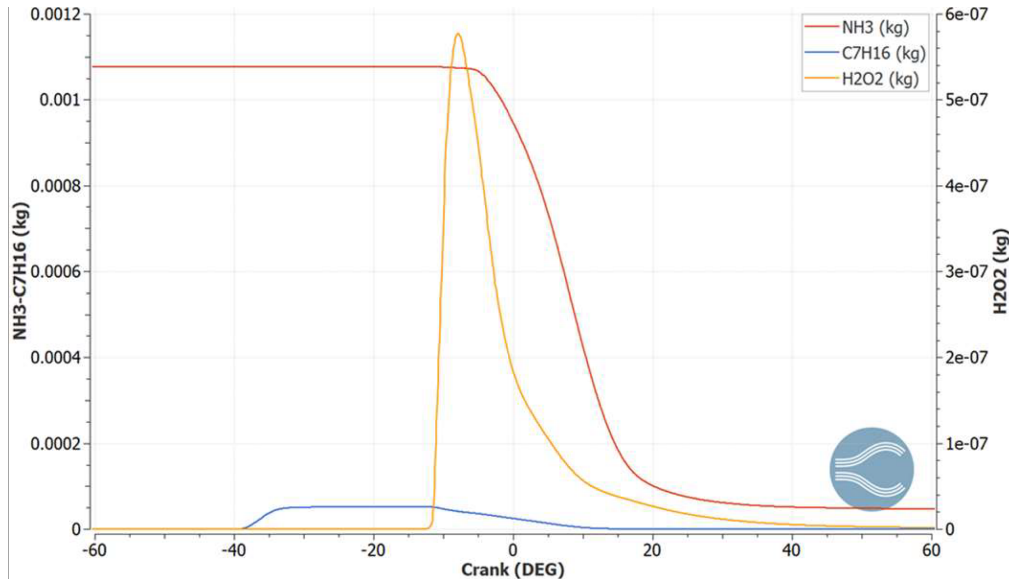


Figure 11.4: Evolution of fuel in the modeling results of Chiera et al. [2022]

As mentioned, there is no experimental data yet of a compression ignition combustion of ammonia, hydrogen, and DME. To validate the model, the results are compared with the modeling and experimental results of Chiera et al. [2022]. The combustion mechanisms of this study and Chiera et al. are different. The engine cylinder model is an HCCI combustion, whilst the model and experiment of Chiera et al. is a RCCI combustion. This difference complicates the comparison. On the other side, the set-ups are very similar, as can be seen in Table 11.1. This overview of engine parameters illustrates the similarity of the experimental set-ups.

Parameter	Chiera et al.	AmmoniaDrive	unit
Stroke	210	220	mm
Bore	170	170	mm
Compression ratio	17	14	-
Inlet temperature	65	up to 70	°C
Inlet pressure	2.4		bar

Table 11.1: Comparison test engines Chiera et al. [2022] and AmmoniaDrive

11.2.3 Comparison with modeling results

The objective of comparing the results of this model and the modeling study of Chiera et al. is to validate this model. Figure 11.4 shows the presence of fuel components in the combustion chamber, approximately $1.08e^{-3}$ kg NH_3 and $5e^{-5}$ kg C_7H_{16} . The LHV of heptane is 44.5 MJ/kg [Zhang et al., 2022]. The amount of injected energy, based on Equation 10.9, is equal to:

$$E_{fuel} = (44.5 \cdot 5e^{-5}) + (1.08e^{-3} \cdot 18.5) = 22.205 \text{ kJ} \quad (11.14)$$

The engine parameters, fuel composition, and injected energy of the Chiera's modeling

study are applied in the engine cylinder model. The input parameters of the engine cylinder model for this validation are:

- 82.5 %_e NH₃
- 17.5 %_e DME
- Fuel energy per cycle 22.2 kJ
- Inlet temp 65 °C
- Inlet pressure 2.4 bar
- Compression ratio 17 [-]
- Equivalence ratio 0.4 [-]

There are significant differences between the combustion concept of Chiera et al. and this study. These differences should align with the discrepancies between the results of the engine cylinder model and the modeling study of Chiera et al..

The most important difference is the combustion strategy. Chiera et al. investigated an RCCI combustion, whereas this model simulates an HCCI combustion. The HCCI combustion strategy will not be able to reach the same ammonia %_e, because the fuel will not ignite. Therefore, the validation is done with 82%_e NH₃ and 18%_e H₂. When the DME %_e is further decreased, the a small undesirable dip, like the one shown in Figure 11.3a start to appear. This indicates the ignition is too late. This aligns with the expectations, that an RCCI combustion concept can achieve a higher %_e NH₃.

Another difference due to the combustion strategies is the pressure. The maximum pressure and maximum pressure rise rate (MPRR) should be higher with an HCCI combustion. This is also confirmed by the modeling results. The maximum pressure in the modeling study of Chiera et al. is 205 bar, whilst the result of the engine cylinder model is 250 bar. The MPRR of Chiera et al. is not given but the engine cylinder model result is 118 bar/CAD, which is certainly beyond the engine limits.

The second difference is the fuel. Chiera et al. consisted of ammonia and diesel. However, their modeling study is done with 90 %_e ammonia and 10 %_e heptane, as can be deduced from Figure 11.4 on the legend. Heptane, C₇H₁₆, is the zero point of the octane number. This means it will ignite easily when being compressed. The reason for using heptane is not mentioned in the publication. It could be due to limitations of available chemical kinetic mechanisms. The engine cylinder model is limited to DME as a carbon-based fuel. The ignition properties of DME and heptane are not the equal. Heptane will have a shorter ignition delay, which means a higher %_e NH₃ can be achieved.

Chiera et al. showed that the heat release is closely related to production of H₂O₂. The engine cylinder model shows a higher and more narrow peak, which is similar to the difference is heat release.

The conclusions on the validation comparison between the modeling results of Chiera et al. and the engine cylinder model are that;

- The discrepancies are as expected based on theoretical expectations.
- It shows similar trends for the H₂O₂.
- The results of the engine cylinder model have the expected order of magnitude based on the results of Chiera et al..

11.2.4 Comparison with experimental results

The experimental results of Chiera et al. are shown in Figure 11.6 for an 81%_e NH₃. Noteworthy is the lower peak pressure, 137 bar, compared to their modeling results, where the peak pressure was 205 bar. The heat release rate of the experimental results of Chiera et al. is unfortunately normalized. This lower peak pressure can possibly be explained by a decrease in supplied fuel energy (Q_f).

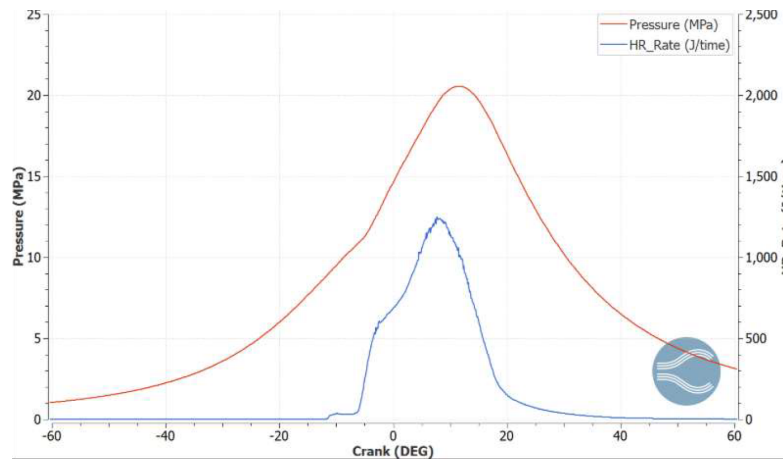


Figure 11.5: Resulting heat release and pressure of Chiera et al. [2022]

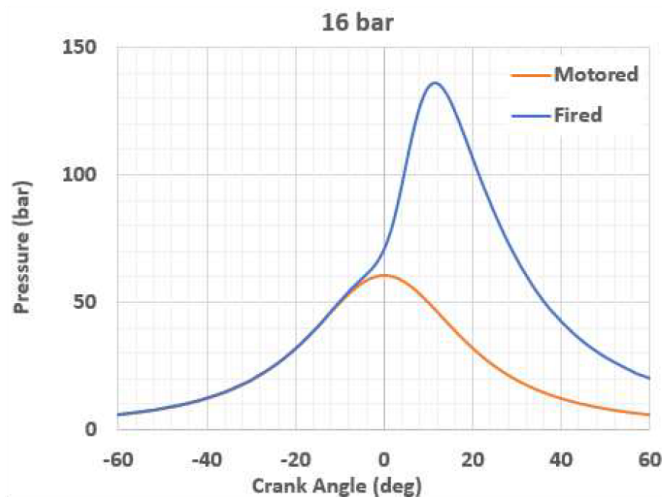


Figure 11.6: Cylinder pressure of the experimental result of Chiera et al. [2022]

To achieve a similar decrease in peak pressure, the injected fuel energy is decreased by 45% by lowering the equivalence ratio to 0.23, whilst keeping the other variables the same. The equivalence ratio is as expected based on the results of the ignition model research.

The objective of the engine cylinder model is providing an initial insight into the possibilities and limitations for CI combustion of ammonia and hydrogen within the AmmoniaDrive project. Considering the verification and validation of the ignition model and the engine cylinder model, these models are capable of fulfilling their objective. For future, more exact predictions of the cylinder performance, experimental data of a mixture with ammonia, hydrogen, and a carbon-based fuel is required.

11.3 Limitations, assumptions, and uncertainties

The limitations, assumptions, and uncertainties of the ignition model are also applicable for the engine cylinder model, except for the one related to the constant volume.

An additional assumption is that the geometric compression ratio is equal to the effective compression ratio.

The main uncertainty comes from the chemical kinetic mechanism, as described in the previous chapter. An additional uncertainty is the heat loss. The heat loss is based on the Hohenberg heat loss equation.

11.4 Results

The investigation of the engine cylinder performance is set up in the same way as the ignition research. It starts with investigating a fuel composition without DME, then DME is added, and the ratio between ammonia and hydrogen is varied. Then research continues with the effect of mixture composition on the CA10, maximum pressure rise rate, and the emissions.

The engine parameters are set at:

- Inlet temp 45 °C
- Inlet pressure at BDC of 2 bar
- Compression ratio 14 [-]
- Equivalence ratio 0.2 [-]

11.4.1 Fueled by ammonia and hydrogen, without DME

The starting point is a fuel composition without DME, analogue to the ignition research. The composition is 80%_e NH₃ and 20%_e with an equivalence ratio (ϕ) of 0.2. Figure 11.7 shows the expected pressure and temperature. The engine cylinder model predicts that there will be no ignition for a fuel without DME in the AmmoniaDrive test engine. Therefore, the research will focus further on a fuel consisting of ammonia, hydrogen, and DME.

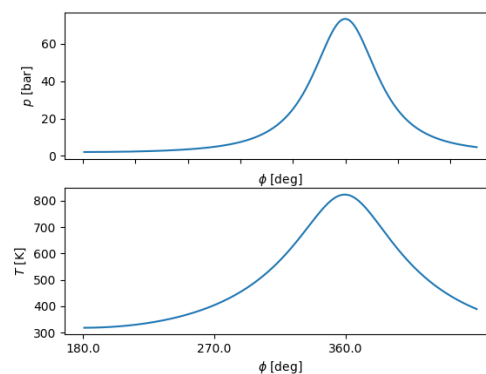


Figure 11.7: Pressure and temperature results of 80%_e NH₃ and 20%_e H₂

11.4.2 Fueled by ammonia, hydrogen, with DME

As seen, the engine cylinder model indicates that there will be no ignition without DME in the AmmoniaDrive test engine. Therefore, the research continues to identify the minimum amount of DME required. This is done by varying the %_e of DME, while the remainder of the energy is split 80/20 between NH₃/H₂. The CA10 and corresponding MPRR are shown in Figure 11.8a. From these results, it can be seen that 17.5%_e, the circled markers, results in a CA10 of 372 CAD and an MPRR of 10 bar/CAD. The MPRR of 10 bar/CAD is approximately the engine limit, however the CA10 is a little late. This can be seen from the corresponding p-V diagram shown in Figure 11.8b, the late ignition results in a dip in the top-right corner of the p-V diagram. The p-V diagram in Figure 11.8b only shows the part where the cylinder is a closed volume. The research on the ignition indicated that hydrogen can improve the ignition. Therefore, the next step is to investigate the effect of changing the ammonia/hydrogen energy ratio.

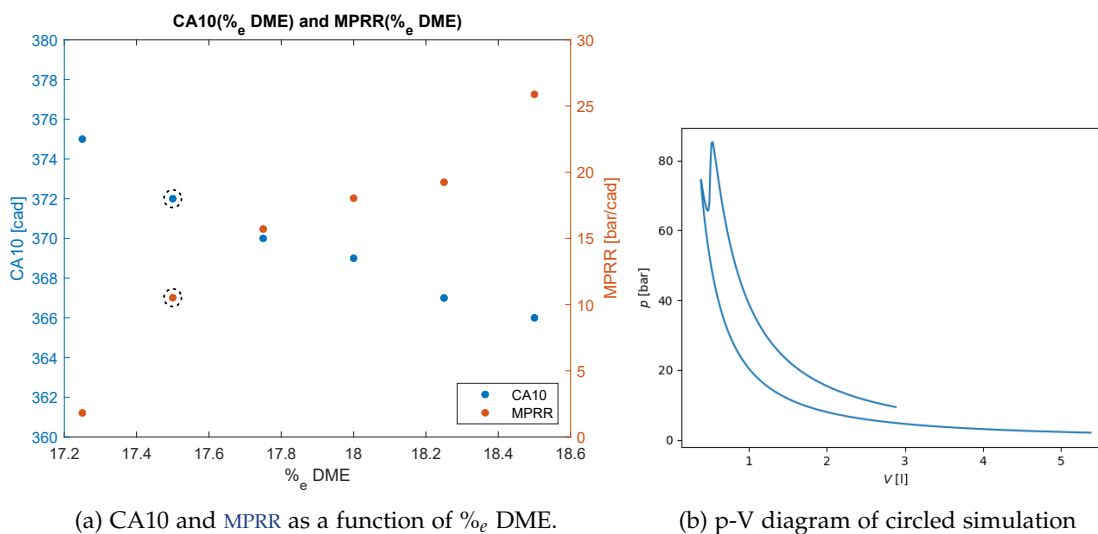


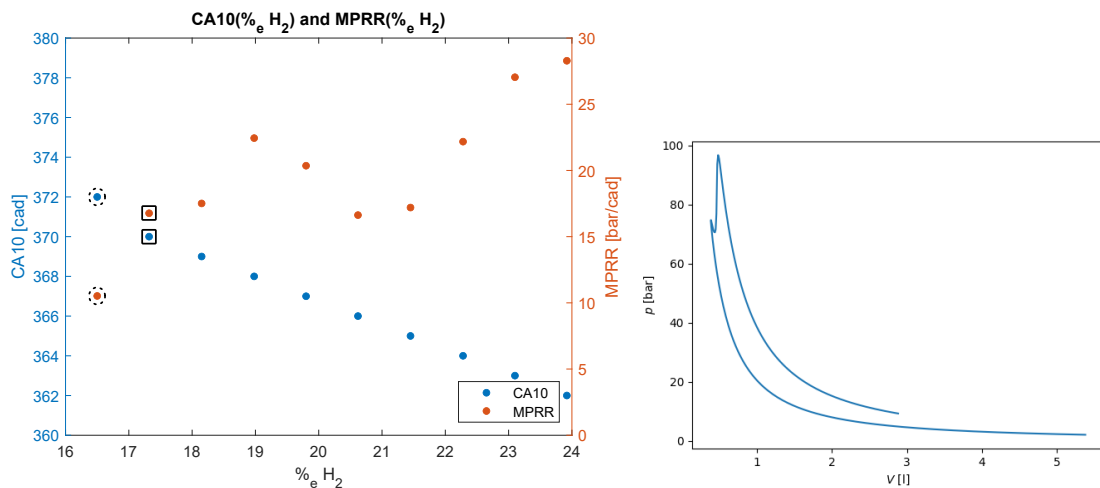
Figure 11.8: Results of varying the energy fraction of DME fraction, with a constant energy ratio between NH₃/H₂ of 80/20%_e

Figure 11.9a shows the effect of varying the H₂ %_e. Between 19-21%_e there appears to be a steep decline. This is remarkable, but could be explained by one of the key points of chapter 3 "There is a threshold in the mixture ratio of ammonia/hydrogen where the ammonia combustion promotion by hydrogen steeply declines. The value of this threshold depends on the operating conditions.". The effect of the hydrogen addition on the p-V diagram is shown in Figure 11.9b. The dip at the top left of the p-V diagram has decreased, which shows that the ignition has been advanced but also the MPRR has increased. This indicates that hydrogen can lower the required amount of DME, but only if the MPRR does not exceed engine limits.

Lastly, the engine cylinder model is used to investigate the expected emissions and how those are influenced by the mixture composition. The DME fraction is constant at 17.5%_e and the energy ratio between NH₃ and H₂ is varied.

It can be seen from Figure 11.10, that a low energy fraction of hydrogen, and thus a high energy fraction of ammonia, leads to higher CO emissions. This is probably due to incomplete combustion. This shows the positive effect of adding hydrogen to this combustion.

11 Engine cylinder modeling



(a) CA10 and MPRR as a function of %_e H₂. The circled marker corresponds to the circled marker in Figure 11.8a. (b) p-V diagram of the simulation corresponding to the marker with a square around it in Figure 11.9a.

Figure 11.9: Results of varying the energy ratio between NH₃ and H₂, with DME fraction constant at 17.5%_e

And there appears to be a reciprocity between NO₂ and NO, when one decreases, the other increases. This can likely be explained by the higher temperature due to the higher hydrogen fraction.

The optimum in terms of emissions is not a straightforward point. Because, as concluded in chapter 6, emissions can only be compared well when the countermeasures, such as an SCR, are considered. And multiple researchers describe the use of the unburned ammonia in an SCR to reduce the NO_x in the exhaust. Which would mean that a higher amount of unburned ammonia directly after the combustion chamber, could lead to lower emissions by the end of the exhaust system.

When reviewing all results, it appears that the amount of energy injected is considerably lower than when a conventional fuel is used. The limiting factor is the pressure rise rate. This shows the need for another combustion mechanism, such as RCCI. The results of the ignition model and engine cylinder model do show the potential for a RCCI combustion. The stratification within the cylinder can be achieved by stratifying the DME and hydrogen.

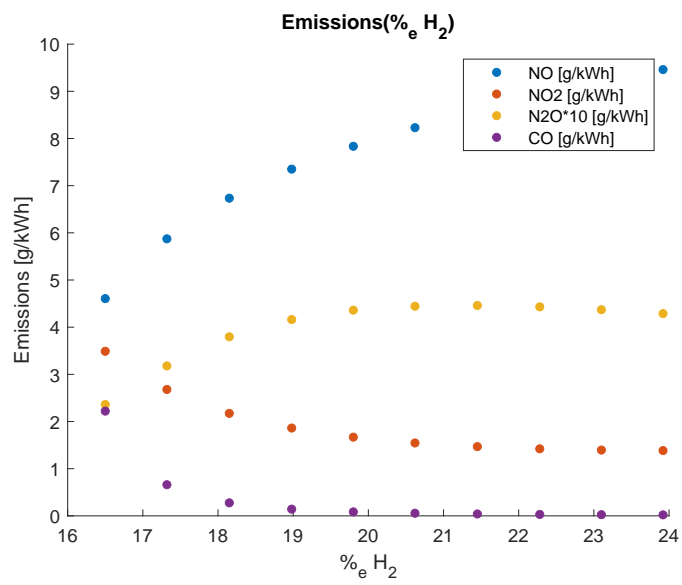


Figure 11.10: Effect on the emissions of varying the energy ratio between NH₃ and H₂, with DME fraction constant at 17.5%_e

Conclusions and future steps

Conclusions on engine cylinder behavior

The ignition of fuel compositions has been investigated with and without DME in the previous chapter. In this chapter, the behavior of the engine cylinder with these fuel compositions has been investigated. Based on the results of this model, the following conclusions can be drawn:

- A carbon-based fuel is required to achieve ignition. Because the required TDC conditions for compression ignition cannot be achieved within the limits of the AmmoniaDrive test engine.
- Hydrogen seems to improve the combustion, as a higher energy fraction of hydrogen, decreases the CO emissions. And hydrogen advances the ignition, which can lower the required amount of DME, but only if the MPRR does not exceed engine limits.
- With HCCI the amount of fuel energy that can be injected, whilst staying within the engine limits, is too low to be feasible. An alternative is a RCCI combustion, where the reactivity is distributed to lower the pressure rise rate. Additional research needs to be done what a good distribution of the reactivity would be and how this distribution can be achieved.
- The engine speed in this research has been set to 1200 rpm, based on the generator version of the AmmoniaDrive test engine. To achieve higher engine speeds, the ignition delay will need to decrease. A decrease in ignition delay can be achieved by a higher T_2 and/or p_2 , but this is not achievable via compression ignition, considering the engine limits of the AmmoniaDrive test engine. Therefore, a lower engine speed, such as 1200 rpm, is recommended. Another option is to investigate spark ignition (SI), as is planned within the AmmoniaDrive project.

Future steps

Multi-zone to model RCCI combustion and SI. Compare results of this model with experimental results of ammonia, hydrogen and DME. Compare the results of different mechanisms, such as the mechanism of [Issayev et al. \[2022\]](#). [Issayev et al.](#) has developed a mechanism for NH_3/DME , together with several authors of the [Shrestha et al. \[2018\]](#) used in this study.

11.5 Reflection on modeling method

This graduation research prepares for further research within the AmmoniaDrive project. Therefore, an important question is 'Is it recommended to continue using this modeling technique?'. The answer to this question comes from an assessment of the accuracy, possibilities, and limitations of the applied modeling technique. However, a definitive answer on the accuracy cannot be given, as there are no experimental results available yet and other chemical kinetic mechanisms should be explored.

An important limitation of a single-zone model is the lack of ability to correctly predict the ignition delay of an RCCI combustion. For an RCCI combustion mechanism, the ignition delay strongly depends on the injection timing. An early injection leads to a longer ignition delay

because the fuel has more time to mix and there will be less fuel rich regions [Chiera et al., 2022]. This effect is not captured by a single-zone model. Which could lead to the suggestion that a single-zone model is more suitable for modeling conventional dual fuel or HCCI, and less for an RCCI combustion.

The chemical kinetic mechanism incorporates the reaction kinetics into a model. An advantage of this is the insight into intermediate species and the formation of pollutants. This was also applied in the validation, where the generation of H_2O_2 corresponded between the different modeling techniques.

The available species in a chemical kinetic mechanism limit the combinations of fuels constituents. This affected this research because the most promising combination, from literature, would be ammonia, hydrogen, and HVO. However, HVO was not available in chemical kinetic mechanisms.

Alternatives to model the combustion are, among others, a Wiebe or Seiliger function. However, this provides no insight into intermediate species and the formation mechanisms of pollutants, and it needs experimental data to determine the Wiebe or Seiliger parameters.

A strategy could be combining a Wiebe function and a chemical kinetic mechanism, although not in the same model. A chemical kinetic mechanism allows for a prediction of the combustion. This can be used to make a more accurate prediction on how a Wiebe function would change, given a change in the fuel or engine parameters. Such a strategy could possibly combine the strong points of both methods.

12 Conclusion

This thesis studied compression ignition (CI) combustion of ammonia and hydrogen within the context of the AmmoniaDrive project. It started with reviewing the literature to gain insight into the available research, fuels, combustion concepts, and the current state-of-the-art experimental and numerical results.

The available research is currently scarce, as there are limited experimental results available of CI combustion of ammonia and even less combining ammonia and hydrogen. The amount of research projects related to the combustion of ammonia in an ICE coming up, however, seems promising. One of those is the AmmoniaDrive project.

The main challenge with using ammonia as the main fuel, is offsetting the high ignition resistance. This has, among others, been successfully experimentally achieved by an HCCI combustion concept of Pochet et al. [2020a] with NH_3/H_2 and an RCCI combustion concept of Chiera et al. [2022] with $\text{NH}_3/\text{diesel}$. The HCCI combustion concept requires a compression ratio of 22, a high intake temperature, and is limited by the maximum pressure rise rate. The RCCI combustion concept has experimentally achieved up to 81%_v NH_3 , but still requires 19%_v diesel.

These concepts are considered the starting point for this research. The next step from the HCCI concept is to lower the required CR and intake temperature. The next step from the RCCI concept is to decrease the amount of required carbon-based fuel. These next steps have to be combined with the properties and limitations of the AmmoniaDrive test engine.

Due to the limitation imposed by the available species in chemical kinetic mechanisms, the chosen carbon-based fuel in the modeling study is DME. For the future experiments, hydrotreated vegetable oil (HVO) seems a more favorable carbon-based fuel, based on experimental results in a constant volume combustion chamber (CVCC) of Hernández et al. [2023].

To research a compression ignition combustion strategy of ammonia and hydrogen within the AmmoniaDrive test engine, a modeling study is performed. This modeling study consists of two models, the ignition model and the engine cylinder model. The ignition model studied the mixture composition and top dead center (TDC) conditions to achieve ignition, whilst staying within the test engine limits, such as a maximum pressure rise rate (MPRR) lower than 10-15 bar. The results of the ignition model answered the first three research questions of this thesis. The research questions are listed in Appendix B.

The first research question of the thesis concerns the effect of the mixture composition of ammonia, hydrogen, DME, and air on the ignition properties. The mixture composition is split into the effect of the equivalence ratio (ϕ) and the effect of the fuel composition. The pressure rise rate rises exponentially with the equivalence ratio for an 80/20%_v ammonia and hydrogen mixture. And an equivalence ratio above 0.225 has a PRR of 10-15 bar/CAD, which exceeds engine limits. Therefore, the equivalence ratio has been kept constant at 0.2. The ignition model also showed an advancement of the ignition with an increasing hydrogen energy fraction, unfortunately this also increased the MPRR beyond engine limits. Increasing the energy fraction of DME also advanced the ignition and with a lower increase of MPRR compared to hydrogen.

12 Conclusion

Then the effect of the p_{TDC} and T_{TDC} on the ignition is investigated with the ignition model. With a p_{TDC} of 50 bar, the T_{TDC} has to be around 1125-1150 to achieve ignition within the required time frame. When the initial pressure is increased to 60 and 70 bar, the ignition delay decreases by approximately 0.4 CAD, unfortunately, it is accompanied by a significant increase in pressure rise rate.

The last research question answered by the ignition model, is the effect of the addition of hydrogen to a mixture of ammonia, air, and DME on the required amount of carbon-based fuel. The ignition advance due to hydrogen comes with more rise of the pressure rise rate compared to increasing DME. This easily exceeds engine limits. Increasing the DME fraction advances the ignition. Especially at the lower temperature of 1100 Kelvin (50 bar and $\phi = 0.2$), the ignition is advanced by +2 CAD by 10%_e DME. This results in a lower possible temperature while still achieving an ignition within the required time (crank angle) frame.

The results of the ignition model are used as input for the engine cylinder model to assess the engine cylinder performance of the AmmoniaDrive test engine (CA10 and MPRR). This starts with a CI combustion of ammonia and hydrogen, without DME. Based on the engine cylinder model, it seems unlikely that ignition will occur without a carbon-based fuel within the AmmoniaDrive test engine. This confirms the expectations based on literature. Therefore, the recommended fuel for the compression ignition concept¹ of the AmmoniaDrive project is ammonia, hydrogen and a carbon-based fuel.

Then the engine cylinder performance of a CI combustion of ammonia, hydrogen, and DME in the AmmoniaDrive test engine is investigated. When keeping the DME fraction constant at 17.5%_e and varying the hydrogen energy fraction, there there appears to be a steep decline 19-21%_e of the MPRR. This is an effect that should be investigated further. Hydrogen does seem to be able to lower the required amount of DME, but only if the MPRR stays within engine limits.

Lastly, the effect of the mixture composition on the emissions is investigated. The DME energy fraction is kept constant and the ammonia/hydrogen ratio is varied. It appears that a low energy fraction of hydrogen, and thus a high energy fraction of ammonia, leads to higher CO emissions. This is probably due to incomplete combustion.

This expected maximum pressure rise rate indicates the need for a RCCI combustion concept, as a HCCI combustion cannot achieve a sufficient power output without exceeding the MPRR limit (10-15 bar/CAD). The engine cylinder model results also indicate that the combination of ammonia, hydrogen, and DME is very suitable for an RCCI combustion concept. This can be seen from the large effect that the %_e of DME has on the CA10. 17.25%_e DME leads to a CA10 of 1 CAD ATDC and 17.5%_e DME leads to a CA10 of 7 CAD ATDC. These numbers should be considered as an initial estimate, as the objective is to identify the order of magnitude and trends. The trend shows that by stratifying the DME concentration throughout the cylinder, it is likely that the MPRR can be reduced. This would allow for a higher power output due to the possibility to inject more fuel energy without exceeding the engine limits.

Combining the literature and modeling results, it is likely that an RCCI combustion concept with ammonia, hydrogen, and HVO will lead to a higher power output and a decreased required amount of carbon-based fuel, whilst staying within engine limits.

The gain of this thesis research exceeds the studied topic. As the modeling method, using

¹This graduation research focuses on a compression ignition combustion concept and the results may not be applicable for the spark ignition concept of the AmmoniaDrive project.

a chemical kinetic mechanism to model the combustion reaction, is new for the Maritime and Transport Technology department. This method could allow for a more adequate forecast of the cylinder performance when there is no experimental data available yet. It is not a substitution of Wiebe function, as a Wiebe function likely will have a better fit as soon as there is experimental data. But when there is the need for extrapolation, a chemical kinetic mechanism can have added value.

13 Discussion and Recommendations

This research can be divided into two parts; a literature study and modeling study. The literature study is the result of reviewing the available literature, to collect what is useful within the scope of the compression ignition concept of the AmmoniaDrive project. The modeling study is the first step to assess the performance of the compression ignition combustion within the AmmoniaDrive test engine.

A discussion point within the literature is the definition of RCCI. There are always two fuels with an RCCI combustion: a high- and low-reactivity fuel. Typically, the LRF is injected via port fuel injection. And the injection strategy of the HRF can determine the mixture reactivity. This provides one certain property of RCCI which is the possibility to adjust the mixture reactivity to the operating conditions. However, when the charge and combustion are homogeneous, but the reactivity of the mixture can be adjusted per cycle based on the measured pressure rise rate of the previous cycle, it will not always be classified as RCCI.

The main limitation for this study is the lack of experimental results for ammonia, hydrogen, and a carbon-based fuel. A reason for those lacking results, is that when a carbon-based pilot or promoter fuel is used, there is no need for hydrogen to enhance the combustion. And as the hydrogen storage and infrastructure has quite an impact, this would not be a favorable option. However, within the AmmoniaDrive project it is, because the hydrogen is supplied by the anode off-gas of the fuel cells. This eliminates a large part of the hydrogen storage. Although it was a limitation for this study, it shows the relevance of the AmmoniaDrive project.

The modeling study made use of a chemical kinetic mechanism to provide the reaction kinetics of the combustion reaction. This method has not been used within the TU Delft Maritime and Transport Technology department.¹ This fact made this graduation research quite an exploration into the unknown. The novelty of this research lies within the choice of fuels and combustion strategy. And additional added value lies within exploring the use of chemical kinetic mechanisms for single-zone thermodynamic models within Maritime and Transport Technology department.

In hindsight, the chemical kinetic mechanism of [Glarborg et al. \[2018\]](#), with some modifications by [Dai et al.](#) could possibly have been a better choice. This should have been identified earlier in the process, but the limited experience with this modeling method has hampered that. This limited experience caused seemingly trivial things, to take a considerable amount of time, such as the transformation of the text-files in which the chemical kinetic mechanism was distributed to a file that was functional with Cantera. This may be a drawback for this study, but it shows good opportunities for follow-up work as well.

Another knowledge gap identified by this study is the lack of applicable phenomenological models and a chemical-kinetic mechanisms for the combustion of ammonia, hydrogen, and a carbon-based fuel under CI engine conditions. The used chemical kinetic mechanism is known to underestimate the ignition delay, and there is no heat loss model which is based on the flow conditions of a combustion with ammonia and hydrogen. As a matter of fact, the flow conditions in the cylinder with these fuels are also largely unknown still. Which is not only relevant for the heat transfer but also for the progress of the combustion due to the turbulence.

¹A chemical kinetic mechanism has not been used to model the combustion reaction, but some have used the Zeldovich chemical mechanism for NO_x production.

13 Discussion and Recommendations

For this study, that is acceptable because the objective is to identify trends and find orders of magnitude. However, when this modeling technique is to be used for finding more accurate numbers, there is the need for appropriate phenomenological models, insight into the flow conditions and applicable chemical-kinetic mechanisms.

There are several follow-up studies directly possible from this graduation:

- Exploring other chemical kinetic mechanisms, such as the chemical mechanism of [Is-sayev et al. \[2022\]](#). And comparing the outcomes of chemical kinetic mechanisms with experimental results.
- A study on the ignition of an ammonia, hydrogen, and a carbon-based fuel, similar to studies used for the validation of the ignition model ([Dai et al. \[2020\]](#) and [Dai et al. \[2021\]](#))
- Investigating the heat loss of compression ignition combustion with a high %_v of ammonia.
- Expanding to a multi-zone model to model a stratified cylinder charge.

And when a chemical kinetic mechanism that gives accurate results for the AmmoniaDrive test engine is found, the number of tests can be limited.

Other combustion strategies can also be studied with this modeling method. Such as the effect of multiple injections on the combustion stability. Within this modeling method, fuel can be added during the combustion simulation. How accurate these results would be, should be validated by experiments. As the single zone thermodynamic model implies that the injected fuel would be instantly spread homogeneously throughout the cylinder, while in reality it may combust directly after injection close to the injector.

This discussion shows multiple opportunities for this modeling method, but it will mainly depend on the comparison with experimental results whether this method will be of added value, i.e. priority should be given to obtaining experimental results.

A Research questions - Literature research

Literature research

The literature research questions concern what is described and/or available in literature.

1. Which studies are available related or relatable to compression ignition combustion of ammonia, hydrogen and optionally a pilot fuel?
2. What are the components and mixture ratio of the fuels used?
3. What is known about compression ignition combustion of a mixture of ammonia & hydrogen?
4. Which combustion mechanisms are known for ammonia and ammonia & hydrogen? Which issues regarding this combustion are known in experimental studies?
5. Which injection strategies are present in literature in similar set-ups? And what are the reasons?
6. Which properties (such as injection pressure, timing and nozzle size) influence the direct injection of hydrogen?
7. What engine properties are suitable for the combustion of ammonia, hydrogen and optionally diesel?
8. Which models are available to numerically investigate the combustion of ammonia, hydrogen and optionally diesel?

B Research questions - Thesis

1. How does the mixture composition of ammonia, hydrogen, DME, and air affect the ignition properties?
2. How do p_{TDC} and T_{TDC} affect the ignition?
3. What effect does the addition of hydrogen to a mixture of ammonia, air, and DME have on the required amount of carbon-based fuel to accomplish an ignition with adequate properties?
4. What is the expected engine cylinder performance (CA10 and MPRR) of a CI combustion of ammonia, hydrogen, without DME in the AmmoniaDrive test engine?
5. What is the expected engine cylinder performance (CA10 and MPRR) of a CI combustion of ammonia, hydrogen, and DME in the AmmoniaDrive test engine?
6. What is the relationship between the mixture composition and (maximum) pressure rise rate?
7. How does the mixture composition affect the emissions?

C Experimental studies

Subscripts e= energy, l=load, v=volume, w=weight, and h=heat. Str = stroke. CO_{2eq} = GHG emissions equivalent to CO_2 over 100 years. Combustion mechanisms correspond to described mechanisms in chapter 4.

Study	Fuel(s)	% NH_3	% H_2	% other	Combustion mechanism	Type	CR	Engine rpm	Bore (mm)	Power (kW)	Emissions (g/kWh or ppm)
Nadimi et al. [2023]	NH_3 , diesel	84.2 % _e	-	15.8 % _e	CDF	1-cyl 4-str	16.5	1200	80	3	$CO_{2eq} = 243$
Kuta et al. [2023]	NH_3 , diesel	63 % _h	-	37 % _{oh}	CDF	1-cyl 4-str	16.5	1500	86.2	2.39	NO_x, N_2O, NH_3
Jin et al. [2023]	NH_3 and diesel	up to 85 % _e	-	down to 15 % _e	CDF/PPCI	1-cyl 4-str	18.5	1500	116	≈ 5	For 50 % _e NH_3 without diesel pre-inj: GHG 493, CO_2 187, NH_3 31, NO_x 7.91, N_2O 1.12 [g/kWh]
Mounaïm-Rousselle et al. [2022]	NH_3	100 %	-	-	SACI (=SI)	1-cyl 4-str	14-17	1000	75	n/a	NO_x, N_2O, NH_3 in ppm
Chiera et al. [2022]	NH_3, H_2 , diesel	81 % _e	-	19 % _e	RCCI	1-cyl 4-str	17	1500	170	≈ 80 +-15 (edu. guess)	$CO_{2eq} = 172$ g/kWh
Yousefi et al. [2022b]	NH_3 , diesel	40 % _e	-	60 % _e	CDF \rightarrow PPCI	1-cyl 4-str	16.25	910	137.2	15	$CO_{2eq} = 606.2$ g/kWh

C Experimental studies

Study	Fuel(s)	% NH ₃	% H ₂	% other	Combustion mechanism	Type	CR	Engine rpm	Bore (mm)	Power (kW)	Emissions (g/kWh or ppm)
Yousefi et al. [2022a]	NH ₃ , diesel	40 % _{o_e}	-	60 % _{o_e}	CDF → PPCI	1-cyl 4-str	16.25	910	137.2	15	CO _{2eq} = 478.10 g/kWh
Nadimi et al. [2022]	NH ₃ , bio-diesel	69.4 % _{o_e}	-	30.6 % _{o_e}	CDF	1-cyl 4-str	16.5	1500	86	3	@100% load 310 CO ₂ , 12.5 NO, 7 CO, 1.5 HC, 37 PM [g/kWh]
Zhang et al. [2022]	NH ₃ , n-heptane	50-70 % _{o_e}	-	50-30 % _{o_e}	RCCI	1-cyl 4-str	15	1000	88	n/a	With 50 % _{o_e} NH ₃ 760ppm NO, 110ppm NH ₃
Niki [2021b]	NH ₃ and diesel	45-60 % _{o_e}	-	% _e	PPCI / RCCI	1-cyl 4-str	18.5	1500	112	n/a	For 60% NH ₃ CO _{2eq} = 420 g/kWh. NOx was not taken into account, NOx is +6800 ppm
Kane and Northrop [2021]	NH ₃ , H ₂ and diesel	55 % _{o_h}	via TCR	45 % _{o_h}	CDF	4-cyl 4-str	17	1500	106	55	CO ₂ 300, soot 0.05, NH ₃ 30, NOx 2.2, N ₂ O 1.2 (before SCR)
Lhuillier et al. [2020]	NH ₃ , H ₂	80 % _{o_v}	20 % _{o_v}	-	SI	1-cyl 4-str	10.5	1500	77	n/a	For phi = 1 and x _{H₂} 20% 6000 NH ₃ and 3000 NOx [ppmv (wet)]
Pochet et al. [2020a]	NH ₃ , H ₂	94 % _{o_v}	6 % _{o_v}	-	HCCI	1-cyl 4-str	22	1500	86	≈2 kW if η _m = 0.8	Not clear. For higher % NH ₃ without EGR: 4000-6800 ppm NOx
Pochet et al. [2017b]	NH ₃ , H ₂ , diesel	up to 69 % _{o_v}	down to 31 % _{o_v}	-	HCCI	1-cyl 4-str	16	1500	88	≈1.5 kW if η _m = 0.8	For 69 % _{o_v} NH ₃ and φ=0.28: 764 ppm NOx
Ryu et al. [2014b]	NH ₃ , DME	40-60 % _{o_w}	-	60-40 % _{o_w}	HCCI for 60% NH ₃	1-cyl 4-str	20	1900	78	4.3	For 60% NH ₃ : 7 g/kWh NOx

Study	Fuel(s)	% NH ₃	% H ₂	% other	Combustion mechanism	Type	CR	Engine rpm	Bore (mm)	Power (kW)	Emissions (g/kWh or ppm)
Reiter and Kong [2011] and Reiter and Kong [2010]	NH ₃ , diesel	up to 80 % _e	-	down to 20 % _e	CDF	4-cyl 4-str	17	1000	106	40	NOx @80 % _e NH ₃ 31 g/kWh, NOx @60 % _e NH ₃ 11 g/kWh
Reiter and Kong [2008]	NH ₃ , diesel	40-80 % _e	-	60-20 % _e	CDF	4-cyl 4-str	17	1000 - 1400	106	≈ 20 @ 50% NH ₃	NOx @80 % _e NH ₃ 1650 ppm, NOx @60 % _e NH ₃ 800 ppm
Gross and Kong [2013]	NH ₃ , DME	up to 40 % _e	-	min 60 % _e	CI	1-cyl 4-str	20	max 3243	78	max 1.74	For the highest power output and 40 % _e NH ₃ +- 5g/kWh NOx

Subscripts e= energy, l=load, v=volume, w=weight, and h=heat. Str = stroke. CO_{2,eq} = GHG emissions equivalent to CO₂ over 100 years. Combustion mechanisms correspond to described mechanisms in chapter 4.

D Results Hernández et al. 2023

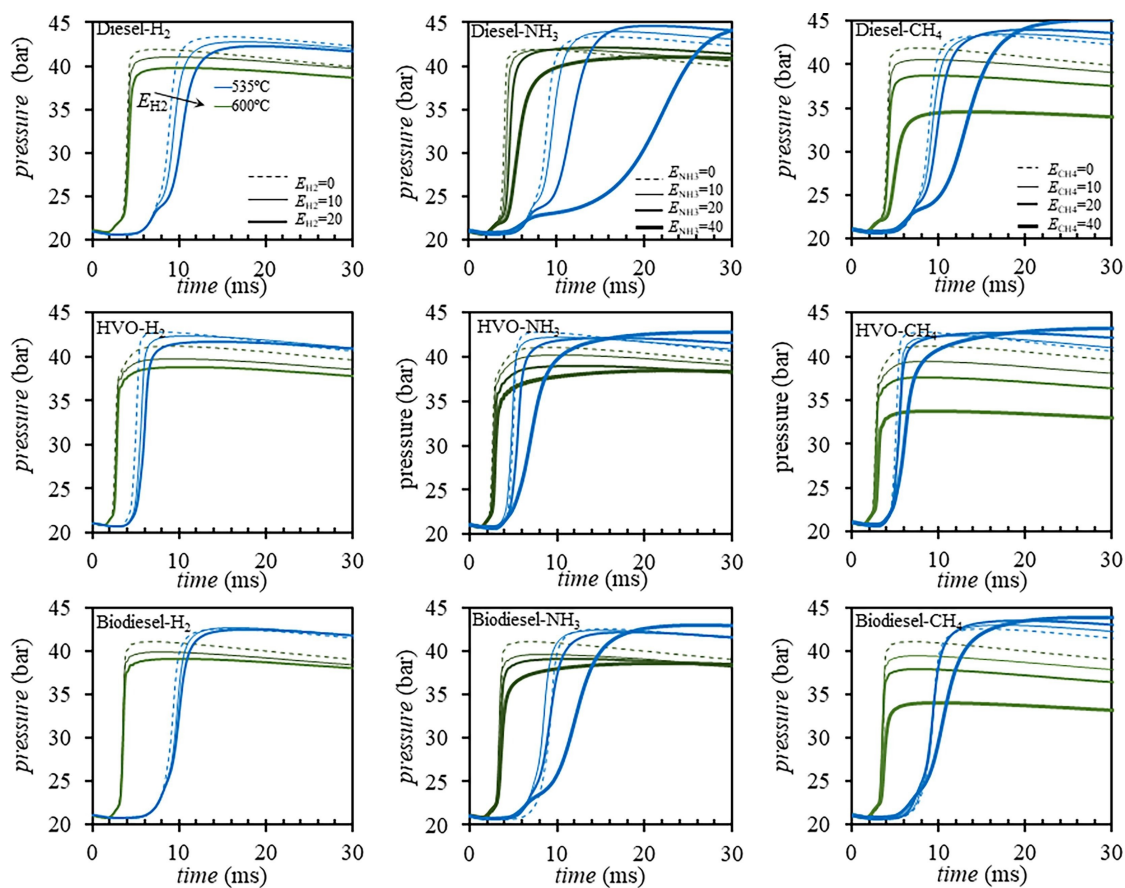


Figure D.1: Pressure traces for different combinations of LRF and HRF from Hernández et al. [2023]

E Spray shape different fuels

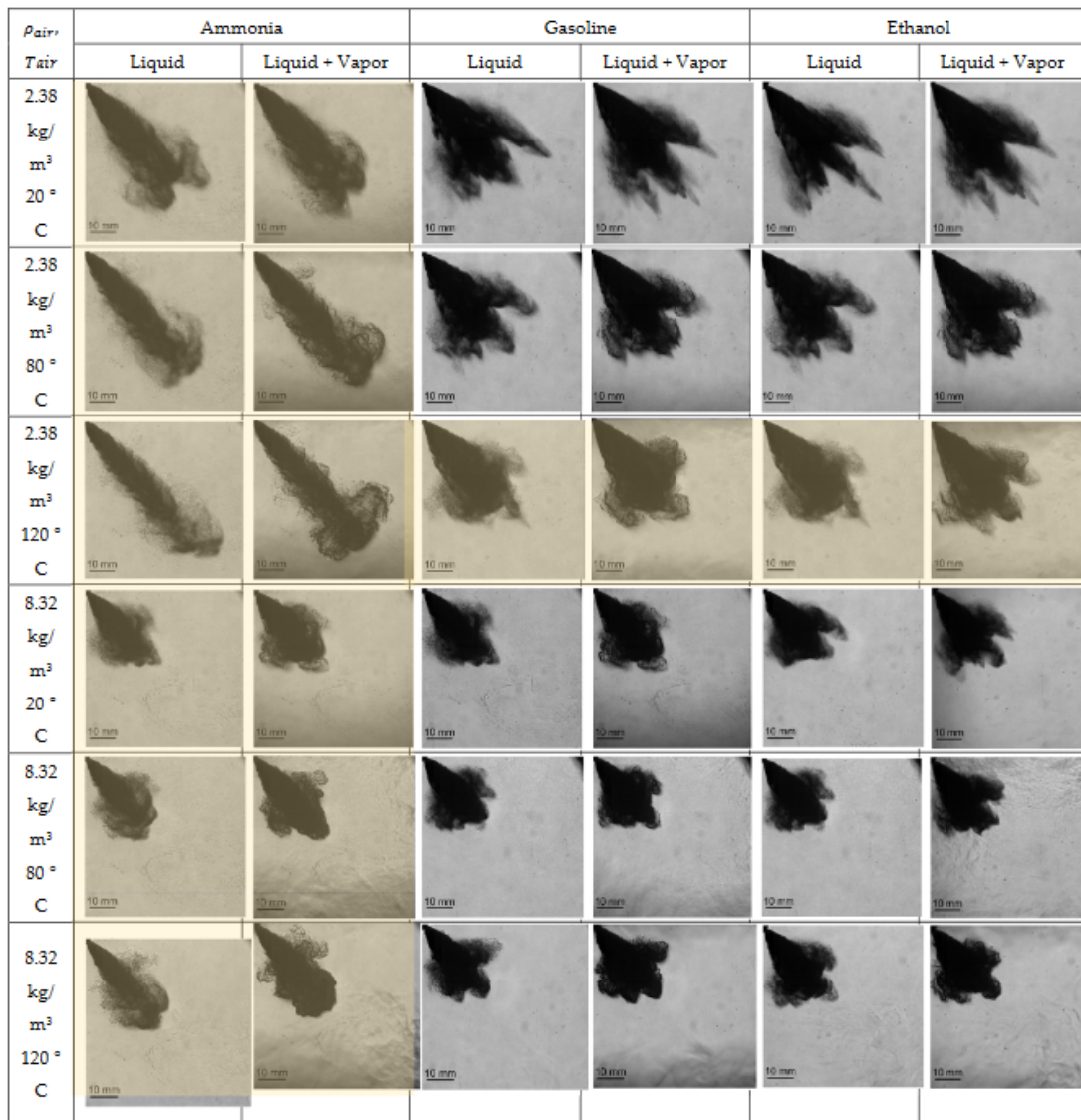


Figure E.1: Spray shapes 1 ms after the start of injection of ammonia, gasoline, and methanol at different conditions. From Pelé et al. [2021]

F Background – Fuel

Quenching distance

The quenching distance, d_q , is the distance between two parallel plates that will extinguish the flame. This phenomenon is the foundation of the miner's safety lamp, a maze where the openings are smaller than the quenching distance [Law, 2006]. Hydrogen has a relatively small quenching distance, while ammonia has a relatively large quenching distance.

Flammability limits

When a mixture of fuel, oxidizer and inert is either very fuel rich or very lean, it will become nonflammable. The flammable-nonflammable boundaries in composition are called the flammability limits and are an empirically observed phenomenon [Law, 2006]. The boundary on the lean side is called the lower flammability limit (LFL) and the boundary on the rich side, the upper flammability limit (UFL). Another empirically observed phenomenon is the widening of flammability limits with increasing temperature. This is important when considering the temperature of the air intake. Increasing the pressure can have different effects, for some fuels the flammability limits widen, for others they narrow [Law, 2006]. A first estimation of the LFL of a mixture can be done with the Châtelier's rule, Equation F.1, in which X_i is the mole fraction of the component.

$$LFL_{mix} = \left[\sum \frac{X_i}{LFL_i} \right]^{-1} \quad (F.1)$$

Flame speed

The laminar flame speed (s_u^0) and the laminar burning velocity (s_L^0) both refer to the propagation speed of a standard premixed flame. Standard stands for a one-dimensional, planar, adiabatic flame in a stationary mixture in an infinite domain. The two terms, laminar flame speed and laminar burning velocity, are used interchangeably, although the first is sometimes more used for the flame motion and the second as a flame property [Law, 2006]. The laminar flame speed depends on the properties of the fuel and on the mixture (composition, temperature, and pressure).

In an engine, the flame will have a turbulent character. However, relevant parameters as the turbulent flame propagation can often be related to the laminar flame speed. Therefore investigating the laminar flame speed of an alternative fuel is relevant.

Cetane number

The cetane number of a diesel fuel describes the ignition quality and is a measure of the tendency of a diesel fuel to knock. The higher the number, the more rapid the fuel autoignites.

F Background – Fuel

Cetane numbers for diesel fuels are typically within 40-55 [Heywood, 2018]. It is determined by the mixture ratio of cetane (CN=100) and heptamethylnonane (CN=15) which has the same ignition delay as the diesel fuel under investigation, as shown in Equation F.2 [Speight, 2015].

$$\text{cetane number} = \% \text{vol n-cetane} + 0.15(\% \text{vol heptamethylnonane}) \quad (\text{F.2})$$

Equivalence ratio

The equivalence ratio is defined as Equation F.3. $\phi > 1$ corresponds to a fuel rich combustion and $\phi < 1$ to a lean combustion.

$$\phi = \frac{m_f/m_{ox}}{(m_f/m_{ox})_{stoic}} \quad (\text{F.3})$$

G Results Niki et al.

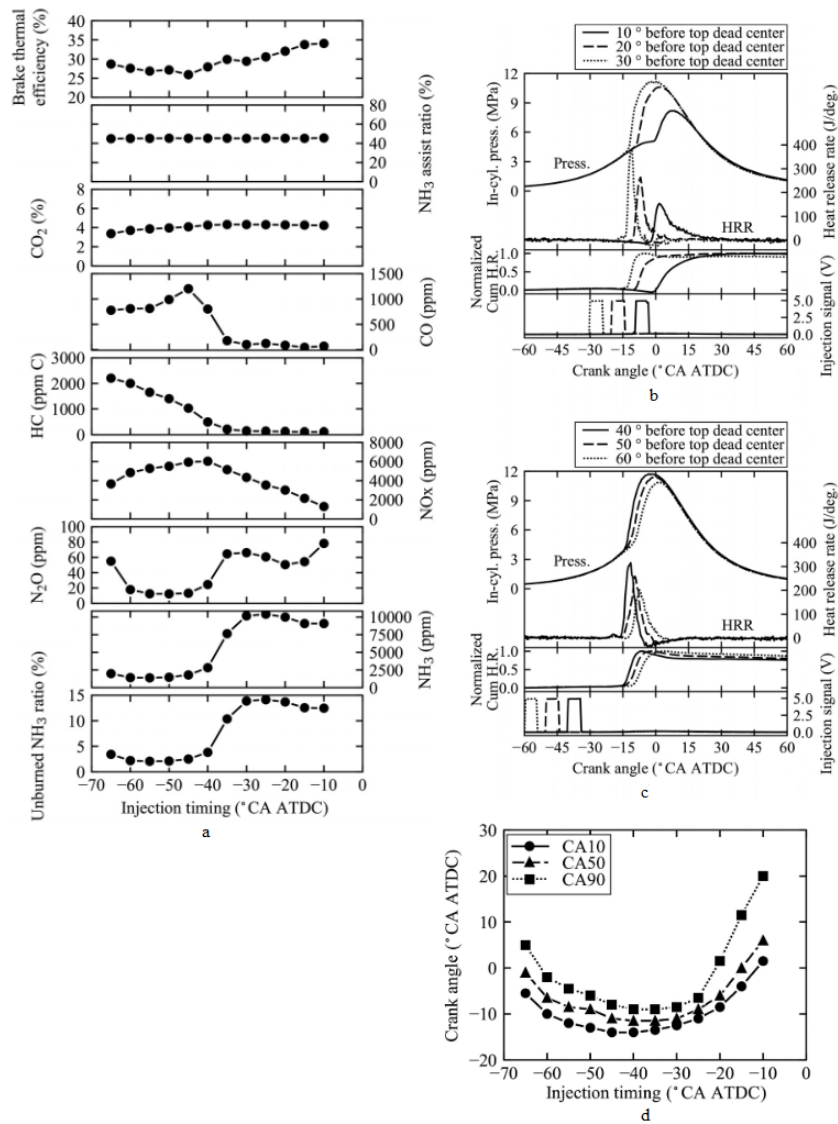


Figure G.1: From Niki [2021b]

H Results Niki et al. - Fuel reactivity

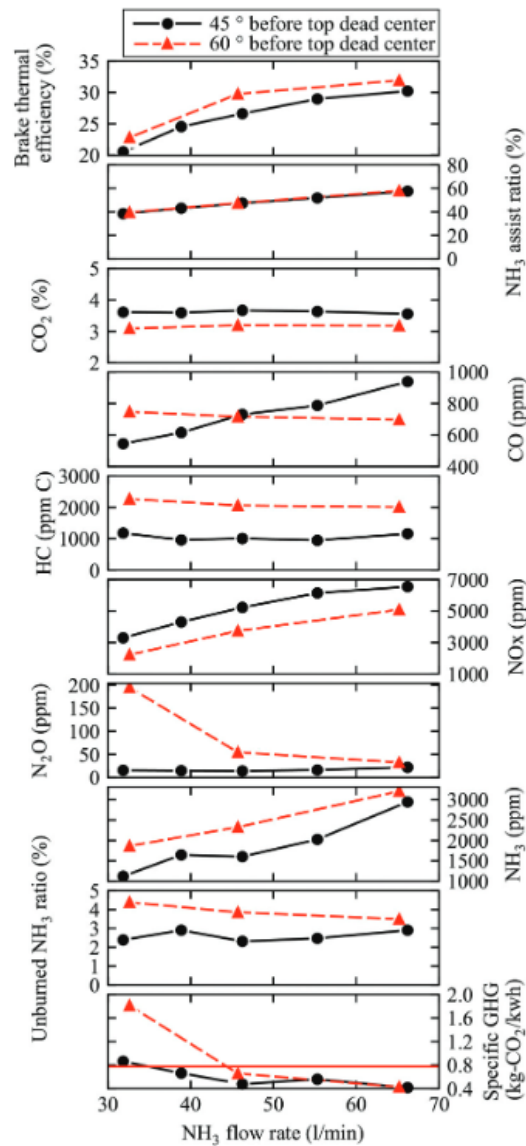


Figure H.1: Effects of different fuel compositions for two pilot injection timings (black = 45 CAD BTDC, red = 60 CAD BTDC). Graphs from Niki [2021b]

I Background - Modeling

The primary distinction between models used for the combustion processes in ICEs is whether the model is thermodynamic or fluid dynamic. This follows from which equations the model is principally built on. A thermodynamic model is based on the conservation of energy. A fluid dynamic model is based on the analysis of fluid motion [Heywood, 2018].

Both fluid dynamic and thermodynamic can make use of phenomenological models and chemical-kinetic mechanisms. Phenomenological models are used to incorporate phenomena, such as the combustion or heat loss, in a model. Chemical-kinetic mechanisms can add chemical reaction details to a model, such as intermediate reactants and the chemical heat release rate.

Thermodynamic models

A thermodynamic model can have different properties, in this literature study the following properties are often encountered:

- 1, 2 or multi-zones
- Phenomenological
- Including reaction kinetics

Zones

Thermodynamic models make use of zones. Zones are modelled as having one set of properties. The combustion mechanism partly determines whether a single-zone or multi-zone is appropriate. For example, HCCI has a homogeneous mixture in the combustion chamber, therefore it is more likely to be accurately modelled with a 1-zone model. A PPCI, however, has different levels of mixing in the combustion chamber, it is then less likely to be accurately modelled by a single-zone model.

Fluid dynamic models

Fluid dynamic models are multidimensional models, as they require the geometry of the engine and predict geometry of the fluid flow. Those models are computational fluid dynamics models (CFD) and are often used in ammonia combustion research. and are outside the scope of this research.

CFD: for combustion. Often CONVERGE - SAGE is used

Phenomenological models

Phenomenological models are used by thermodynamic or fluid dynamic models to incorporate phenomena which cannot be described by governing equations. Phenomenological models are based on simplified descriptions of the underlying physics and/or chemistry [Heywood, 2018]. For example, Woschni is used to incorporate the heat loss.

Chemical-kinetic mechanisms

Including reaction kinetics, means the model makes use of a chemical kinetic mechanism. The chemical-kinetic mechanism contains the sequence of elementary reactions by which the overall reaction occurs and can predict the chemical heat release rate. To model the combustion, models can make use of specific chemical-kinetic mechanisms. Chemical-kinetic mechanisms can give more information about intermediate species during the combustion compared to a phenomenological model. A drawback of chemical-kinetic mechanisms is the increase in computational time [Heywood, 2018].

J Overview chemical kinetic mechanisms

Table from Cai et al. [2023].

Mixture composition	No. of species/ reaction steps	Evaluation indexes	Ref.
NH ₃ /O ₂ , NH ₃ /H ₂ /O ₂	22/98	Flame structure	Miller et al. [1983]
H/N/O	19/73	Flame structure	Miller and Bowman [1989]
NH ₃ /H ₂ /O ₂ /N ₂ , NH ₃ /NO/H ₂ /O ₂ , NH ₃ /O ₂	21/95	Flame structure	Lindstedt et al. [1994]
H/N/O	31/238	NO _x formation	Konnov and De Ruyck [2000]
NH ₃ /NO/CO/H ₂ /O ₂ /N ₂ , NH ₃ /CO/H ₂ /O ₂ /N ₂	34/191	NO _x formation and flame structure	Skreiberg et al. [2004]
NH ₃ /CH ₄ /O ₂ /Ar	84/703	Flame structure	Tian et al. [2009]
H/N/C/O	85/1200	NO _x formation	Konnov [2009]
NH ₃ /CH ₄ /O ₂ /CO ₂ /N ₂	97/779	NO _x formation and flame structure	Mendiara and Glarborg [2009]
NH ₃ /H ₂ /O ₂ /Ar	19/80	Flame structure and NO _x formation	Duynslaegher et al. [2012]
NH ₃ /H ₂ /air	21/91	Laminar burning velocity	Nozari and Karabeyoglu [2015]
NH ₃ /O ₂ /Ar	35/159	Ignition delay time, NO _x formation, and flame structure	Mathieu and Petersen [2015]
NH ₃ /CH ₄ /O ₂ /Ar	48/500	Ignition delay time, NO _x formation, and flame structure	Xiao et al. [2016]
NH ₃ /O ₂	32/204	Ignition delay time	Song et al. [2016]
NH ₃ /air	38/232	Ignition delay time, laminar burning velocity, and flame structure	Nakamura et al. [2017]
CH ₄ /NH ₃ /air	59/365	Laminar burning velocity	Okafor et al. [2018]

J Overview chemical kinetic mechanisms

NH3/air	34/264	Ignition delay time, laminar burning velocity, and flame structure	Shrestha et al. [2018]
NH3/air, NH3/H2/air	32/213	Ignition delay time and laminar burning velocity	Otomo et al. [2018]
CH4/NH3/air	38/140	Laminar burning velocity	Okafor et al. [2019]
NH3/O2/N2	38/265	Laminar burning velocity	Mei et al. [2019]
NH3/H2/air	28/213	Ignition delay time, laminar burning velocity, and flame structure	Li et al. [2019]
NH3/CH4/air	51/420	Ignition delay time, laminar burning velocity, and flame structure	Li et al. [2019]
NH3/O2/Ar NH3/air	31/203	Laminar burning velocity and flame structure	Stagni et al. [2020]
NH3/syngas/air	35/177	Laminar burning velocity	Han et al. [2020]
NH3/CH3OH/air, NH3/C2H5OH/air	91/444	Laminar burning velocity	Wang et al. [2021]
NH3/air	32/259	Ignition delay time, laminar burning velocity, and flame structure	Singh et al. [2021]
NH3/DME/air	176/1419	Ignition delay time and laminar burning velocity	Issayev et al. [2022]
NH3/DEE/air	280/2238	Laminar burning velocity, ignition delay time, and flame structure	Shrestha et al. [2022]
NH3/H2/air	26/119	Laminar burning velocity	Gotama et al. [2022]
NH3/air, NH3/H2/air	20/89	Laminar burning velocity and ignition delay time	Cai et al. [2022]
NH3/CH4/air	187/1571	Soot volume fraction	Yang et al. [2023]

K Species Chemical Kinetic Mechanism

Species in the chemical kinetic mechanism of [Shrestha et al. \[2018\]](#). Many of the species are intermediate species.

<i>In TXT-file</i>	<i>Chemical formula</i>	<i>Remark</i>
AR	Ar	Argon
HE	He	Helium
N2	N ₂	Nitrogen
H	H	
O	O	
OH	OH	
H2	H ₂	Hydrogen
O2	O ₂	Oxygen
HO2	HO ₂	
H2O2	H ₂ O ₂	
H2O	H ₂ O	Water
OH*	OH	
CO	CO	Carbon monoxide
CO2	CO ₂	Carbon dioxide
HCO	HCO	
CH2O	CH ₂ O	
CH	CH	
C	C	
CH2-3	CH ₂	
CH2-1	CH ₂	
C2H2	C ₂ H ₂	
CH3	CH ₃	
CH4	CH ₄	Methane
HOCHO	HOCHO	
CH2OH	CH ₂ OH	
OCHO	OCHO	
CH3O	CH ₃ O	
C2H4	C ₂ H ₄	
CH2CO	CH ₂ CO	
C2H6	C ₂ H ₆	
CH3OH	CH ₃ OH	
CH3O2	CH ₃ O ₂	
CH3O2H	CH ₃ O ₂ H	
C2H3	C ₂ H ₃	
C2H5	C ₂ H ₅	
C2H5OH	C ₂ H ₅ OH	
C2H5O	C ₂ H ₅ O	
CH3CHO	CH ₃ CHO	

K Species Chemical Kinetic Mechanism

<i>In TXT-file</i>	<i>Chemical formula</i>	<i>Remark</i>
CH3CO	CH ₃ CO	
CH2O2H	CH ₂ O ₂ H	
C2H	C ₂ H	
C2	C ₂	
C2O	C ₂ O	
HCCO	HCCO	
H2CC	H ₂ CC	
C3H3	C ₃ H ₃	
C4H2	C ₄ H ₂	
C3H5	C ₃ H ₅	
CH2CHO	CH ₂ CHO	
C2H3OO	C ₂ H ₃ OO	
HCCOH	HCCOH	
C4H4	C ₄ H ₄	
C2H2OH	C ₂ H ₂ OH	
C2H3CHO	C ₂ H ₃ CHO	
C3H4O	C ₃ H ₄ O	
CHCHO	CHCHO	
CHOCHO	CHOCHO	
CHOCO	CH ₃ CO	
CH3CO2	CH ₃ CO ₂	
CH3CO3	CH ₃ CO ₃	
CH3CO3H	CH ₃ CO ₃ H	
C3H6	C ₃ H ₆	
C3H8	C ₃ H ₈	
I-C3H7	C ₃ H ₇	
N-C3H7	C ₃ H ₇	
C3H4	C ₃ H ₄	
C3H4P	C ₃ H ₄ P	
CH2CHOH	CH ₂ CHOH	
CH3CHOH	CH ₃ CHOH	
CH2CH2OH	CH ₂ CH ₂ OH	
C2H5O2	C ₂ H ₅ O ₂	
C2H4O1-2	C ₂ H ₄ O	
C2H5O2H	C ₂ H ₅ O ₂ H	
C2H5CHO	C ₂ H ₅ CHO	
C2H5CO	C ₂ H ₅ CO	
C2H4O2H	C ₂ H ₄ O ₂ H	
C2H3O1-2	C ₂ H ₃ O	
CH3OCH3-DME	CH ₃ OCH ₃	Dimethyl ether
CH3OCH2	CH ₃ OCH ₂	
CH3OCH2O2	CH ₃ OCH ₂ O ₂	
CH3OCH2O2H	CH ₃ OCH ₂ O ₂ H	
CH3OCH2O	CH ₃ OCH ₂ O	
CH3OCHO	CH ₃ OCHO	
CH2OCHO	CH ₂ OCHO	
CH3OCO	CH ₃ OCO	
CH2OCH2O2H	CH ₂ OCH ₂ O ₂ H	

<i>In TXT-file</i>	<i>Chemical formula</i>	<i>Remark</i>
O2CH2OCH2O2H	O ₂ CH ₂ OCH ₂ O ₂ H	
HO2CH2OCHO	HO ₂ CH ₂ OCHO	
OCH2OCHO	OCH ₂ OCHO	
HOCH2OCO	HOCH ₂ OCO	
HOCH2O	HOCH ₂ O	
CH*	CH	
N	N	
NO	NO	Nitrogen oxide
N2O	N ₂ O	Nitrous oxide
NO2	NO ₂	Nitrogen dioxide
NH	NH	
NH2	NH ₂	
NH3	NH ₃	Ammonia
HNO	HNO	
HONO	HONO	
H2NO	H ₂ NO	
NNH	NNH	
N2H2	N ₂ H ₂	
N2H3	N ₂ H ₃	
N2H4	N ₂ H ₄	
H2NN	H ₂ NN	
HNOH	HNOH	
NH2O	NH ₂ OH	
HNO2	HNO ₂	
HONO	HONO ₂	
NO3	NO ₃	
HNO3	HNO ₃	
CN	CN	
HCN	HCN	
HCNO	HCNO	
NCN	NCN	
HNC	HNC	
HNCN	HNCN	
H2CN	H ₂ CN	
C2N2	C ₂ N ₂	
HOCN	HOCN	
HNCO	HNCO	
NCO	NCO	
HON	HON	

L Converting chemical kinetic model to YAML

Shrestha et al. [2018] provided three TXT files containing the kinetic mechanism, the thermochemistry, and transport properties. The original TXT files have been modified to create a chemical kinetic mechanism in YAML format. This YAML format can be used in Cantera. The modifications listed are in the kinetic mechanism and are listed in chronological order.

1. Line 293 reaction equation "CH2-3(+M)=C+H2(+M)" changed to "CH2-3+M=C+H2+M"
2. Line 295 reaction equation "CH2-3(+M)=CH+H(+M)" changed to "CH2-3+M=CH+H+M"
3. Line 344 reaction equation "CH3(+M)=CH2-3+H(+M)" changed to "CH3+M=CH2-3+H+M"
4. Line 346 reaction equation "CH3(+M)=CH+H2(+M)" changed to "CH3+M=CH+H2+M"
5. Line 404 reaction equation "CH3O(+M)=CH2OH(+M)" changed to "CH3O+M=CH2OH+M"
6. Line 1745 reaction equation "OH*+Ar=OH+Ar" changed to "OH*+AR=OH+AR"
7. Line 1745 reaction equation "OH*+Ar=OH+Ar" changed to "OH*+AR=OH+AR"
8. Added "DUPLICATE" to equations on 1063 and 1201 (1201 becomes 1202 after adding DUPLICATE to reaction of 1063)
9. Added "DUPLICATE" to equation 1827

The original files can be found here: <https://pubs-acsc-org.tudelft.idm.oclc.org/doi/10.1021/acs.energyfuels.8b01056>

M Cantera

Several Cantera objects are employed as building blocks of the model. These objects are the ideal gas reactor, wall, reservoir, and mass flow controller. This section describes their properties and governing equations. This appendix is not a general description of Cantera, only the objects that are relevant for the ignition and engine cylinder model are described.

The employed Cantera objects are;

- Ideal gas reactor
- Wall
- Reservoir

M.1 Ideal Gas Reactor

The ideal gas reactor is a reactor with a homogeneous phase and distribution of ideal gases. It is defined by four state variables; the reactor volume, temperature, the mass of the content, and the mass fraction of each species. The governing equations of the Ideal Gas Reactor determine the governing equations of the model.

M.2 Wall

Walls are objects in between reactors, for example, a wall can represent the piston by being placed in between a reservoir (the environment) and an ideal gas reactor (the combustion chamber). A reactor can be combined with one or multiple walls that influence the chemical reactions in the reactor. The influence on the reactor is by changing the volume, transferring heat or providing a location for surface reactions. In this work, the option for a surface reaction is not used and will therefore not be described.

Walls can have a set velocity and with that change the volume of the adjacent reactors. Positive values for \dot{V} , the change in volume, correspond to increases in the volume of the reactor on the left, and decreases in the volume of the reactor on the right.

Walls allow heat transfer between reactors, and provide a location for surface reactions to take place.

The construct "wall" is defined by two files, [Wall.h](#) and [Wall.cpp](#). Both files are available on the Cantera website.

M.2.1 Wall parameters

The properties of the wall are defined by parameters. These parameters are used in the definitions of the properties, for example, K and A appear in the wall velocity function. The following parameters are used in the model in this work:

- K - expansion rate coefficient
- A - wall area

- h - heat transfer coefficient

Other parameters, for example 'k' which describes the specie covering the wall, are not used in this model and therefore not described in this appendix.

Wall velocity

The wall velocity is defined by [Equation M.1](#), where v is the wall velocity [[Cantera, 2023b](#)]. The defined wall velocity can be found at line 70 of Wall.cpp.

$$v = K (P_{\text{left}} - P_{\text{right}}) + v_0(t) \quad (\text{M.1})$$

$v_0(t)$ corresponds to m_{vf} in the files 'Wall.h' and 'Wall.cpp'. This wall velocity function can be set by using

Heat transfer The heat transfer in the model is described by [Equation M.2](#).

$$H = h \cdot A_{\text{cyl}} \cdot T_{\text{cyl}} \quad (\text{M.2})$$

In which

H	heat flux	$[W]$
h	heat transfer coefficient from Equation 11.13	$[\frac{W}{m^2K}]$
A_{cyl}	Instantaneous area of the cylinder	$[m^2]$
T_{cyl}	Cylinder temperature	K

To incorporate this in the model, the heat flux property of the Cantera 'Wall' object is used. The unit of the heat flux property of the Wall is $W/m^2/K$.

In the [source code](#) (line 140) of the Wall object, the heat flux is described by:

$$Q = hA(T_{\text{left}} - T_{\text{right}}) + AG(t) \quad (\text{M.3})$$

In which h is the heat transfer coefficient, A is the wall area, and $G(t)$ is a specified function of time. To implement the heat transfer model of Hohenberg, h in [Equation M.3](#) has to be zero, A the instantaneous cylinder area and $G(t)$ equals [Equation 11.13](#) multiplied by T_{cyl} .

M.3 Reservoir

A reservoir is a reactor that has a constant state. Therefore, the reservoirs' temperature, pressure, and chemical composition never change from their initial values.

N Ignition model results

The output of the ignition model consists of several graphs and a list with the set-up variables and the calculated results.

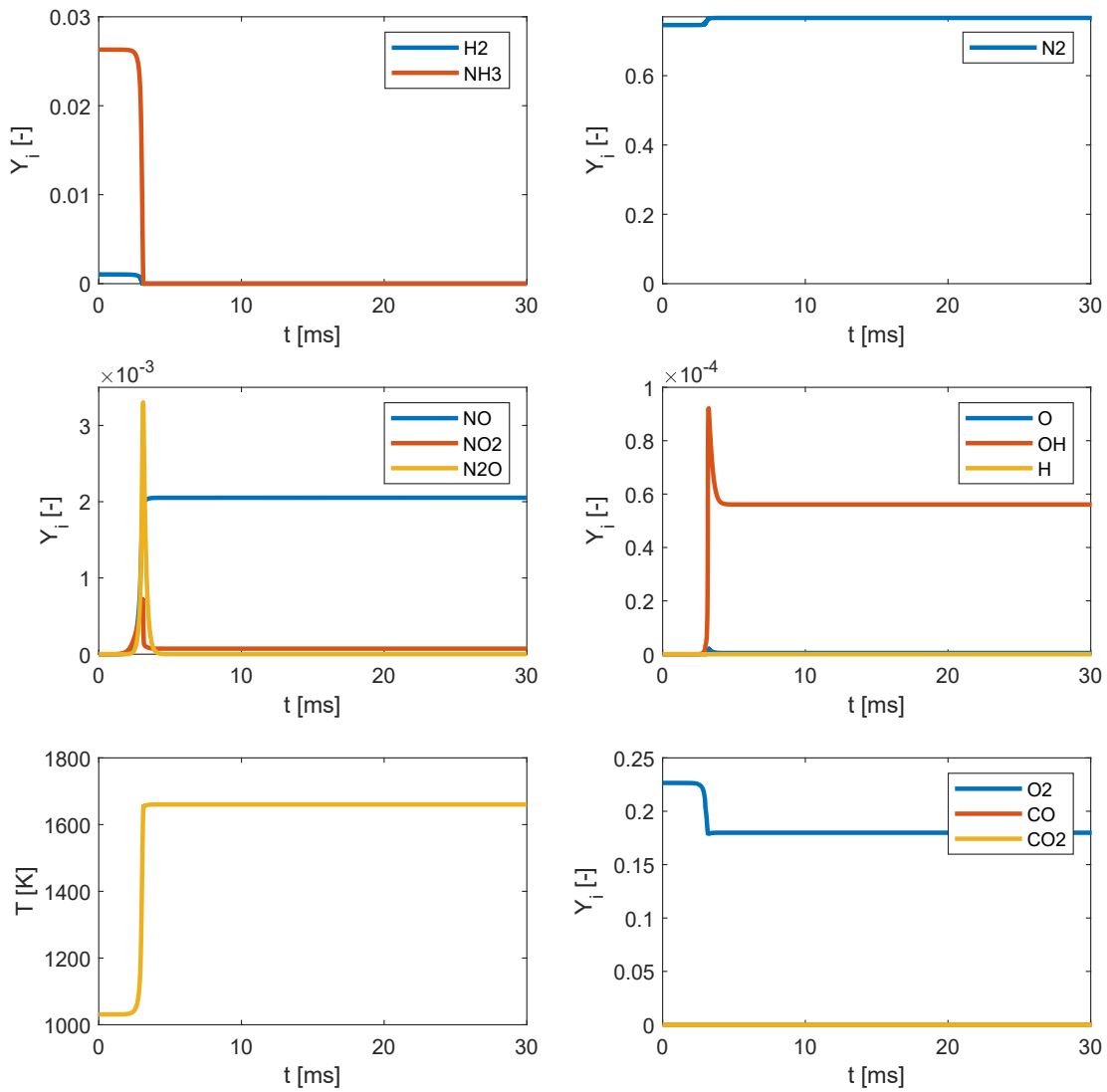


Figure N.1: Graphical results of the ignition model

N Ignition model results

Molar fraction NH3 [-]	0.75
Molar fraction H2 [%]	0.25
Molar fraction DME [%]	0
Energy in fuel [kJ]	8.651
Energy fraction NH3 [%]	79.622
Energy fraction H2 [%]	20.378
Energy fraction DME [%]	0
Equivalence set	0.2
$T_{initial}$	1031
$P_{initial}$	43.4
CA10 [cad]	20.454
CA10 [ms]	2.841
CA10 T [K]	1108.82
dT t0-CA10 [K]	77.82
CA10 @ PRR [bar/CAD]	3.048

Table N.1: Export of set-up and results of the ignition model

O Engine cylinder model results

The output of the engine cylinder model consist of numbers and graphs.

Set up summary

$\%_e$ NH3	0.64
$\%_e$ H2	0.16
$\%_e$ DME	0.2
Fuel mass [g]	0.4303
Fuel energy per cycle [kJ]	9.9659
Engine speed [rps]	20
Inlet temp [C]	45
Compression ratio	14
Stoichiometric afr	7.4185
Equivalence ratio	0.2
AFR_{mass}	37.0924

Result summary

CA10 [CAD]	361
CA90 [CAD]	364
Combustion duration [CAD]	3
Heat release [kW]	236.343
Heat loss [kW]	12.4955
Expansion power per cyl [kW]	29.1973
Indicated work [kJ]	2.9197
Efficiency W_i/Q_{in} [%]	29.2973
Maximum temperature [K]	1458.971
Maximum pressure [bar]	128.2118
Maximum pressure rise rate [bar/cad]	27.8594
MPPRR ave top2 [bar/cad]	21.5418

Emissions

NH3 [mg]	0
NO [g/kWh]	9.6283
NO2 [g/kWh]	0.8381
N2O [g/kWh]	0.3622
CO [g/kWh]	0.0007
CO2 [g/kWh]	48.8502

Table O.1: Export of set-up and results of the engine cylinder model

O Engine cylinder model results

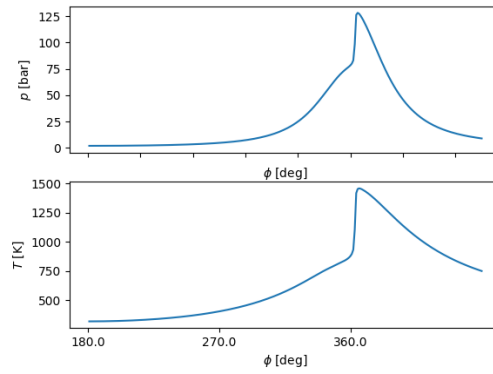
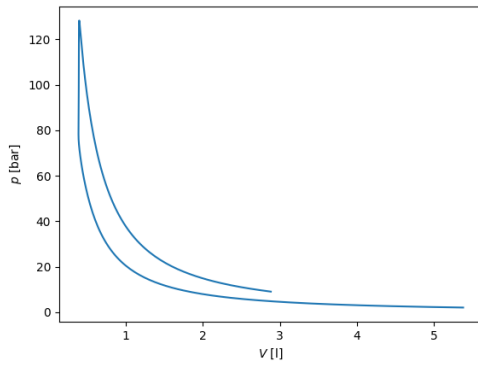
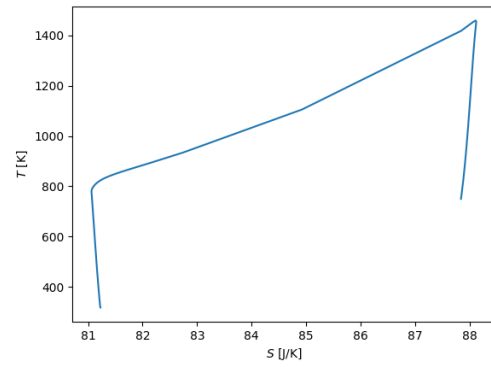


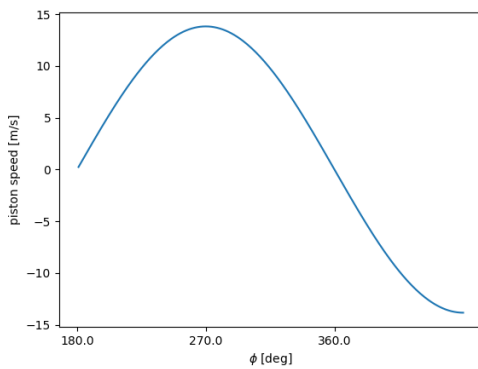
Figure O.1: Pressure and temperature



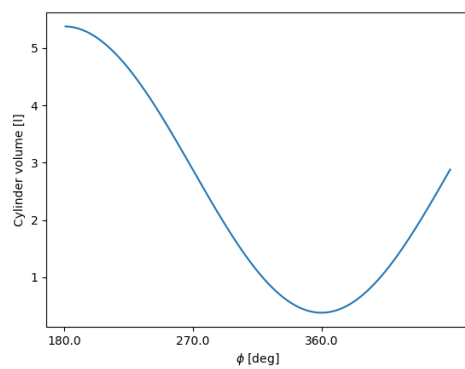
(a) The partial p-V diagram



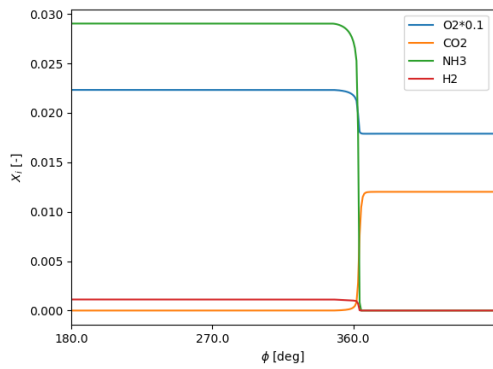
(b) The partial T-S diagram



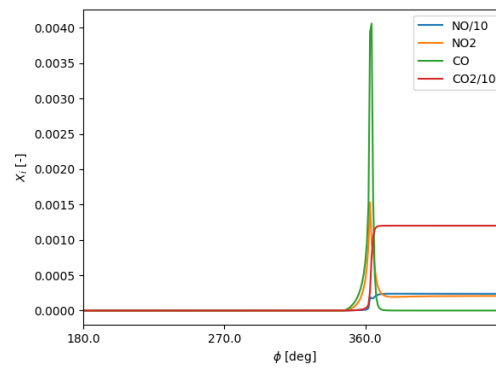
(a) The piston speed



(b) The reactor (cylinder) volume



(a) The molar fractions of the fuel and oxidizer



(b) The molar fractions of the emissions

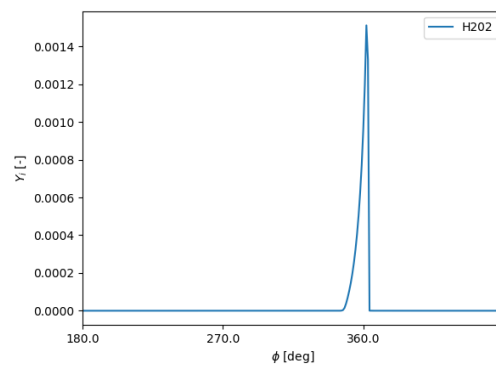


Figure O.5: Mass fraction H₂O₂

Bibliography

- AEA. About – Ammonia Energy Association, 2023. URL <https://www.ammoniaenergy.org/about/>.
- L.-Z. Bao, B.-G. Sun, Q.-H. Luo, J.-C. Li, D.-C. Qian, H.-Y. Ma, and Y.-J. Guo. Development of a turbocharged direct-injection hydrogen engine to achieve clean, efficient, and high-power performance. *Fuel*, 324, 2022. doi: 10.1016/j.fuel.2022.124713.
- A. Bertolino, M. Fürst, A. Stagni, A. Frassoldati, M. Pelucchi, C. Cavallotti, T. Faravelli, and A. Parente. An evolutionary, data-driven approach for mechanism optimization: theory and application to ammonia combustion. *Combustion and Flame*, 229, 7 2021. ISSN 15562921. doi: 10.1016/J.COMBUSTFLAME.2021.02.012.
- Stijn Broekaert, Thomas De Cuyper, Kam Chana, Michel De Paepe, and Sebastian Verhelst. Assessment of Empirical Heat Transfer Models for a CFR Engine Operated in HCCI Mode. *SAE Technical Papers*, 2015-April(April), 4 2015. ISSN 01487191. doi: 10.4271/2015-01-1750.
- Tao Cai, Dan Zhao, Siew Hwa Chan, and Mohammad Shahsavari. Tailoring reduced mechanisms for predicting flame propagation and ignition characteristics in ammonia and ammonia/hydrogen mixtures. *Energy*, 260:125090, 12 2022. ISSN 0360-5442. doi: 10.1016/J.ENERGY.2022.125090.
- Tao Cai, Dan Zhao, and Ephraim Gutmark. Overview of fundamental kinetic mechanisms and emission mitigation in ammonia combustion. *Chemical Engineering Journal*, 458:141391, 2 2023. ISSN 1385-8947. doi: 10.1016/J.CEJ.2023.141391.
- Cantera. Ideal Gas Reactor — Cantera, 2023a. URL <https://cantera.org/science/reactors/idealgasreactor.html>.
- Cantera. Python Examples — Cantera, 2023b. URL <https://cantera.org/examples/python/index.html>.
- Domenico Chiera, James Wood, Andrew Jones, Michael Buehner, Nolan Polley, and Gregory J. Hampson. Method to reach high substitution of an ammonia fueled engine using dual fuel RCCI and active combustion control. *Proceedings of ASME 2022 ICE Forward Conference, ICEF 2022*, 2022. doi: 10.1115/ICEF2022-88759.
- Rodolfo Cavaliere da Rocha, Mário Costa, and Xue Song Bai. Chemical kinetic modelling of ammonia/hydrogen/air ignition, premixed flame propagation and NO emission. *Fuel*, 246: 24–33, 6 2019. ISSN 0016-2361. doi: 10.1016/J.FUEL.2019.02.102.
- Liming Dai, Sander Gersen, Peter Glarborg, Howard Levinsky, and Anatoli Mokhov. Experimental and numerical analysis of the autoignition behavior of NH₃ and NH₃/H₂ mixtures at high pressure. *Combustion and Flame*, 215:134–144, 5 2020. ISSN 15562921. doi: 10.1016/J.COMBUSTFLAME.2020.01.023.

Bibliography

- Liming Dai, Hamid Hashemi, Peter Glarborg, Sander Gersen, Paul Marshall, Anatoli Mokhov, and Howard Levinsky. Ignition delay times of NH₃ /DME blends at high pressure and low DME fraction: RCM experiments and simulations. *Combustion and Flame*, 227:120–134, 5 2021. ISSN 0010-2180. doi: 10.1016/J.COMBUSTFLAME.2020.12.048.
- Vincenzo De Bellis, Enrica Malfi, Alfredo Lanotte, Giovanni Fasulo, Fabio Bozza, Alberto Cafari, Gennaro Caputo, and Jari Hyvönen. Development of a phenomenological model for the description of RCCI combustion in a dual-fuel marine internal combustion engine. *Applied Energy*, 325:119919, 11 2022. ISSN 0306-2619. doi: 10.1016/J.APENERGY.2022.119919.
- P. de Vos. Case study w12v31, 2022.
- P. de Vos, L. M. T. Somers, T. Tinga, E. M. Foekema, B. van der Zwaan, and R. R. Negenborn. The ammoniadrive research project. *SWZ Maritime*, 143(7/8):24–27, 2022.
- Pavlos Dimitriou and Rahat Javaid. A review of ammonia as a compression ignition engine fuel. *International Journal of Hydrogen Energy*, 45(11):7098–7118, 2 2020. ISSN 0360-3199. doi: 10.1016/J.IJHYDENE.2019.12.209.
- M.H. Dinesh, J.K. Pandey, and G.N. Kumar. Study of performance, combustion, and NO_x emission behavior of an SI engine fuelled with ammonia/hydrogen blends at various compression ratio. *International Journal of Hydrogen Energy*, 47(60):25391–25403, 2022. doi: 10.1016/j.ijhydene.2022.05.287.
- C. Duynslaegher, F. Contino, J. Vandooren, and H. Jeanmart. Modeling of ammonia combustion at low pressure. *Combustion and Flame*, 159(9):2799–2805, 2012. doi: 10.1016/j.combustflame.2012.06.003.
- S. Frankl, S. Gleis, S. Karmann, M. Prager, and G. Wachtmeister. Investigation of ammonia and hydrogen as CO₂-free fuels for heavy duty engines using a high pressure dual fuel combustion process. *International Journal of Engine Research*, 22(10):3196–3208, 2021. doi: 10.1177/1468087420967873.
- Stefano Frigo and Roberto Gentili. Analysis of the behaviour of a 4-stroke Si engine fuelled with ammonia and hydrogen. *International Journal of Hydrogen Energy*, 38(3):1607–1615, 2 2013. ISSN 0360-3199. doi: 10.1016/J.IJHYDENE.2012.10.114.
- J. Frost, A. Tall, A.M. Sheriff, A. Schönborn, and P. Hellier. An experimental and modelling study of dual fuel aqueous ammonia and diesel combustion in a single cylinder compression ignition engine. *International Journal of Hydrogen Energy*, 46(71):35495–35510, 2021. doi: 10.1016/j.ijhydene.2021.08.089.
- Peter Glarborg, James A Miller, Branko Ruscic, and Stephen J Klippenstein. Modeling nitrogen chemistry in combustion. *Progress in energy and combustion science*, 67:31–68, 2018.
- Gabriel J. Gotama, Akihiro Hayakawa, Ekenechukwu C. Okafor, Ryuhei Kanoshima, Masao Hayashi, Taku Kudo, and Hideaki Kobayashi. Measurement of the laminar burning velocity and kinetics study of the importance of the hydrogen recovery mechanism of ammonia/hydrogen/air premixed flames. *Combustion and Flame*, 236:111753, 2 2022. ISSN 0010-2180. doi: 10.1016/J.COMBUSTFLAME.2021.111753.
- James T. Gray, Edward Dimitroff, Nelson T. Meckel, and R. D. Quillian. Ammonia Fuel - Engine Compatibility and Combustion. *SAE Technical Papers*, 2 1966. ISSN 0148-7191. doi: 10.4271/660156. URL <https://www-sae-org.tudelft.idm.oclc.org/publications/technical-papers/content/660156/>.

- Christopher W. Gross and Song Charng Kong. Performance characteristics of a compression-ignition engine using direct-injection ammonia-DME mixtures. *Fuel*, 103:1069–1079, 1 2013. ISSN 00162361. doi: 10.1016/J.FUEL.2012.08.026.
- Xinlu Han, Zhihua Wang, Yong He, Yanqun Zhu, and Kefa Cen. Experimental and kinetic modeling study of laminar burning velocities of NH₃/syngas/air premixed flames. *Combustion and Flame*, 213:1–13, 3 2020. ISSN 0010-2180. doi: 10.1016/J.COMBUSTFLAME.2019.11.032.
- Reed M. Hanson, Sage L. Kokjohn, Derek A. Splitter, and Rolf D. Reitz. An experimental investigation of fuel reactivity controlled PCCI combustion in a heavy-duty engine. *SAE Technical Papers*, pages 700–716, 2010. ISSN 26883627. doi: 10.4271/2010-01-0864.
- J.J. Hernández, A. Cova-Bonillo, H. Wu, J. Barba, and J. Rodríguez-Fernández. Low temperature autoignition of diesel fuel under dual operation with hydrogen and hydrogen-carriers. *Energy Conversion and Management*, 258, 2022. doi: 10.1016/j.enconman.2022.115516.
- Juan J. Hernández, A. Cova-Bonillo, A. Ramos, H. Wu, and J. Rodríguez-Fernández. Autoignition of sustainable fuels under dual operation with H₂-carriers in a constant volume combustion chamber. *Fuel*, 339, 5 2023. ISSN 00162361. doi: 10.1016/J.FUEL.2023.127487.
- John B. Heywood. *Internal Combustion Engine Fundamentals*. McGraw-Hill Education, 2018. ISBN 9781260116106. URL <https://www.accessengineeringlibrary.com/content/book/9781260116106><https://www.accessengineeringlibrary.com/content/book/9781260116106.abstract>.
- Günter F. Hohenberg. Advanced Approaches for Heat Transfer Calculations. *SAE Technical Papers*, 2 1979. ISSN 0148-7191. doi: 10.4271/790825. URL <https://www-sae-org.tudelft.idm.oclc.org/publications/technical-papers/content/790825/>.
- Hy2Gen Inc Canada. CANADA — HY2GEN AG, 2023. URL <https://hy2gen.com/canada/>.
- IMarEST Marine Professional. Ammonia’s Achilles heel, 3 2023. URL <https://www.imarest.org/themarineprofessional/on-the-radar/6783-ammonia-s-achilles-heel>.
- IMO. International Maritime Organization, 2023. URL <https://www.imo.org/en/>.
- Gani Issayev, Binod Raj Giri, Ayman M. Elbaz, Krishna P. Shrestha, Fabian Mauss, William L. Roberts, and Aamir Farooq. Ignition delay time and laminar flame speed measurements of ammonia blended with dimethyl ether: A promising low carbon fuel blend. *Renewable Energy*, 181:1353–1370, 1 2022. ISSN 0960-1481. doi: 10.1016/J.RENENE.2021.09.117.
- Shouying Jin, Binyang Wu, Zhenyuan Zi, Puze Yang, Taifeng Shi, and Junhong Zhang. Effects of fuel injection strategy and ammonia energy ratio on combustion and emissions of ammonia-diesel dual-fuel engine. *Fuel*, 341:127668, 2023. doi: 10.1016/j.fuel.2023.127668. URL <https://doi.org/10.1016/j.fuel.2023.127668>.
- S.P. Kane and W.F. Northrop. Thermochemical recuperation to enable efficient ammonia-diesel dual-fuel combustion in a compression ignition engine. *Energies*, 14(22), 2021. doi: 10.3390/en14227540.
- Stephen J Klippenstein, Lawrence B Harding, Peter Glarborg, and James A Miller. The role of n₂h in NO formation and control. *Combustion and Flame*, 158(4):774–789, 2011.

Bibliography

- E Koch. Ammonia—a fuel for motor buses. *J. Inst. Pet*, 31:213, 1945.
- S. L. Kokjohn and R. D. Reitz. Investigation of charge preparation strategies for controlled premixed charge compression ignition combustion using a variable pressure injection system. *International Journal of Engine Research*, 11(4):257–282, 8 2010. ISSN 14680874. doi: 10.1243/14680874JER06409.
- S. L. Kokjohn, R. M. Hanson, D. A. Splitter, and R. D. Reitz. Fuel reactivity controlled compression ignition (RCCI): A pathway to controlled high-efficiency clean combustion. *International Journal of Engine Research*, 12(3):209–226, 6 2011. ISSN 14680874. doi: 10.1177/1468087411401548/FORMAT/EPUB.
- Sage L. Kokjohn, Reed M. Hanson, Derek A. Splitter, and Rolf D. Reitz. Experiments and modeling of dual-fuel HCCI and PCCI combustion using in-cylinder fuel blending. *SAE International Journal of Engines*, 2(2):24–39, 2010. ISSN 19463936. doi: 10.4271/2009-01-2647.
- A. A. Konnov. Implementation of the NCN pathway of prompt-NO formation in the detailed reaction mechanism. *Combustion and Flame*, 156(11):2093–2105, 11 2009. ISSN 0010-2180. doi: 10.1016/J.COMBUSTFLAME.2009.03.016.
- A. A. Konnov and J. De Ruyck. Kinetic modeling of the thermal decomposition of ammonia. *Combustion science and technology*, 152(1):23–37, 2000. ISSN 00102202. doi: 10.1080/00102200008952125.
- R. Senthil Kumar, M. Loganathan, and E. James Gunasekaran. Performance, emission and combustion characteristics of CI engine fuelled with diesel and hydrogen. *Frontiers in Energy*, 9(4):486–494, 12 2015. ISSN 20951698. doi: 10.1007/S11708-015-0368-4/METRICS. URL <https://link-springer-com.tudelft.idm.oclc.org/article/10.1007/s11708-015-0368-4>.
- Caneon Kurien and Mayank Mittal. Review on the production and utilization of green ammonia as an alternate fuel in dual-fuel compression ignition engines. *Energy Conversion and Management*, 251, 1 2022. ISSN 01968904. doi: 10.1016/J.ENCONMAN.2021.114990.
- K. Kuta, G. Przybyła, D. Kurzydym, and Z. Żmudka. Experimental and numerical investigation of dual-fuel CI ammonia engine emissions and after-treatment with V2O5/SiO–TiO2 SCR. *Fuel*, 334, 2023. doi: 10.1016/j.fuel.2022.126523.
- J. Lasocki, M. Bednarski, and M. Sikora. Simulation of ammonia combustion in dual-fuel compression-ignition engine. *IOP Conference Series: Earth and Environmental Science*, 214(1), 1 2019. ISSN 17551315. doi: 10.1088/1755-1315/214/1/012081.
- Chung K. Law. *Combustion physics*. Cambridge University Press,, Cambridge ;, 2006. ISBN 0521870526. URL <http://books.google.com/books?id=vWgJvKMXwQ8C&pgis=1>.
- H. Lesmana, Z. Zhang, X. Li, M. Zhu, W. Xu, and D. Zhang. NH3 as a transport fuel in internal combustion engines: A technical review. *Journal of Energy Resources Technology, Transactions of the ASME*, 141(7), 2019. doi: 10.1115/1.4042915.
- C. Lhuillier, P. Brequigny, F. Contino, and C. Mounaim-Rousselle. Experimental study on ammonia/hydrogen/air combustion in spark ignition engine conditions. *Fuel*, 269, 2020. doi: 10.1016/j.fuel.2020.117448.

- Rui Li, Alexander A. Konnov, Guoqiang He, Fei Qin, and Duo Zhang. Chemical mechanism development and reduction for combustion of NH₃/H₂/CH₄ mixtures. *Fuel*, 257:116059, 12 2019. ISSN 0016-2361. doi: 10.1016/J.FUEL.2019.116059.
- Tie Li, Xinyi Zhou, Ning Wang, Xinran Wang, Run Chen, Shiyan Li, and Ping Yi. A comparison between low- and high-pressure injection dual-fuel modes of diesel-pilot-ignition ammonia combustion engines. *Journal of the Energy Institute*, 102:362–373, 6 2022. ISSN 1743-9671. doi: 10.1016/J.JOEL.2022.04.009.
- Wanxiong Liao, Zhaohan Chu, Yiru Wang, Shuiqing Li, and Bin Yang. An experimental and modeling study on auto-ignition of ammonia in an RCM with N₂O and H₂ addition. *Proceedings of the Combustion Institute*, 11 2022. ISSN 15407489. doi: 10.1016/J.PROCI.2022.07.264. URL <https://linkinghub.elsevier.com/retrieve/pii/S1540748922005090>.
- R. P. Lindstedt, F. C. Lockwood, and M. A. Selim. Detailed Kinetic Modelling of Chemistry and Temperature Effects on Ammonia Oxidation. *Combustion Science and Technology*, 99(4-6): 253–276, 9 1994. ISSN 1563521X. doi: 10.1080/00102209408935436.
- L. Liu, F. Tan, Z. Wu, Y. Wang, and H. Liu. Comparison of the combustion and emission characteristics of NH₃/NH₄NO₂ and NH₃/H₂ in a two-stroke low speed marine engine. *International Journal of Hydrogen Energy*, 47(40):17778–17787, 2022. doi: 10.1016/j.ijhydene.2022.03.239.
- MAN Energy Solutions. Man b&w two-stroke engine operating on ammonia, 2019. URL https://www.man-es.com/docs/default-source/marine/tools/man-b-w-two-stroke-engine-operating-on-ammonia.pdf?sfvrsn=544dc811_10.
- Olivier Mathieu and Eric L. Petersen. Experimental and modeling study on the high-temperature oxidation of Ammonia and related NO_x chemistry. *Combustion and Flame*, 162(3):554–570, 3 2015. ISSN 0010-2180. doi: 10.1016/J.COMBUSTFLAME.2014.08.022.
- Bowen Mei, Xiaoyuan Zhang, Siyuan Ma, Mingli Cui, Hanwen Guo, Zhihao Cao, and Yuyang Li. Experimental and kinetic modeling investigation on the laminar flame propagation of ammonia under oxygen enrichment and elevated pressure conditions. *Combustion and Flame*, 210:236–246, 12 2019. ISSN 0010-2180. doi: 10.1016/J.COMBUSTFLAME.2019.08.033.
- Teresa Mendiara and Peter Glarborg. Ammonia chemistry in oxy-fuel combustion of methane. *Combustion and Flame*, 156:1937–1949, 2009. doi: 10.1016/j.combustflame.2009.07.006.
- X. Meng, C. Zhao, Z. Cui, X. Zhang, M. Zhang, J. Tian, W. Long, and M. Bi. Understanding of combustion characteristics and NO generation process with pure ammonia in the pre-chamber jet-induced ignition system. *Fuel*, 331, 2023. doi: 10.1016/j.fuel.2022.125743.
- James A. Miller and Craig T. Bowman. Mechanism and modeling of nitrogen chemistry in combustion. *Progress in Energy and Combustion Science*, 15(4):287–338, 1 1989. ISSN 0360-1285. doi: 10.1016/0360-1285(89)90017-8.
- James A. Miller, Mitchell D. Smooke, Robert M. Green, and Robert J. Kee. Kinetic Modeling of the Oxidation of Ammonia in Flames. *Combustion Science and Technology*, 34(1-6):149–176, 10 1983. ISSN 1563521X. doi: 10.1080/00102208308923691.
- MMMCZCS. Managing Emissions from Ammonia-Fueled Vessels. Technical report, MMMCZCS, 2 2023. URL https://cms.zerocarbonshipping.com/media/uploads/documents/Ammonia-emissions-reduction-position-paper_v4.pdf.

Bibliography

- Christine Mounaïm-Rousselle, Adrien Mercier, Pierre Brequigny, Clément Dumand, Jean Bourriot, and Sébastien Houillé. Performance of ammonia fuel in a spark assisted compression Ignition engine. *International Journal of Engine Research*, 23(5):781–792, 5 2022. ISSN 20413149. doi: 10.1177/14680874211038726.
- E. Nadimi, G. Przybyła, D. Emberson, T. Løvås, Ł. Ziółkowski, and W. Adamczyk. Effects of using ammonia as a primary fuel on engine performance and emissions in an ammonia/biodiesel dual-fuel CI engine. *International Journal of Energy Research*, 46(11):15347–15361, 2022. doi: 10.1002/er.8235.
- Ebrahim Nadimi, Grzegorz Przybyła, Michał T. Lewandowski, and Wojciech Adamczyk. Effects of ammonia on combustion, emissions, and performance of the ammonia/diesel dual-fuel compression ignition engine. *Journal of the Energy Institute*, 107:101158, 4 2023. ISSN 1743-9671. doi: 10.1016/J.JOEL.2022.101158.
- Suraj Nair, Gregory Hampson, and Jeffrey Carlson. Controlled multi-staged combustion strategy for overcoming load limitations of fuel flexible gas-diesel engines. *New Engine Developments – Gas & Dual Fuel. CIMAC Congress Vancouver*, 2019.
- Hisashi Nakamura, Susumu Hasegawa, and Takuya Tezuka. Kinetic modeling of ammonia/air weak flames in a micro flow reactor with a controlled temperature profile. *Combustion and Flame*, 185:16–27, 11 2017. ISSN 0010-2180. doi: 10.1016/J.COMBUSTFLAME.2017.06.021.
- Yoichi Niki. Experimental investigation of effects of split diesel-pilot injection on emissions from ammonia-diesel dual fuel engine. *Proceedings of ASME 2021 Internal Combustion Engine Division Fall Technical Conference, ICEF 2021*, 2021a. doi: 10.1115/ICEF2021-66341.
- Yoichi Niki. Reductions in Unburned Ammonia and Nitrous Oxide Emissions From an Ammonia-Assisted Diesel Engine With Early Timing Diesel Pilot Injection. *Journal of Engineering for Gas Turbines and Power*, 143(9), 9 2021b. ISSN 15288919. doi: 10.1115/1.4051002.
- Yoichi Niki, Yoshifuru Nitta, Hidenori Sekiguchi, and Koichi Hirata. Diesel fuel multiple injection effects on emission characteristics of diesel engine mixed ammonia gas into intake air. *Journal of Engineering for Gas Turbines and Power*, 141(6), 6 2019. ISSN 15288919. doi: 10.1115/1.4042507.
- Hadi Nozari and Arif Karabeyoglu. Numerical study of combustion characteristics of ammonia as a renewable fuel and establishment of reduced reaction mechanisms. *Fuel*, 159:223–233, 11 2015. ISSN 0016-2361. doi: 10.1016/J.FUEL.2015.06.075.
- NRC. Toezichthouder: kans op grote incidenten met waterstof in havens, 2023. URL <https://www.nrc.nl/nieuws/2023/02/20/veiligheidsproblemen-met-ammoniak-in-rotterdamse-haven-vertragen-energietransitie-a4157651>.
- Ekenechukwu C. Okafor, Yuji Naito, Sophie Colson, Akinori Ichikawa, Taku Kudo, Akihiro Hayakawa, and Hideaki Kobayashi. Experimental and numerical study of the laminar burning velocity of CH₄-NH₃-air premixed flames. *Combustion and Flame*, 187:185–198, 1 2018. ISSN 0010-2180. doi: 10.1016/J.COMBUSTFLAME.2017.09.002.
- Ekenechukwu Chijioke Okafor, Yuji Naito, Sophie Colson, Akinori Ichikawa, Taku Kudo, Akihiro Hayakawa, and Hideaki Kobayashi. Measurement and modelling of the laminar burning velocity of methane-ammonia-air flames at high pressures using a reduced reaction mechanism. *Combustion and Flame*, 204:162–175, 6 2019. ISSN 0010-2180. doi: 10.1016/J.COMBUSTFLAME.2019.03.008.

- Junichiro Otomo, Mitsuo Koshi, Teruo Mitsumori, Hiroshi Iwasaki, and Koichi Yamada. Chemical kinetic modeling of ammonia oxidation with improved reaction mechanism for ammonia/air and ammonia/hydrogen/air combustion. *International Journal of Hydrogen Energy*, 43 (5):3004–3014, 2 2018. ISSN 0360-3199. doi: 10.1016/J.IJHYDENE.2017.12.066.
- Thomas J. Pearsall and Charles G. Garabedian. Combustion of Anhydrous Ammonia in Diesel Engines. *SAE Technical Papers*, 2 1967. ISSN 0148-7191. doi: 10.4271/670947. URL <https://www-sae-org.tudelft.idm.oclc.org/publications/technical-papers/content/670947/>.
- Ronan Pelé, Christine Mounaïm-Rousselle, Pierre Bréquigny, Camille Hespel, Jérôme Bellettre, Steven Begg, and Nwabueze Emekwuru. First Study on Ammonia Spray Characteristics with a Current GDI Engine Injector. *Fuels* 2021, Vol. 2, Pages 253-271, 2(3):253–271, 6 2021. ISSN 2673-3994. doi: 10.3390/FUELS2030015. URL [https://www.mdpi.com/2673-3994/2/3/15](https://www.mdpi.com/2673-3994/2/3/15/html). URL <https://www.mdpi.com/2673-3994/2/3/15>.
- M. Pochet, H. Jeanmart, and F. Contino. A 22:1 Compression Ratio Ammonia-Hydrogen HCCI Engine: Combustion, Load, and Emission Performances. *Frontiers in Mechanical Engineering*, 6, 2020a. doi: 10.3389/fmech.2020.00043.
- Maxime Pochet, Véronique Dias, Hervé Jeanmart, Sebastian Verhelst, and Francesco Contino. Multifuel CHP HCCI Engine towards Flexible Power-to-fuel: Numerical Study of Operating Range. *Energy Procedia*, 105:1532–1538, 2017a. ISSN 18766102. doi: 10.1016/J.EGYPRO.2017.03.468.
- Maxime Pochet, Ida Truedsson, Fabrice Foucher, Hervé Jeanmart, and Francesco Contino. Ammonia-Hydrogen Blends in Homogeneous-Charge Compression-Ignition Engine. *SAE Technical Papers*, 2017-September(September), 9 2017b. ISSN 01487191. doi: 10.4271/2017-24-0087.
- Maxime Pochet, Véronique Dias, Bruno Moreau, Fabrice Foucher, Hervé Jeanmart, and Francesco Contino. Experimental and numerical study, under LTC conditions, of ammonia ignition delay with and without hydrogen addition. *Proceedings of the Combustion Institute*, 37:621–629, 2019. ISSN 1540-7489. doi: 10.1016/j.proci.2018.05.138. URL www.sciencedirect.com www.elsevier.com/locate/proci.
- Maxime Pochet, Hervé Jeanmart, and Francesco Contino. Uncertainty quantification from raw measurements to post-processed data: A general methodology and its application to a homogeneous-charge compression-ignition engine. *International Journal of Engine Research*, 21(9):1709–1737, 11 2020b. ISSN 20413149. doi: 10.1177/1468087419892697.
- Aaron J. Reiter and Song Charng Kong. Demonstration of compression-ignition engine combustion using ammonia in reducing greenhouse gas emissions. *Energy and Fuels*, 22(5):2963–2971, 9 2008. ISSN 08870624. doi: 10.1021/EF800140F.
- Aaron J. Reiter and Song Charng Kong. Diesel engine operation using ammonia as a carbon-free fuel. *American Society of Mechanical Engineers, Internal Combustion Engine Division (Publication) ICE*, pages 111–117, 2010. ISSN 10665048. doi: 10.1115/ICEF2010-35026.
- A.J. Reiter and S.-C. Kong. Combustion and emissions characteristics of compression-ignition engine using dual ammonia-diesel fuel. *Fuel*, 90(1):87–97, 2011. doi: 10.1016/j.fuel.2010.07.055.

Bibliography

- Rolf D. Reitz and Ganesh Duraisamy. Review of high efficiency and clean reactivity controlled compression ignition (RCCI) combustion in internal combustion engines. *Progress in Energy and Combustion Science*, 46:12–71, 2 2015. ISSN 0360-1285. doi: 10.1016/J.PECS.2014.05.003.
- K. Ryu, G.E. Zacharakis-Jutz, and S.-C. Kong. Performance enhancement of ammonia-fueled engine by using dissociation catalyst for hydrogen generation. *International Journal of Hydrogen Energy*, 39(5):2390–2398, 2014a. doi: 10.1016/j.ijhydene.2013.11.098.
- Kyunghyun Ryu, George E. Zacharakis-Jutz, and Song Charng Kong. Performance characteristics of compression-ignition engine using high concentration of ammonia mixed with dimethyl ether. *Applied Energy*, 113:488–499, 2014b. ISSN 03062619. doi: 10.1016/J.APENERGY.2013.07.065.
- A. Schönborn. Aqueous solution of ammonia as marine fuel. *Proceedings of the Institution of Mechanical Engineers Part M: Journal of Engineering for the Maritime Environment*, 235(1): 142–151, 2021. doi: 10.1177/1475090220937153.
- Krishna P. Shrestha, Lars Seidel, Thomas Zeuch, and Fabian Mauss. Detailed Kinetic Mechanism for the Oxidation of Ammonia Including the Formation and Reduction of Nitrogen Oxides. *Energy and Fuels*, 32(10):10202–10217, 10 2018. ISSN 15205029. doi: 10.1021/ACS.ENERGYFUELS.8B01056.
- Krishna Prasad Shrestha, Charles Lhuillier, Amanda Alves Barbosa, Pierre Brequigny, Francesco Contino, Christine Mounaïm-Rousselle, Lars Seidel, and Fabian Mauss. An experimental and modeling study of ammonia with enriched oxygen content and ammonia/hydrogen laminar flame speed at elevated pressure and temperature. *Proceedings of the Combustion Institute*, 38(2):2163–2174, 1 2021. ISSN 1540-7489. doi: 10.1016/J.PROCI.2020.06.197.
- Krishna Prasad Shrestha, Binod Raj Giri, Ayman M Elbaz, Gani Issayev, William L Roberts, Lars Seidel, Fabian Mauss, and Aamir Farooq. A detailed chemical insights into the kinetics of diethyl ether enhancing ammonia combustion and the importance of NO_x recycling mechanism. *Fuel Communications*, 10:100051, 3 2022. ISSN 2666-0520. doi: 10.1016/J.JFUECO.2022.100051.
- Anand Shankar Singh, Subhankar Mohapatra, Raghu Boyapati, Ayman M. Elbaz, Sukanta Kumar Dash, William L. Roberts, and V. Mahendra Reddy. Chemical Kinetic Modeling of the Autoignition Properties of Ammonia at Low-Intermediate Temperature and High Pressure using a Newly Proposed Reaction Mechanism. *Energy and Fuels*, 35(16):13506–13522, 8 2021. ISSN 15205029. doi: 10.1021/ACS.ENERGYFUELS.1C01243/ASSET/IMAGES/LARGE/EF1C01243{_}0017.JPEG. URL <https://pubs-acsc-org.tudelft.idm.oclc.org/doi/full/10.1021/acs.energyfuels.1c01243>.
- Øyvind Skreiberg, Pia Kilpinen, and Peter Glarborg. Ammonia chemistry below 1400 K under fuel-rich conditions in a flow reactor. *Combustion and Flame*, 136(4):501–518, 3 2004. ISSN 0010-2180. doi: 10.1016/J.COMBUSTFLAME.2003.12.008.
- Yu Song, Hamid Hashemi, Jakob Munkholt Christensen, Chun Zou, Paul Marshall, and Peter Glarborg. Ammonia oxidation at high pressure and intermediate temperatures. *Fuel*, 181: 358–365, 10 2016. ISSN 00162361. doi: 10.1016/J.FUEL.2016.04.100.
- James G. Speight. *Handbook of Petroleum Product Analysis (2nd Edition)*. John Wiley & Sons, 2015. ISBN 978-1-118-36926-5. URL <https://app.knovel.com/hotlink/khtml/id:kt011BR4BT/handbook-petroleum-product/cetane-number>.

- Derek Splitter, Sage Kokjohn, Keith Rein, Reed Hanson, Scott Sanders, and Rolf Reitz. An optical investigation of ignition processes in fuel reactivity controlled PCCI combustion. *SAE Technical Papers*, pages 142–162, 2010. ISSN 26883627. doi: 10.4271/2010-01-0345.
- Alessandro Stagni, Carlo Cavallotti, Suphaporn Arunthanayothin, Yu Song, Olivier Herbinet, Frédérique Battin-Leclerc, and Tiziano Faravelli. An experimental, theoretical and kinetic-modeling study of the gas-phase oxidation of ammonia. *Reaction Chemistry and Engineering*, 5(4):696–711, 4 2020. ISSN 20589883. doi: 10.1039/C9RE00429G.
- Douwe Stapersma. *Diesel Engines - Volume 5 Thermodynamical principles I*. TU Delft, 2009.
- Douwe Stapersma. *Diesel Engines - Volume 1 Performance Analysis*. TU Delft, 2010a.
- Douwe Stapersma. *Diesel Engines - Volume 3 Combustion*. TU Delft, 2010b.
- E. S. Starkman, G. E. James, and H. K. Newhall. Ammonia as a Diesel Engine Fuel: Theory and Application. *SAE Technical Papers*, 2 1967. ISSN 0148-7191. doi: 10.4271/670946. URL <https://www-sae-org.tudelft.idm.oclc.org/publications/technical-papers/content/670946/https://www-sae-org.tudelft.idm.oclc.org/publications/technical-papers/content/670946/?src=670947>.
- Yong Sun, Eric D Weninger, and Rolf D Reitz. Adaptive Injection Strategies (AIS) for Ultra-Low Emissions Diesel Engines. *SAE Technical Papers*, 2007.
- James P Szybist, Samuel Mclaughlin, Volvo North, and America Suresh Iyer. Emissions and Performance Benchmarking of a Prototype Dimethyl Ether-Fueled Heavy-Duty Truck. *Oak Ridge National Laboratory*, 2014. URL <http://www.osti.gov/contact.html>.
- B H Thacker, S W Doebbling, F M Hemez, M C Anderson, J E Pepin, and E A Rodriguez. Concepts of Model Verification and Validation. *Office of Scientific and Technical Information*, 10 2004. doi: 10.2172/835920. URL <http://www.osti.gov/servlets/purl/835920-Y180w3/native/>.
- Zhenyu Tian, Lidong Zhang, Yuyang Li, Tao Yuan, and Fei Qi. An experimental and kinetic modeling study of a premixed nitromethane flame at low pressure. *Proceedings of the Combustion Institute*, 32(1):311–318, 1 2009. ISSN 1540-7489. doi: 10.1016/J.PROCI.2008.06.098.
- US Department of Energy. Alternative Fuels Data Center: Dimethyl Ether, 2023. URL https://afdc.energy.gov/fuels/emerging_dme.html.
- U.S. Environmental Protection Agency US EPA. Understanding Global Warming Potentials — US EPA, 2023. URL <https://www.epa.gov/ghgemissions/understanding-global-warming-potentials>.
- B. Wang, C. Yang, H. Wang, D. Hu, and Y. Wang. Effect of Diesel-Ignited Ammonia/Hydrogen mixture fuel combustion on engine combustion and emission performance. *Fuel*, 331, 2023. doi: 10.1016/j.fuel.2022.125865.
- Y. Wang, X. Zhou, and L. Liu. Feasibility study of hydrogen jet flame ignition of ammonia fuel in marine low speed engine. *International Journal of Hydrogen Energy*, 2022. doi: 10.1016/j.ijhydene.2022.09.198.

Bibliography

Zhihua Wang, Xinlu Han, Yong He, Runfan Zhu, Yanqun Zhu, Zhijun Zhou, and Kefa Cen. Experimental and kinetic study on the laminar burning velocities of NH₃ mixing with CH₃OH and C₂H₅OH in premixed flames. *Combustion and Flame*, 229:111392, 7 2021. ISSN 0010-2180. doi: 10.1016/J.COMBUSTFLAME.2021.02.038.

Woodward. About woodward, 2023. URL <https://www.woodward.com/en/about>.

Wärtsilä. World's first full scale ammonia engine test - an important step towards carbon free shipping, 2020. URL <https://www.wartsila.com/media/news/30-06-2020-world-s-first-full-scale-ammonia-engine-test---an-important-step-towards-carbon>

Hua Xiao, Micheal Howard, Agustin Valera-Medina, Stephen Dooley, and Philip J. Bowen. Study on Reduced Chemical Mechanisms of Ammonia/Methane Combustion under Gas Turbine Conditions. *Energy and Fuels*, 30(10):8701–8710, 10 2016. ISSN 15205029. doi: 10.1021/ACS.ENERGYFUELS.6B01556/SUPPL{_}FILE/EF6B01556{_}SI{_}002.PDF. URL <https://pubs-acsc.org.tudelft.idm.oclc.org/doi/full/10.1021/acs.energyfuels.6b01556>.

Yu Yang, Shu Zheng, Ran Sui, and Qiang Lu. Impact of ammonia addition on soot and NO/N₂O formation in methane/air co-flow diffusion flames. *Combustion and Flame*, 247: 112483, 1 2023. ISSN 0010-2180. doi: 10.1016/J.COMBUSTFLAME.2022.112483.

Lindsay D. Yee, Jill S. Craven, Christine L. Loza, Katherine A. Schilling, Nga Lee Ng, Manjula R. Canagaratna, Paul J. Ziemann, Richard C. Flagan, and John H. Seinfeld. Secondary organic aerosol formation from low-NO_x photooxidation of dodecane: Evolution of multi-generation gas-phase chemistry and aerosol composition. *Journal of Physical Chemistry A*, 116(24):6211–6230, 6 2012. ISSN 10895639. doi: 10.1021/JP211531H.

A. Yousefi, H. Guo, S. Dev, S. Lafrance, and B. Liko. A study on split diesel injection on thermal efficiency and emissions of an ammonia/diesel dual-fuel engine. *Fuel*, 316:123412, 5 2022a. ISSN 0016-2361. doi: 10.1016/J.FUEL.2022.123412.

A. Yousefi, H. Guo, S. Dev, B. Liko, and S. Lafrance. Effects of ammonia energy fraction and diesel injection timing on combustion and emissions of an ammonia/diesel dual-fuel engine. *Fuel*, 314, 2022b. doi: 10.1016/j.fuel.2021.122723.

Ren Zhang, Lin Chen, Haiqiao Wei, Jinguang Li, Yi Ding, Rui Chen, and Jiaying Pan. Experimental investigation on reactivity-controlled compression ignition (RCCI) combustion characteristic of n-heptane/ammonia based on an optical engine. *International Journal of Engine Research*, 2022. ISSN 20413149. doi: 10.1177/14680874221124452/FORMAT/EPUB.

Xiao Sen Zheng. An investigation of hydrogen-ammonia combustion inside internal combustion engines, 2020. URL <https://repository.tudelft.nl/islandora/object/uuid%3A2372f356-c197-4286-b6fe-5b2873b40539>.

Yuanxian Zhu and Liyun Fan. Fuel Delivery System for Alternative Fuel Engines: A Review. *Energy, Environment, and Sustainability*, pages 67–95, 2022. ISSN 25228374. doi: 10.1007/978-981-16-8414-2{_}4.

Seif Zitouni, Pierre Brequigny, and Christine Mounaim-Rousselle. Turbulent flame speed and morphology of pure ammonia flames and blends with methane or hydrogen. *Proceedings of the Combustion Institute*, 2022. ISSN 15407489. doi: 10.1016/J.PROCI.2022.07.179.

Colophon

This document was typeset using L^AT_EX, using the KOMA-Script class scrbook. The main font is Palatino.

